

A MEGABRECCIA WITH ASSOCIATED STRATIGRAPHY OF THE
CHERRY CANYON AND BELL CANYON FORMATIONS TRANSITION
(GUADALUPIAN, MIDDLE PERMIAN), SOUTHERN DELAWARE
MOUNTAINS, WEST TEXAS

by

JOHNATHON LEE BOGACZ

Presented to the Faculty of the Graduate School of
The University of Texas at Arlington in Partial Fulfillment
of the Requirements
for the Degree of

MASTER OF SCIENCE IN ENVIRONMENTAL AND EARTH SCIENCES

THE UNIVERSITY OF TEXAS AT ARLINGTON

May 2017

Copyright © by JOHNATHON LEE BOGACZ 2017

All Rights Reserved



Acknowledgements

I am appreciative and thankful of my advisor Merlynd Nestell, Galina Nestell, and John Wickham for their guidance and patience during my work on this project. I would like to thank George Snyder, George Strickhousen, Kenny Frasier, T. J. Shipp, and Paul Blankenburg for allowing access to their private properties and use of facilities. I am also grateful for my field partners and friends Michael Sweatt and Zach Sutton. I extend sincere thanks to my wife Sana Bogacz and my parents John and Brenda Bogacz for their support towards my success. Lastly, I wish to thank all my friends and family members for their encouragements in all my endeavors.

April 24, 2017

Abstract

A MEGABRECCIA WITH ASSOCIATED STRATIGRAPHY OF THE
CHERRY CANYON AND BELL CANYON FORMATIONS TRANSITION
(GUADALUPIAN, MIDDLE PERMIAN), SOUTHERN DELAWARE
MOUNTAINS, WEST TEXAS

Johnathon Lee Bogacz, MS

The University of Texas at Arlington, 2017

Supervising Professor: Merlynd Nestell

The Cherry Canyon and Bell Canyon Formations (Guadalupian, Middle Permian) are well exposed in the southern part of the Delaware Mountains, West Texas and are marked by the presence of several distinct and widespread debris flows. Various lithostratigraphic units (members) of these two formations were originally named for exposures in the Guadalupe Mountains and the northern part of the Delaware Mountains, West Texas. These units are not easily recognized litho-stratigraphically in the southern part of the Delaware Mountains, but some correlations can be made by using biostratigraphic methods. One of the easily recognizable debris flows in the southern Delaware Mountains is a megabreccia named the B-debris that is well exposed in a road cut along Texas FM road 2185

about 25 miles from a bird's eye view to the northeast of Van Horn and can be traced to the northwest into the southern part of the Delaware Mountains where it is extensively exposed. The first objective of this study was to map the lateral extent of the B-debris flow that may be traced along the upper parts of the ridges in the 42 mi² study area. The second objective was to describe the litho- and biofacies of a well exposed stratigraphic section, named the WP-section, of the Cherry Canyon and Bell Canyon Formations transition, and is capped by the B-debris. The WP-section appears to include the upper part of the Cherry Canyon and lower part of the Bell Canyon Formations. This study discusses the exposed lateral extent of the B-debris from Texas FM road 2185 to the north-northwest into the southern part of the Delaware Mountains.

Table of Contents

Acknowledgements.....	iii
Abstract.....	iv
List of Illustrations.....	viii
Chapter 1.....	1
INTRODUCTION.....	1
1.1 Geographic Setting.....	1
1.2 Location.....	5
1.3 Previous Work of Study Area.....	9
1.4 Methods.....	13
1.5 Scope of Current Study.....	13
Chapter 2.....	17
STRATIGRAPHY.....	17
2.1 Introduction.....	17
2.2 Cherry Canyon Formation.....	19
2.3 Bell Canyon Formation.....	20
2.4 WP-Section.....	21
2.5 Package A.....	24
2.6 Package B.....	52
2.7 Package C.....	62
2.8 Package D.....	72

Chapter 3.....	83
MAPPING	83
3.1 Introduction.....	83
3.2 Study Area	83
3.3 B-Debris Map.....	85
3.4 Extent of Exposure.....	86
Chapter 4.....	88
STRUCTURE.....	88
4.1 Introduction.....	88
4.2 Structural Interpretation	91
Chapter 5.....	100
B-DEBRIS	100
5.1 Introduction.....	100
5.2 Rheology.....	101
5.3 Source of the B-debris	114
Chapter 6.....	116
CONCLUSIONS	116
References.....	119
Biographical Information.....	124

List of Illustrations

Figure 1.1: General location of Capitan Reef today.	1
Figure 1.2: Structural province of Permian Basin.	2
Figure 1.3: Guadalupe Mountains area geologic time scale (Middle Permian)	3
Figure 1.4: Location of prominent monoclinial flexures	4
Figure 1.5: Topographic map of Culberson County	6
Figure 1.6: Sections along Texas FM road 2185	7
Figure 1.7: Topographic map of study area	8
Figure 1.8: Photograph of the WP-section.....	8
Figure 1.9: Reference photograph of the B-debris.....	14
Figure 1.10: Photograph of the BWK-section	15
Figure 2.1: Stratigraphic columns of the reference WP-section.	19
Figure 2.2: Field photographs of samples WP-0 through WP-4.....	25
Figure 2.3: Thin sections of samples WP-0, 4, 5B, and 7.....	26
Figure 2.4: Field photographs of samples WP-5A through WP-7.....	27
Figure 2.5: Field photograph of samples WP-8A through WP-11	29
Figure 2.6: Thin sections of samples WP-8A, 8B, 10, and 11.....	30
Figure 2.7: Field photograph of samples WP-12 through WP-15	32
Figure 2.8: Thin sections of samples WP-13, 14, 16A, and 16D	33
Figure 2.9: Field photograph of samples WP-12 through WP-15	34
Figure 2.10: Field photograph of samples WP-17A through WP-18A	36

Figure 2.11: Thin sections of samples WP-17B, 17C, and 17F.....	38
Figure 2.12: Field photograph of samples WP-18C through WP-19B.....	39
Figure 2.13: Thin sections of samples WP-18A, 18B, 19A, and 21.....	41
Figure 2.14: Field photograph of sample WP-20.....	42
Figure 2.15: Field photograph of samples WP-23 through WP-25.....	44
Figure 2.16: Thin sections of samples WP-23, 25, 27, and 28B.....	45
Figure 2.17: Field photograph of samples WP-26 though WP-32.....	47
Figure 2.18: Field photograph of samples WP-33 through WP-37.....	49
Figure 2.19: Thin sections of samples WP-30, 31, and 32.....	50
Figure 2.20: Thin sections of samples WP-35 and 37.....	51
Figure 2.21: Field photograph of samples WP-38 through WP-42.....	53
Figure 2.22: Thin sections of samples WP-38, 39A, 39B, and 41.....	54
Figure 2.23: Thin sections of smaples WP-42, 43, 45, and 46.....	57
Figure 2.24: Field photograph of samples WP-43 through WP-45.....	58
Figure 2.25: Field photograph of samples WP-46 though WP-51B.....	59
Figure 2.26: Thin sections of samples WP-47 and 49.....	60
Figure 2.27: Thin sections of samples WP-50, 51A, and 51B.....	61
Figure 2.28: Field photograph of samples WP-53 through WP-54C.....	63
Figure 2.29: Thin sections of samples WP-52, 53, and 54A.....	64
Figure 2.30: Thin section of sample WP-54C.....	65
Figure 2.31: Field photograph of sample WP-55.....	66

Figure 2.32: Thin sections of samples WP-55, 56, and 56.	67
Figure 2.33: Field photograph of sample WP-56.....	68
Figure 2.34: Thin sections of samples WP-57, 58, 59, and 60.	71
Figure 2.35: Field photograph of samples WP-59 and WP-60.....	72
Figure 2.36: Field photograph of sample WP-61.....	73
Figure 2.37: Thin sections of samples WP-61, 63, and 64.	74
Figure 2.38: Thin sections of samples WP-65, 66, 67, and 68.	77
Figure 2.39: Thin sections of samples WP-69, 70, and 71.	79
Figure 2.40: Field photograph of the B-debris near top of WP-section.....	81
Figure 3.1: Topographic map showing edge of exposures of major units.....	84
Figure 3.2: Cross-section along A-A' (west to east).....	85
Figure 3.3: Outcrop map of the extent of the B-debris	86
Figure 4.1: Problematic faulted blocks	89
Figure 4.2: Illustrations of structural dynamics	90
Figure 4.3: Photographs showing faulted block and faulted section	92
Figure 4.4: Photograph showing a down faulted section.....	93
Figure 4.5: Photographs showing displacement and joint fractures	94
Figure 4.6: Photographs showing down-dropped blocks.....	95
Figure 4.7: Photographs showing fault scarp and associated displacement.....	96
Figure 4.8: Photographs showing faulting and associated displacement.....	97
Figure 5.1: Kennedy (2009) original photographs of B-debris zones	102

Figure 5.2: Photographs showing western study area zone distribution.....	104
Figure 5.3: Photographs showing floating clast and boulders	106
Figure 5.4: Photographs showing ditribution of clasts	108
Figure 5.5: Photographs showing boulder and complete section of B-debris	109
Figure 5.6: Photographs showing B-debris range of thickness and limit	110
Figure 5.7: Photograph showing boulder and complete section of B-debris	112
Figure 5.8: Photographs showing boulder and lower contact of B-debris.....	113
Figure 5.9: Illustration showing theoretical transport mechanism.....	115

Chapter 1

INTRODUCTION

1.1 Geographic Setting

The Permian Reef complex contains the Capitan Reef (figure 1.1), which mostly surrounds the Delaware Basin, located in the Trans-Pecos region of West Texas and southeastern New Mexico and contains strata from shelf, marginal, and basinal paleoenvironments (King, 1942; Newell, 1953). The Delaware Basin is a part of a much larger basin known as the Permian Basin (figure 1.2), which from west to east is made up of the Delaware Basin, Central Basin Platform, and the

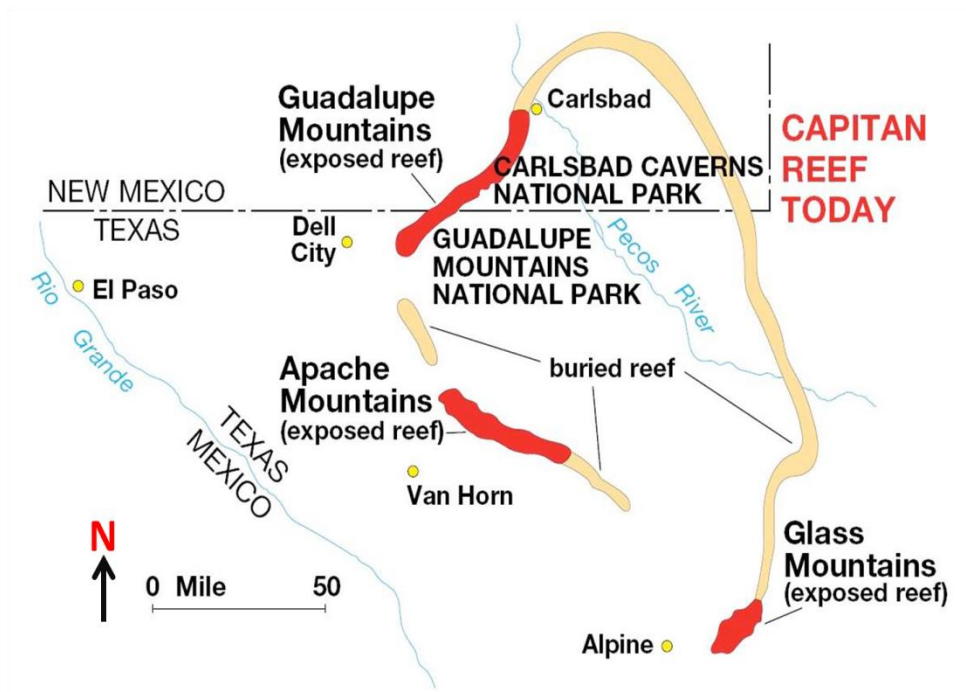


Figure 1.1: General location of the exposed Capitan Reef in the Guadalupe, Apache, and Glass Mountains, West Texas and New Mexico (Image is available via the Guadalupe Mountains National Park Service website www.nps.gov/gumo/naturescience/geologicformations.htm).

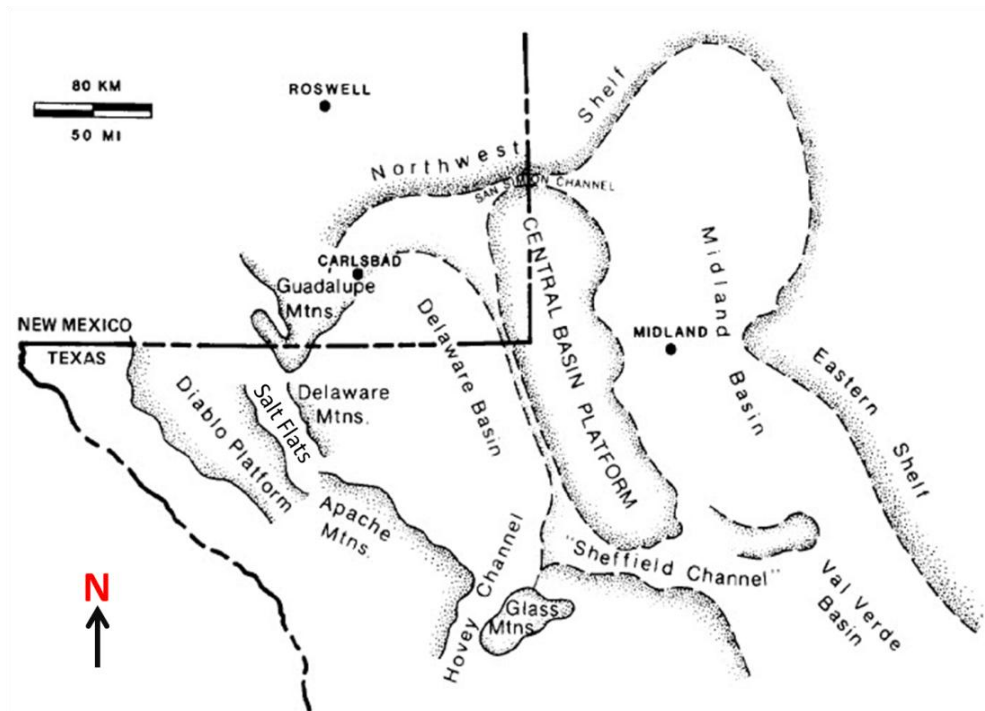


Figure 1.2: Large scale features of the Permian Basin with the general location of the Delaware Mountains relative to the Guadalupe and Apache Mountains (after Ward et al., 1986).

Midland Basin. The Delaware Basin is an asymmetric block-faulted basin with its axis parallel to the western edge of the Central Basin Platform (Garber et al., 1989). The Delaware Mountains are located in the western part of the Delaware Basin (figure 1.2), which contains the uplifted and exposed basinal strata of the Delaware Mountain Group (figure 1.3) (King, 1942). Shelf and marginal strata are exposed in the Guadalupe and Apache Mountains (figure 1.2) to the north and south of the Delaware Mountains, respectively (King, 1942; Newell, 1953).

System		North America, Guadalupe Mountains (Glenister et al., 1992, 1999; Wardlaw, 2004; Nestell and Nestell, 2006)						
Series	Stage	Ag (Ma)	FA of conodont species	Shelf	Margin	Basin		
Permian	Lopingian	Wuchiapingian lower	259.8	<i>C. postbitteri</i>	Castile Fm			
	Guadalupian	Capitanian	265.1	<i>Jinogondolella postserrata</i>			Tansill Fm	Capitan Fm
		Wordian	268.8	<i>J. asserata</i>	Yates Fm	McComb mbr		
		Roadian	272.3	<i>J. nanjingensis</i>	Seven Rivers Fm	Rader mbr Pinery mbr		
		Cisuralian	Leonardian upper		Queen Fm	Goat Seep Fm	Hegler mbr	Cherry Canyon Fm
					Grayburg Fm	Manzanita mbr South Wells mbr Getaway mbr	Brushy Canyon Fm	
					upper San Andres Fm	Cutoff Fm		
					lower San Andres Fm	Victorio Peak Fm	Bone Spring Limestone	Delaware Mountain Group

Figure 1.3: Correlation chart of Middle Permian strata in the Delaware Basin, West Texas (modified from Nestell and Nestell, 2006). *J.* – *Jinogondolella*; *C.* – *Clarkina*.

Towards the end of the Pennsylvanian, subsidence of the Delaware Basin began as monoclinical structures (figure 1.4) that were activated along the Bone Spring, Babb, and Victorio flexures (King, 1942; McNutt, 1948). As the flexures down warped the region, marine water flowed into the basin from the open ocean through the Hovey channel (figure 1.2). This channel is perceived to have opened between the Apache and Glass Mountains (King, 1942; Hills, 1942). It was suggested by Hills (1942) that the Hovey channel allowed circulation of water in and out of the Delaware Basin. By the end of the deposition of strata of the Guadalupian Series (figure 1.3), the Hovey channel area was uplifted and the rate

of flow into the basin was diminished, which ultimately caused the formation of the evaporites that make up the Castile Formation of the overlying Lopingian Series (Upper Permian) (King, 1948; Hill, 1999).

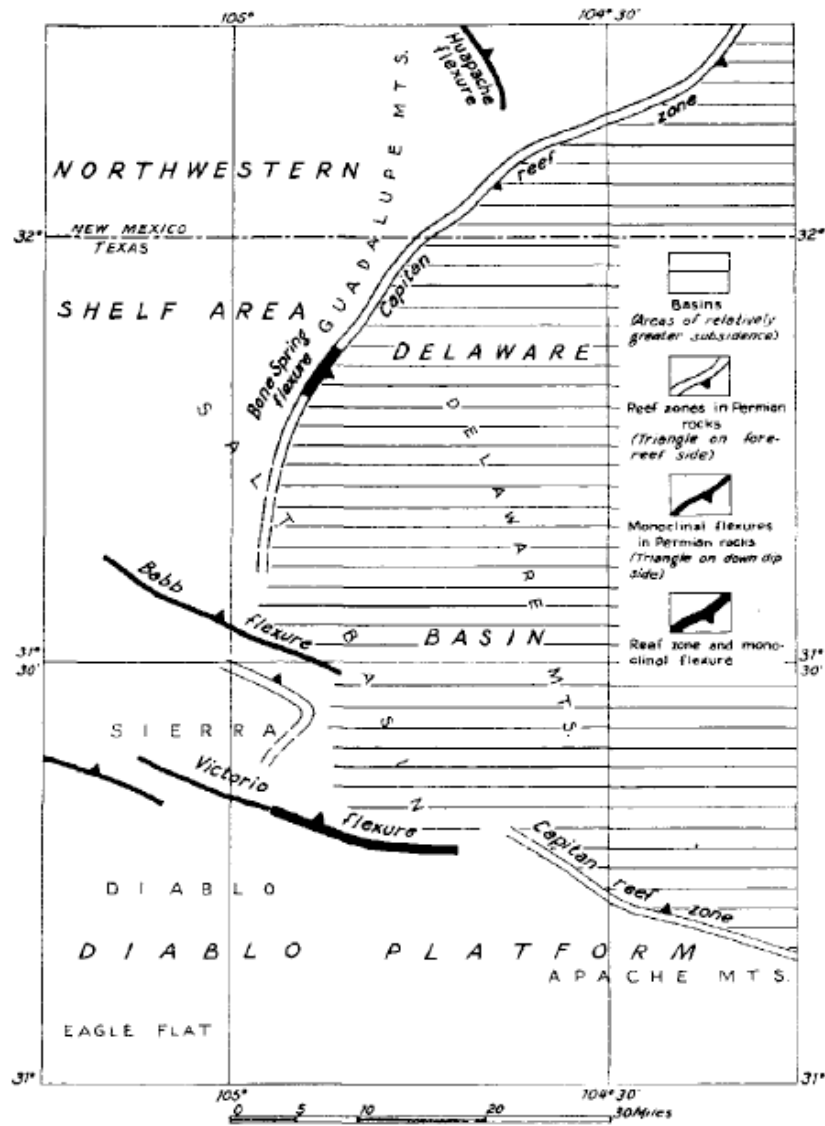


Figure 1.4: Location of the monoclinal flexures that down warp the Delaware Basin of West Texas (after King, 1942).

As the Delaware Basin subsided, organisms such as algae, brachiopods, bryozoans, foraminifers, sponges, conodonts, and ammonoids started to inhabit the edges of the basin on the Permian Reef complex (Newell, 1953). Remains of these organisms are associated with carbonate and siliciclastic strata that make up the preserved sedimentary sequence within the Delaware Basin. The rate of subsidence in the Delaware Basin and the rate of organism growth are believed to be the same (Sweatt, 2009). Different sea levels resulted in the distribution of highstand deposits of mixed carbonate-siliciclastics on the shelves, and lowstand deposits of shelf-derived siliclastic rocks and margin-derived carbonate rocks in the basin (Silver and Todd, 1969; Meissner, 1972). The sediment supply into the Delaware Basin was at a low enough rate that the basin subsidence was much faster, which left the basin in deep water conditions until the deposition of evaporate strata of the Lopingian Series (Nance, 2014). Overall the Delaware Basin during the deposition of the Guadalupian Series accumulated approximately 1,370 m (4,500 ft) of highstand and lowstand deposits (Dutton et al., 2005; Nance, 2014).

1.2 Location

The map area is located in Culberson County, West Texas, approximately 25 miles (~40.2 kilometers) from a bird's eye view, north northeast of Van Horn, in the southern part of the Delaware Mountains (figure 1.5). The map area covers a 42 mi² (~67.6 km²) area with the corners approximately located at:

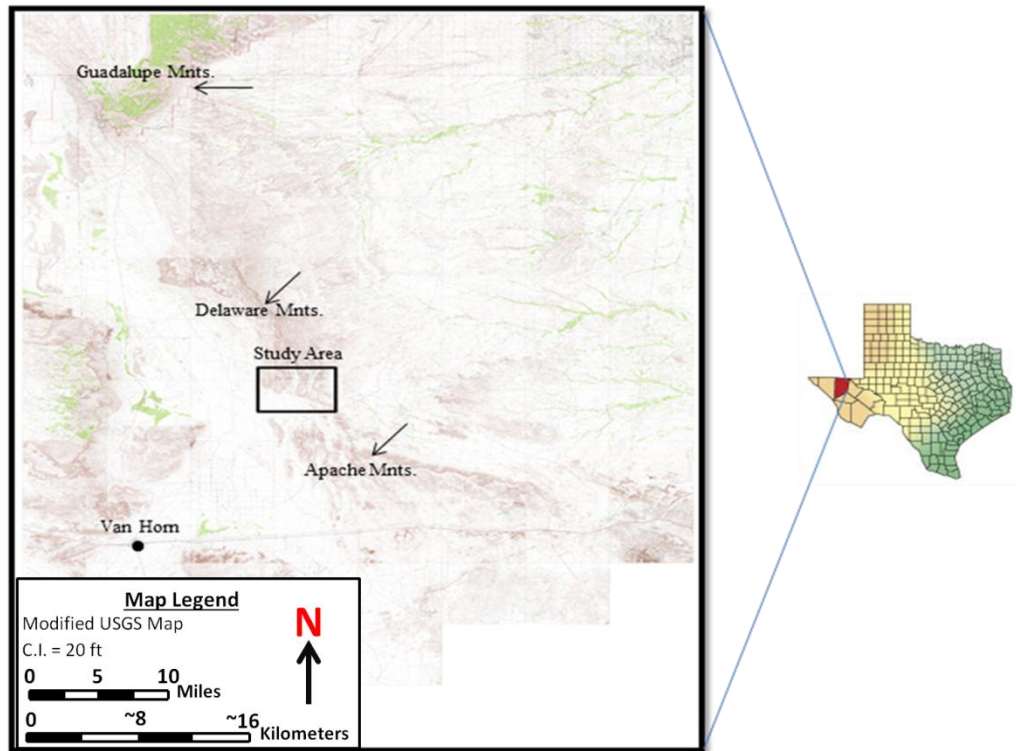


Figure 1.5: Culberson County, West Texas, (highlighted in red), is seen enlarged as a USGS topographic map with major features labeled. Modified from USGS Service website: <http://www.usgs.gov/pubprod/index.html>.

north-northwest (31.4 N, 104.65 W), north east (31.4 N, 104.5 W), southeast (31.3 N, 104.5 W), and southwest (31.3 N, 104.65 W). The southeast corner of the map area includes an excellent exposure of the B-debris in a road cut along Texas FM road 2185 (figures 1.6 and 1.7). The map area in the Delaware Mountains includes the geographical features from west to east: Square Mesa, Scott Canyon, Ed Ray Canyon (also called Trew Canyon), Wildcat Canyon, and Trew Gap (figure 1.7). The base of the WP-section is located at the south western end of Scott Canyon at 31.358514 N, 104.606519 W (figure 1.7). It is reached by an unnamed dirt road

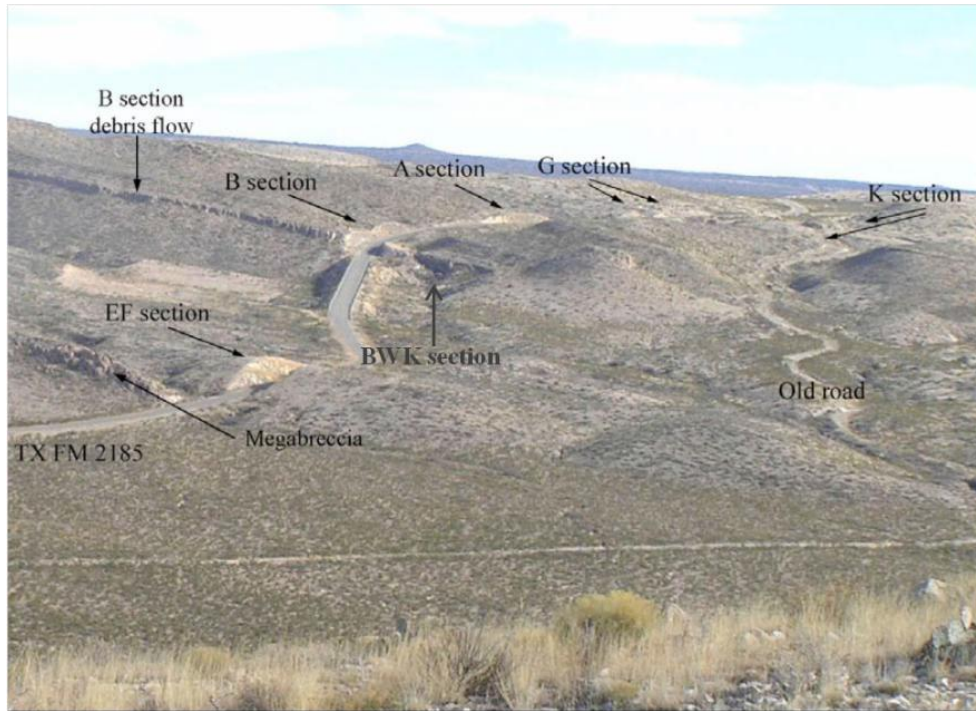


Figure 1.6: Location of the road cuts along Texas FM road 2185, which shows the B-section (with an elongate exposed section of the B-debris) with associated sections from (Nestell et al., 2006).

which connects to Jay-Capp road and leads to an old well pad site. The WP-section is located just to the south of the old well pad site on the west flank of Scott Canyon and is in the third drainage wash coming down from the flank (figure 1.8).

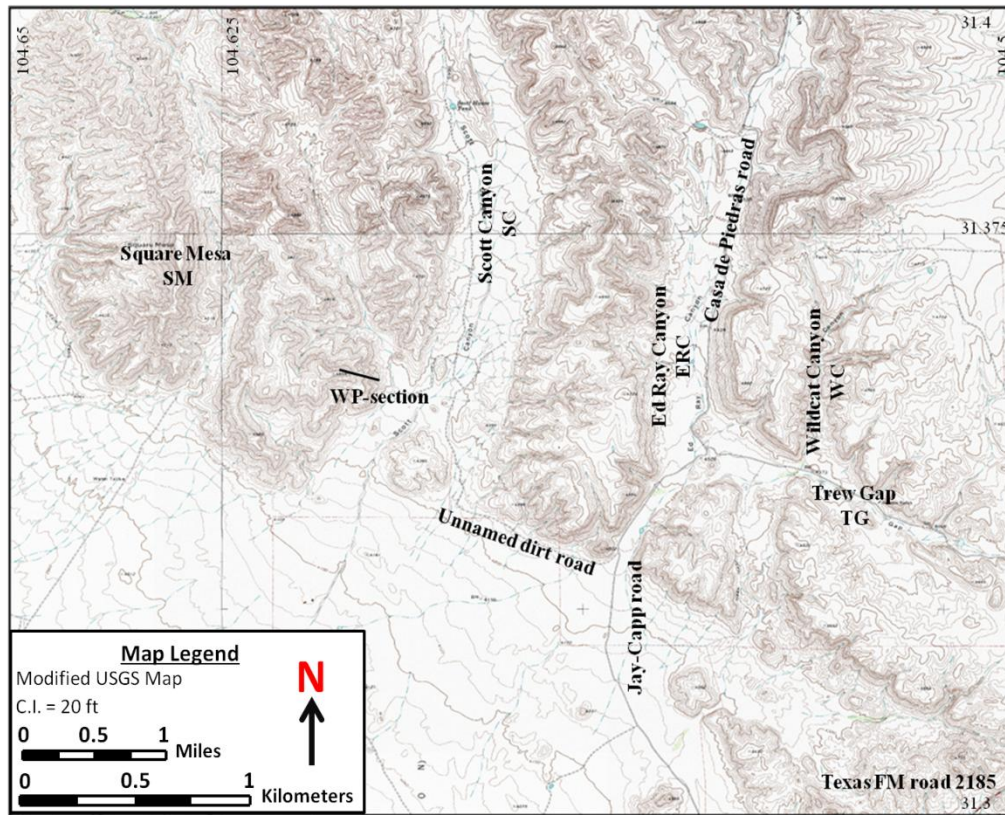


Figure 1.7: Closer view of the study area with major features labeled and the WP-section marked (modified from USGS Service website, <http://www.usgs.gov/pubprod/index.html>).

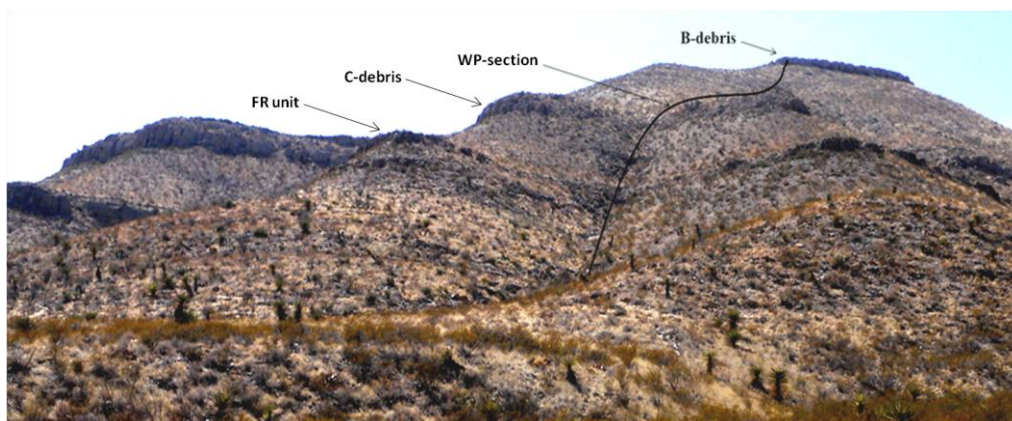


Figure 1.8: Photo of the WP-section taken from the base of the section showing up to the peak topped by the B-debris with associated units.

1.3 Previous Work of Study Area

The Delaware Mountains, which consist of exposed stratigraphic units of the Delaware Mountain Group (Guadalupian Series), were first visited by the geologist G. G. Shumard (King, 1948; McNutt, 1948) who was a member of an artesian well experimental party under Captain John Pope from 1855 to 1857 (Shumard G. G., 1858). Shumard took detailed notes on his journey and collected many samples from geological sections in the Trans-Pecos region, specifically from the Guadalupe Mountains located north of the Delaware Mountains (King, 1948). He noted at the time that his samples were of Pennsylvanian age (Shumard G. G., 1858). Later, Shumard's brother, B. F. Shumard, examined the samples and determined them to be of Permian age (Shumard B. F., 1858). The geology of the Guadalupe Mountains were also mentioned in early reports by Von Streeruwitz (1890, 1893), Dumble (1903), and Hill (1900), as they traveled in the area.

The sequence of strata of the Delaware Mountain Group was first described by Richardson (1904), who included the exposed strata from the Guadalupe Mountains up to the Capitan Limestone and strata from the Delaware Mountains up to the Castile Gypsum. Richardson (1904) discussed the geometric lateral variability of the Delaware Mountain Group strata, which includes slope and basinal deposits. Depositional facies of the strata were recognized by Beede (1924) as a succession of three sequences. King (1942) used Beede's tripartite observation of the Delaware Mountain Group divisional lithological units by

formally naming them from oldest to youngest: the Brushy Canyon, Cherry Canyon, and Bell Canyon Formations (figure 1.3), and elevated the rank of the Delaware Mountain Group succession to its current rank of a Group. The underlying Bone Spring Limestone was originally a part of the Delaware Mountain Group of Richardson (1904), but was separated from the Delaware Mountain Group and formally named the Bone Spring Limestone Formation by King (1942). The classification of the Bone Spring Limestone Formation was changed due to work by King and King (1929). They considered that the formation was of Leonardian age and should be separated from the Delaware Mountain Group because of a pronounced unconformity and dissimilar lithologies (figure 1.3).

King (1942) introduced the names of the members of the Cherry Canyon and Bell Canyon Formations of the Delaware Mountain Group. The Cherry Canyon Formation overlies the Brushy Canyon Formation unconformably and starts with the Getaway Limestone Member. The limestone members of the Cherry Canyon Formation are from oldest to youngest: Getaway, South Wells, and Manzanita Limestone (figure 1.3) and are inter-fingered with siltstone/sandstone. The overlying Bell Canyon Formation contains limestone members from oldest to youngest: Hegler, Pinery, Rader, McCombs, and Lamar Limestone (figure 1.3) also inter-fingered with siltstone/sandstone (Lang, 1937; King, 1942; King and Newell, 1956). Wilde et al. (1999) established a new

member, the Reef Trial Member (figure 1.3), which overlies the older Lamar Limestone Member and had previously been called the “post Lamar” beds. King (1948) revised the correlative strata in the Guadalupe Mountains and the northern part of the Delaware Mountains, which included cross-sections and geologic maps that are still considered correct. Cross-sections and geologic maps of King (1948) refined the shelfal, marginal, and basinal strata correlations in the Guadalupe Mountains area.

The top of the Cherry Canyon Formation is marked biostratigraphically by the last occurrence of the fusulinid genus *Parafusulina* as described by Dunbar and Skinner (1931; 1937) from the Manzanita Limestone Member (King, 1942; Newell et al., 1953). The base of the Bell Canyon Formation is marked biostratigraphically by the first occurrence of the fusulinid genus *Polydiexodina* as described by Dunbar and Skinner (1931; 1937) in the Hegler Limestone Member (King, 1942; Newell et al., 1953). In the Guadalupe Mountains area lithologically the Manzanita Limestone Member and the Hegler Limestone Member are separated by siltstone/sandstone. The Cherry Canyon Formation formally ends at the top of the Manzanita Limestone Member and the Bell Canyon Formation begins with siltstone/sandstone deposits underlying the Hegler Limestone Member (McNutt, 1948, Hayes, 1946).

Faunas from Permian age strata of the Guadalupe Mountains area were described by Girty (1908) and contained various brachiopod, sponge, gastropod,

and pelecypod species (King, 1948). Dunbar and Skinner (1931; 1937) formally described the first Permian fusulinids from West Texas, and discussed their morphologies, classification, correlations, and zonations. Newell et al. (1953) in famous monograph “The Permian Reef Complex”, provided biostratigraphic correlations based on distribution of the species of different group of fauna. In Newell’s species correlation of the fusulinids, *Parafusulina* and *Polydiexodina* are considered as benchmark markers between the reef and reef-transported Goat Seep Member and the overlying Hegler Member. After several decades Wilde et al. (1999) modified Newell’s faunal correlations. Wilde incorrectly considered the “post-Lamar” beds, which he later named as the Reef Trail Member, to belong to the Lopingian Series (Upper Permian) based on his observations and correlations with no conodont data considered. However, based on conodonts, the Reef Trail Member was later correctly placed in the Guadalupian Series (Wardlaw et al., 2001).

Wood (1965) discussed the geology and rock correlations of the Apache Mountains, which included the shelfal, shelf-marginal, and basinal facies that are age equivalent to those of the Guadalupe Mountains. Wood’s lithological correlations were reproduced by Wilde and Todd (1968), but were correlated by surface and subsurface fusulinid data. Wilde and Todd’s biostratigraphic correlations showed the importance of the use of fusulinids to aid in correlations of age equivalent strata from marginal to basinal facies.

1.4 Methods

Field work was conducted in a time frame of two and half years during seven visits, totaling approximately six weeks. The field work consists of reconnaissance of the B-debris (figure 1.8), mapping and measuring the thickness of the B-debris, and describing the lithofacies and collecting samples from the WP-section (figure 1.8). Mapping of the exposed B-debris was done with a Garmin Rhino 120 GPS receiver that recorded tracking and waypoint data. Thickness measurements of the exposed B-debris were recorded at each waypoint.

Laboratory work consisted of cutting the samples for polished hand specimens and making thin sections. The descriptions of the hand samples and thin sections follow the Dunham classification (Dunham, 1962). A stratigraphic column of the WP-section is constructed to give the age range of the units measured.

1.5 Scope of Current Study

The B-debris outcrops over a large area north-northwest of the Apache Mountains about 25 miles from a bird's eye view, northeast of Van Horn, West Texas. The outcrop area of Guadalupian-age B-debris of the Bell Canyon Formation is located in the Delaware Basin north-northwest of the Apache Mountains and may be traced into the southern part of the Delaware Mountains. The distinctive megabreccia facies of the B-debris makes it easy to distinguish

from other thick debris units found below and above it (figure 1.9). The measured B-section along a road cut on Texas FM road 2185 identified the B-debris as belonging to strata in age equivalence to the Pinery Limestone Member of the Guadalupe Mountains area (Kennedy, 2009; Wardlaw and Nestell, 2010). Because of its distinctive lithofacies, the B-debris can be traced throughout a large area along the ridges of the southern part of the Delaware Mountains.



Figure 1.9: Base of the B-debris rising above a one and half meter J-staff along the edge of Texas FM road 2185.

In a road cut on Texas FM road 2185 northeast of Van Horn, the underlying BWK-section (figures 1.6, and 1.10), the B-debris, and the overlying B-section are stratigraphically the lower most aged units exposed (Kennedy,

2009). The ten meter thick BWK- section exposed below the B-debris is correlated to the Hegler Limestone Member (Kennedy, 2009; Nestell and Wardlaw, 2010).



Figure 1.10: Photograph of the B-section that contains the B-debris with the older BWK-section on the east side of Texas FM road 2185 (after Nestell and Wardlaw, 2010).

The ridges of the southern part of the Delaware Mountains are mostly topped by the B-debris and exhibit stratigraphically exposed sections of up to two hundred meters below the B-debris. Physical mapping of the extent of the exposed B-debris in the southern part of the Delaware Mountains provides a direct

correlation back to the B-section exposed along the road cut on Texas FM road 2185.

The main priorities of this study is to trace and map the B-debris from the original locality of Kennedy (2009), north-northwest into the southern part of the Delaware Mountains to determine the exposed extent of the debris in the area, provide a reference stratigraphic section in the southern part of the Delaware Mountains that contains the B-debris and older in age strata, measure and describe the litho- and biostratigraphy of the stratigraphic section. Use biostratigraphic methods to determine the transitional zone between the Cherry Canyon and Bell Canyon Formations.

Chapter 2

STRATIGRAPHY

2.1 Introduction

The Guadalupe and Apache Mountains appear to have equivalent Middle Permian age rocks using correlations by biostratigraphic methods, but distinct differences in lithofacies exist between the two areas. Formational names such as Cherry Canyon and Bell Canyon have been used in both areas, but member name usage is certainly suspect because of differences in lithofacies. In the only major work done in this area, McNutt (1948) used both formational and member names to compare exposed rocks in the Apache and southern part of the Delaware Mountains to those of the Guadalupe Mountains. In his geological study of the area, he correctly considered by using his interpretation of the lithofacies and biofacies of the area to conclude that the upper part of the Cherry Canyon Formation and some of the lower part of the Bell Canyon Formation could be identified in the southern part of the Delaware Mountains. He also considered that lithofacies of age equivalent Getaway, South Wells, and Manzanita Limestone Members of the Cherry Canyon Formation (figure 1.3) were also recognizable in the southern part of the Delaware Mountains. He also stated that strata age equivalent to the Hegler Limestone Member, the lowest named member of the Bell Canyon Formation (figure 1.3), are also present in the southern part of the Delaware Mountains. He further concluded the contact between strata of the

uppermost age equivalent Manzanita Limestone Member of the Cherry Canyon Formation and the overlying siltstone/sandstone underlying the Hegler Limestone Member of the lower part of the Bell Canyon Formation is present in the southern part of the Delaware Mountains. McNutt (1948) incorrectly inferred that the capping limestone (an extensive debris flow) seen along the ridges in the southern part of the Delaware Mountains belonged to the Rader Limestone Member of the Bell Canyon Formation (figure 1.3) as originally described in the Guadalupe Mountains. Using biostratigraphic analysis of the conodont succession in strata present in a road cut along Texas FM road 2185 (figure 1.6), this observation was discredited by Kennedy (2009) and Nestell and Wardlaw (2010), who considered that this debris flow, now called the B-debris, belongs to an older age rock unit of the Bell Canyon Formation, and is equivalent in age to the Pinery Limestone Member (figure 1.3). The latter locality is located in a heavily faulted transitional zone between the Apache and Delaware Mountains. Major objectives of the present study were to map exposures of the B-debris (as seen in figure 1.6) north-northwest into the southern part of the Delaware Mountains and to find a well exposed section to measure and describe (the WP-section) (figures 1.7 and 2.1), to use it as a reference stratigraphic section for the southern part of the Delaware Mountains. Ultimately, the careful description of the WP-section will allow its use as a tool to identify similar stratigraphic sequences to the east and north-east, and over to the Texas FM road 2185 area.

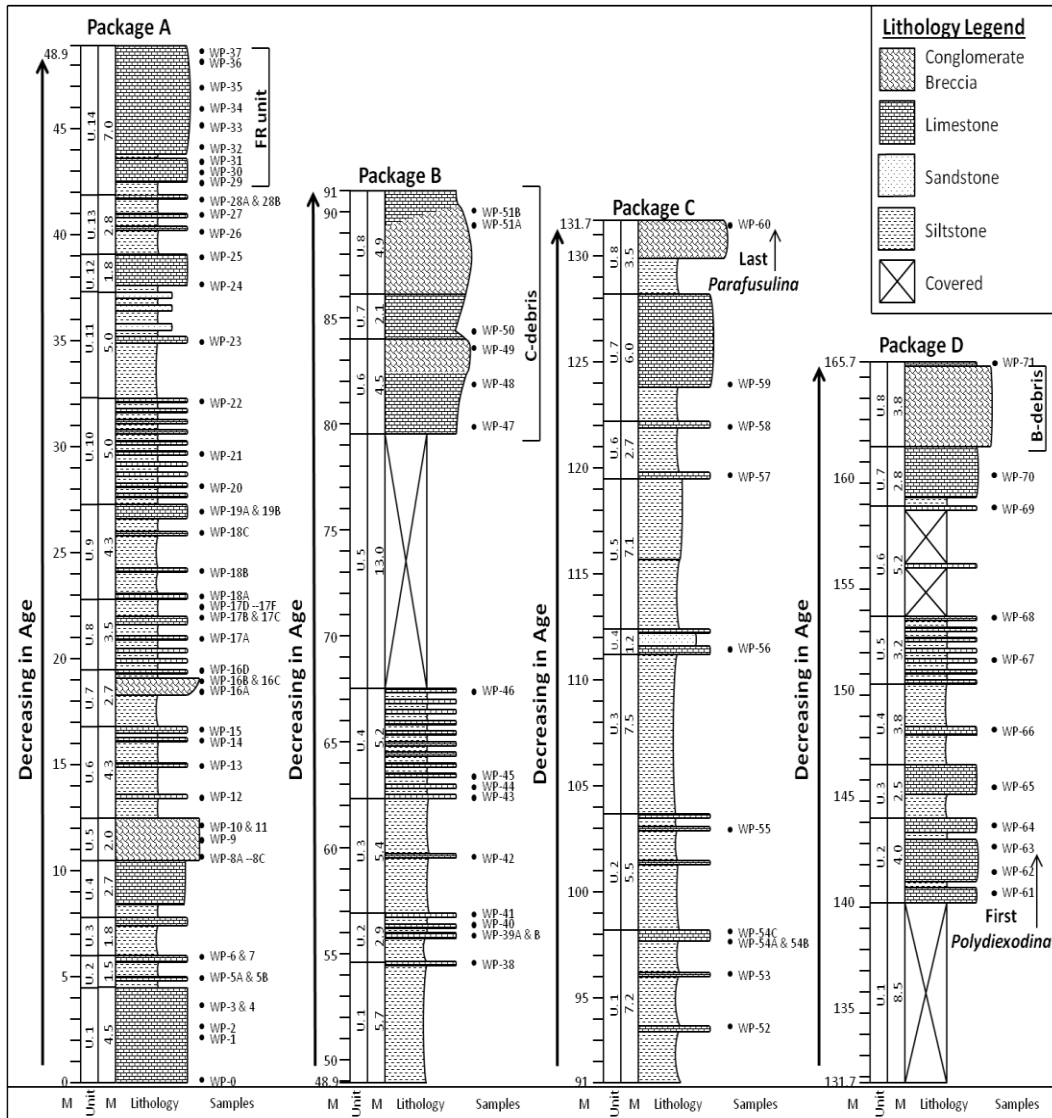


Figure 2.1: Stratigraphic column of the reference WP-section for the southern part of the Delaware Mountains showing oldest to youngest units in ascending order.

2.2 Cherry Canyon Formation

The Cherry Canyon Formation composes the middle part of the Delaware Mountains Group (figure 1.3) and was first named and described by King (1942) for exposures in a shallow canyon in the northern part of the Delaware Mountains.

King (1942) described the Cherry Canyon Formation to be siltstone/sandstone interbedded with three prominent limestone beds given member names, from oldest to youngest: Getaway, South Wells, and Manzanita Limestone Members. As previously mentioned, McNutt (1948) considered these members of the Cherry Canyon Formation to be present as equivalent aged exposed rocks in the southern part of the Delaware Mountains. The study of McNutt (1948) used limited biostratigraphic methods to help define his lithologic boundaries on the western flank of the southern part of the Delaware Mountains facing the Salt Flats (figure 1.2). For the purpose of this study, the youngest and upper-most strata considered as age equivalent to the Manzanita Limestone Member of the Cherry Canyon Formation can be identified in the WP-section by identifying the last occurrence of the fusulinaceans genus *Parafusulina* and species *Leëlla fragilis* (Dunbar and Skinner, 1937), as identified in the Guadalupe Mountains area.

2.3 Bell Canyon Formation

The Bell Canyon Formation of the upper part of the Delaware Mountain Group (figure 1.3), was first named and described by King (1942) for exposures located a few miles northeast of Guadalupe Peak along the U.S. Highway 62 in the Guadalupe Mountains. King (1942) described the Bell Canyon Formation as siltstone/sandstone interbedded with limestone beds. Six of the prominent limestone beds have been given member names. These are from oldest to youngest the Hegler, Pinery, Rader, and McCombs Limestone Members (King,

1942), Lamar Limestone Member (Lang, 1937), and Reef Trail Limestone Member (Wilde et al., 1999) (figure 1.3). McNutt (1948) considered the lower part of the Bell Canyon Formation to be present as equivalent aged exposed rocks in the southern part of the Delaware Mountains as to those identified in the Guadalupe Mountains. The study of McNutt (1948) used limited biostratigraphic methods to identify the lower lithological boundary of the Bell Canyon Formation on the western flank of the southern part of the Delaware Mountains just to the east of the Salt Flats (figure 1.2). In this study strata considered as age equivalent to the Hegler Limestone Member of the Bell Canyon Formation is present in the WP-section as identified by the first occurrence of fusulinacean *Polydiexodina*, as is also used in the Guadalupe Mountains area. The underlying siltstone/sandstone sequence of several meters with some thin limestone beds are considered to belong to the lowermost part of the Bell Canyon Formation and to have been deposited above the Manzanita Limestone Member of the Cherry Canyon Formation.

2.4 WP-Section

The WP-section is a 165.7 meter thick stratigraphic section measured and sampled for this study (figure 2.1). The base of the WP-section is located at the southwestern end of Scott Canyon where the base is at 31.358514 N, 104.606519 W (figure 1.7). An unnamed dirt road, which connects to Jay-Capp road, leads to an old well pad site close to the WP-section. The WP-section is located just to the

south of the old well pad site on the west flank of Scott Canyon and is in the third drainage wash coming down from the flank (figure 1.8). Measurements and sample collection began in the drainage wash, with the first in place exposed limestone. The WP-section ends at the top of the hill where less than a meter of exposed strata is present on top of the B-debris.

The WP-section is for the most part composed of beds of siltstone, sandstone, and limestone. The siltstone and sandstone intervals are usually fossil poor and have carbonate cement, but also have rare lag deposits comprised of mostly fusulinids of the genus *Parafusulina* in the lower part and *Polydiexodina* in the upper part of the section. The limestone lithofacies varies from mudstone with radiolarians and sponge spicules to megabreccia with algae, foraminifers, crinoids, echinoid spines, rugose corals, bryozoans, mollusks, ammonoids, and brachiopods.

Three distinct beds can be mapped in the area along the local ridges; in order of oldest to youngest: the FR unit, C-debris, and the B-debris (figure 2.1). The FR unit is generally about 7 meters thick as extended laterally, and is located about 42 meters from the base in the measured section. It is a fusulinid (*Parafusulina*) rich wackestone to packstone with some mudstone. The C-debris is located approximately 80 meters from the base of the measured section and is 11.5 meters thick. It also can be traced laterally with varying thickness from the measured section. The megabreccia B-debris is 3.6 meters thick near the top of

the measured section at approximately 162 meters from the base. The beds directly below the B-debris contain the fusulinid genus *Polydiexodina*, which is an index-fossil of the Bell Canyon Formation in the Guadalupe Mountains area and occur in the Hegler, Pinery, Rader, and McCombs Members. The occurrence of *Polydiexodina* in these beds below the B-debris suggest that at least those beds and those deposited above in some areas in the study area are age equivalent to the lower part of the Bell Canyon Formation. This measured section is significant in that it represents an age equivalent continuous section of the upper part of the Cherry Canyon Formation and the lower part of the Bell Canyon Formation in the southern part of the Delaware Mountains.

This WP-section located in the southwestern part of the Delaware Mountains of West Texas is significant because it contains a microfossil succession in strata of Middle to Late Guadalupian age that can be directly correlated to equivalent age strata present in the upper part of the Cherry Canyon Formation and the lower part of the Bell Canyon Formation in the Guadalupe Mountains.

The correlation of the transitional strata of the Cherry Canyon and Bell Canyon Formations in the Guadalupe Mountains to equivalent age strata in the southernmost part of the Delaware Mountains is done by biostratigraphic correlation because of differences in the lithofacies between the two areas. Biostratigraphic correlations can be made by using several key microfossils

present in Cherry Canyon and Bell Canyon age strata in both the southern part of the Delaware and Guadalupe Mountains, such as the fusulinacean genera *Parafusulina*, *Leëlla*, *Codonofusiella*, and *Polydiexodina*.

The fusulinacean genus *Parafusulina*, a key microfossil for the Cherry Canyon Formation, is abundantly present in the WP-section up from the base at sample WP-1 up to sample WP-60 (figure 2.1). Species of this genus are mentioned by Dunbar and Skinner (1931; 1937) and McNutt (1948) as found in the top of the Cherry Canyon Formation within the Manzanita Limestone. This genus is the primary constituent in the FR unit and is also present in most of the wackestone and packstone beds; it is also present in lag deposits in the siltstone and sandstone packages. The fusulinacean species *Leëlla fragilis* is found in the Cherry Canyon Formation, whereas species *Leëlla bellula* is found in the Bell Canyon Formation (Dunbar and Skinner, 1937). As noted above the fusulinacean genus *Polydiexodina* is a key microfossil for the lower part of the Bell Canyon Formation as it marks the presence of strata equivalent in age to the Hegler Member of the Bell Canyon Formation in the Guadalupe Mountains area. The fusulinacean genus *Polydiexodina* first appears in sample WP-63 approximately 143 meters from the base of the WP-section (figure 2.1).

2.5 Package A

Unit 1 of Package A is a 4.5 meter thick wavy nodular limestone unit with some intervals of laminated limestone beds with interbedded darker colored

limestone lenses; the lower contact is obscured by vegetation (figure 2.2 (A and B)). Five samples were taken

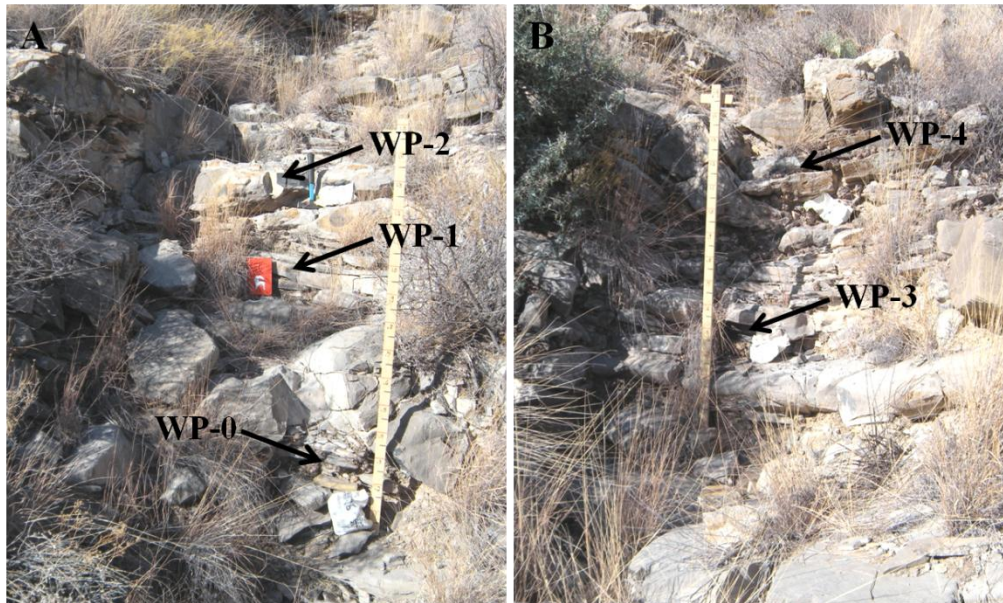


Figure 2.2: Photographs (A) and (B) of Package A, unit 1; showing where samples WP-0 through WP-4 were collected.

from the unit. Bed with sample WP-0 is a spiculitic carbonate mudstone, dark brown, weathers grey and contains small foraminifers, sponge spicules, rare ostracodes, and rare medium sized angular lithoclasts (figure 2.3 (A)). Sample WP-1 was taken from thin fusulinid/bryozoan packstone lens present in the middle part of the unit and is a poorly sorted biosparite, approximately 10x40 cm that is brown and weathers grey with *Parafusulina*, echinoid spines, rare small foraminifers, and small ammonoids. At the base of the thin section from the

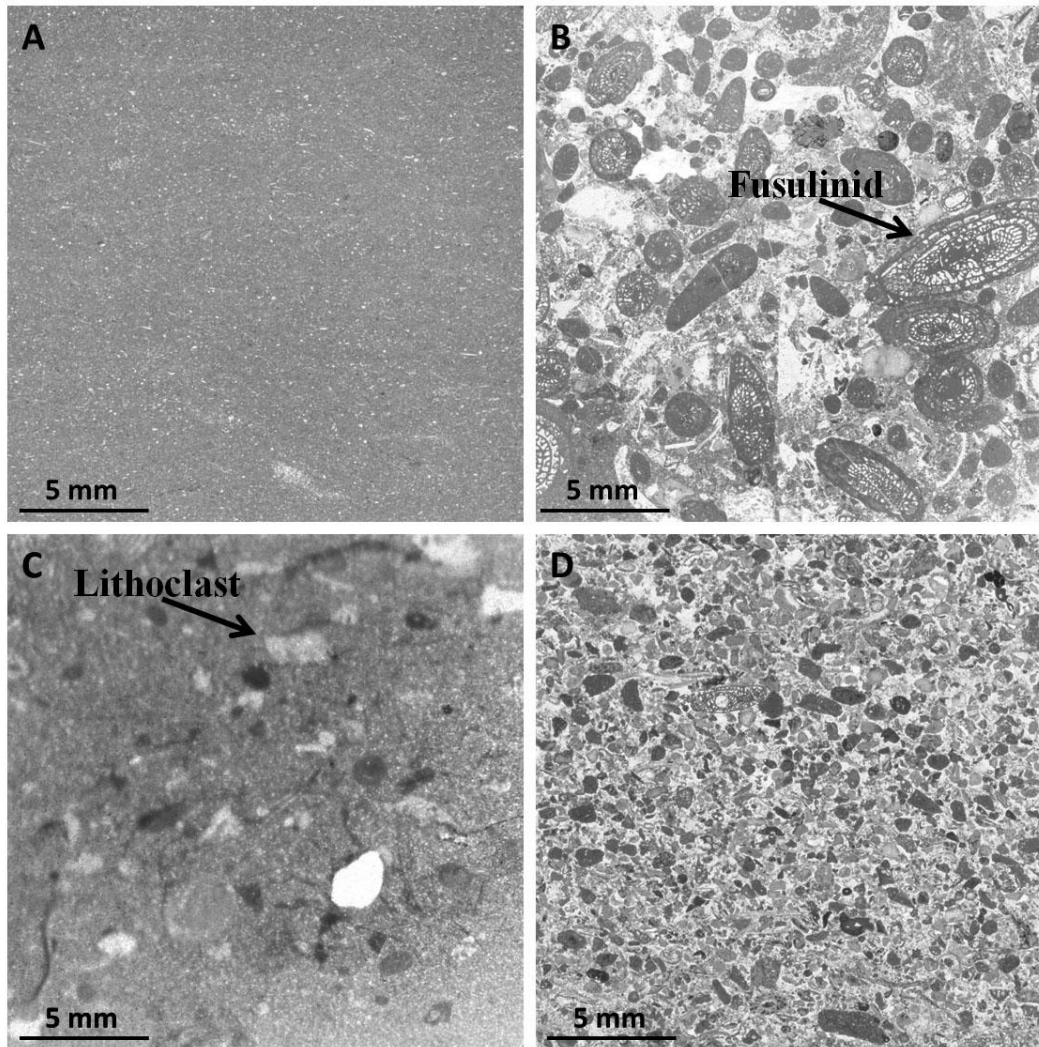


Figure 2.3: Thin sections of Package A, unit 1 (A) and (B); unit 2 (C) and (D) showing the texture of the rock samples. (A) is sample WP-0 of a spiculitic carbonate mudstone; (B) is sample WP-4 of a fusulinid/bryozoan packstone where the fusulinids are of the genus *Parafusulina*; (C) is sample WP-5B of a wackestone with lithoclasts; and (D) is sample WP-7 of a fine- to medium grained packstone.

sample there is a transitional contact from the underlying mudstone into the packstone. Bed with sample WP-2 (a nodule in the middle part of the unit) is dark brown and weathers grey, a sponge spicule mudstone with scattered small

foraminifers and ostracodes. Bed with sample WP-3 is a sponge spicule mudstone; brown with wavy black laminations and weathers light grey; bed contains a few small foraminifers. One of the lenses in the upper part of sample WP-4 has a very similar texture to sample WP-1 (figure 2.3 (B)).

Unit 2 is a 1.5 meter thick and mostly consists of siltstone with its lower contact irregular; unit also includes two limestone beds with the thin-bedded lower limestone and the medium-bedded upper limestone capping the unit (figure 2.4). The siltstone is very fine-grained; weathers light grey with tan patches.



Figure 2.4: Photographs of Package A, unit 2; showing where samples WP-5A and 5B were collected in the lower part and where samples WP-6 and 7 were collected in the upper part of the unit. Strata above sample WP-7 belongs mostly to unit 3 and the lower part of unit 4.

Lower limestone bed samples WP-5A and 5B are a mudstone and grade upward into a wackestone; parts of the wackestone contain 5% to 10% fine- to medium-grained scattered angular quartz grains in the matrix; dark brown and weathers grey with lithoclasts that are very coarse sized, subrounded to angular; contains small foraminifers, fusulinids (*Parafusulina*), ostracodes, *Tubiphytes*, and sponge spicules found in mudstone clasts (figure 2.3 (C)). Upper limestone bed samples WP-6 and WP-7 are a packstone with some sparite and coarsens upwards into a much finer packstone; brown to dark grey, weathers light grey with some orange streaks and a few vugs; angular to subrounded lithoclasts, some silicified, and are fine to very coarse sized debris; contains small foraminifers, fusulinids (*Parafusulina*), echinoid spines, crinoids, brachiopods, bryozoans, and mollusk fragments (figure 2.3 (D)).

Unit 3 is 1.8 meters with no samples taken; unit is mostly a siltstone with vegetation and rock debris scattered over the exposure and a medium-bedded limestone bed topping the unit; the lower contact of the unit is sharp (figure 2.4). The siltstone bed is very fine-grained; weathers light grey. The uppermost limestone bed weathers dark grey and is partially covered by debris.

Unit 4 is 2.7 meters with no samples taken; the lower part is a siltstone; weathers light grey with a very thick limestone bed in the middle and upper parts; lower contact of the unit is sharp. The limestone has sparse fusulinids visible to

the naked eye at the top of the exposed bed. Unit is mostly covered by vegetation and rock debris.

Unit 5 is 2.0 meter thick debris and sampled in the lower, middle, and upper parts with six random samples taken; unit is slightly wavy bedded; brown, weathers grey; lower contact of the unit is irregular (figure 2.5). The lower part

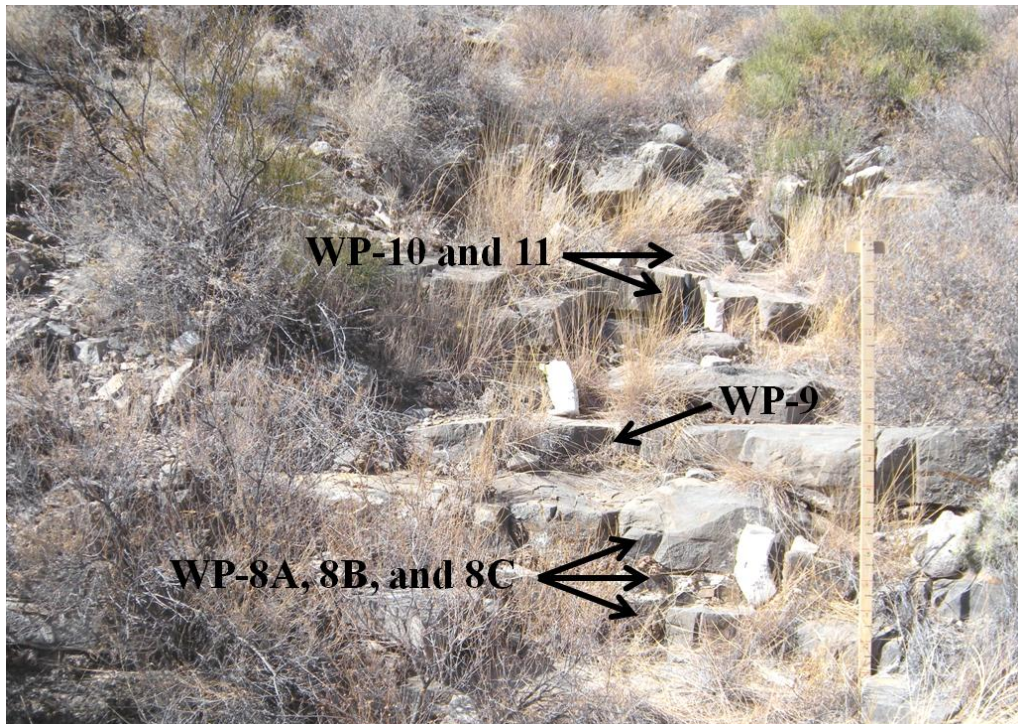


Figure 2.5: Photograph of Package A, unit 5; showing where samples WP-8A through WP-11 were collected.

samples WP-8A, 8B, and 8C were taken to show the diversity of the debris textures present. Rock sample WP-8A is a quartzose fusulinid/bryozoan packstone with 20% quartz grains, medium- to coarse-grained, poorly sorted, subrounded to angular; coarsens upwards; contains *Parafusulina*, small foraminifers, brachiopods, crinoids, and medium to coarse sized lithoclasts (figure

2.6 (A)). Directly above the rock with sample WP-8A is a rock where sample WP-8B was collected is quartzose wackestone with some lag deposits of

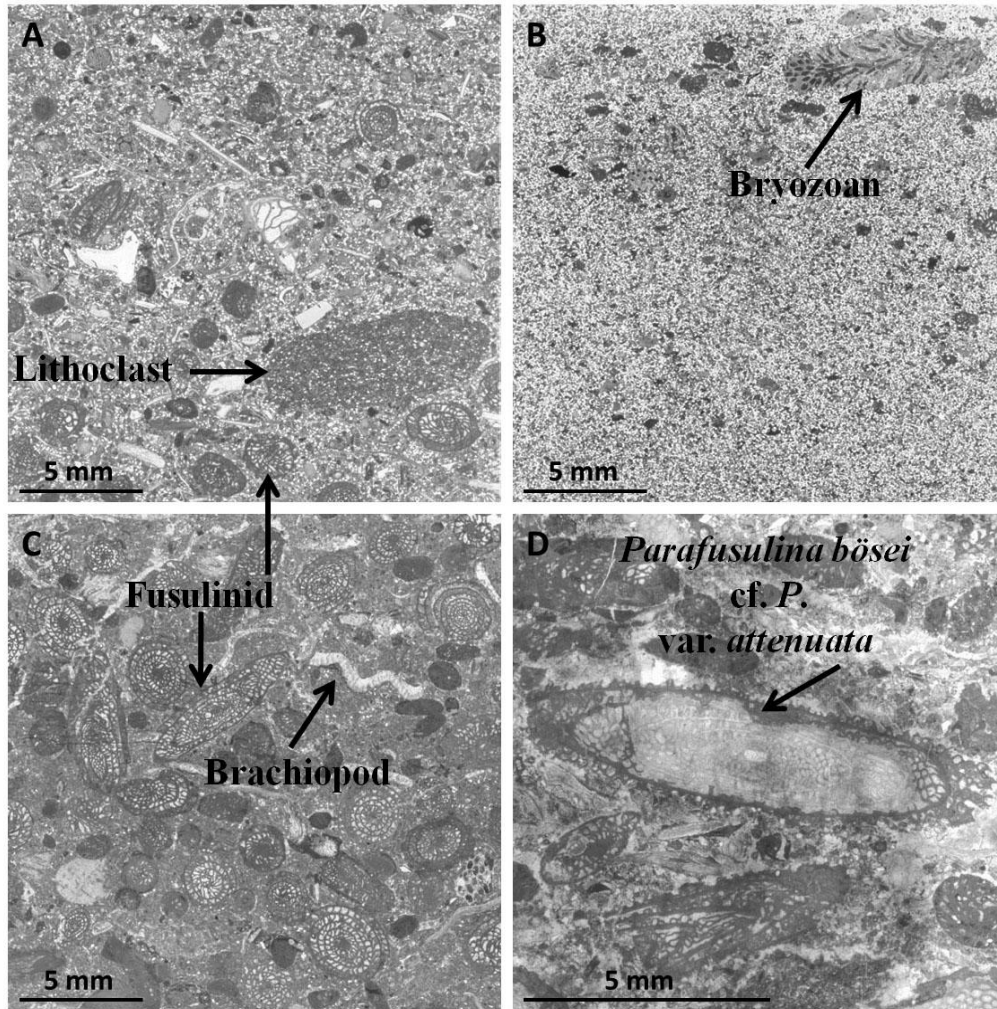


Figure 2.6: Thin sections (A), (B), (C), and (D) of Package A, unit 5; showing the texture of the rock samples. (A) is sample WP-8A of a quartzose fusulinid/bryozoan packstone with variable sized lithoclasts; (B) is sample WP-8B of a quartzose wackestone with lag deposits in the upper part; (C) is sample WP-10 of a fusulinid packstone with brachiopod fragments; and (D) is sample WP-11 of a fusulinid packstone with a partially silicified axial section of *Parafusulina* cf. *P. bösei* var. *attenuata* (Dunbar and Skinner, 1937).

fragmented fossil constituents; quartz grains are medium- to coarse-grained, well sorted, subrounded to angular (figure 2.6 (B)); fossil fragments consist of bryozoans, echinoid spines, crinoids, and some fusulinids (*Parafusulina*) in the lower part of the thin section. Rock sample WP-8C is a quartzose bryozoan packstone with slightly more mud; contains small foraminifers, fusulinids (*Parafusulina*), brachiopods, and medium to coarse lithoclasts; one of the lithoclasts was recognized as ripped up piece from the rock with sample WP-8B. Sample WP-9 was taken in the middle part of the unit and is quartzose sandstone that grades upwards into a packstone; contains brachiopods, bryozoans, and some fusulinids (*Parafusulina*). Rock sample WP-10 was taken in the upper part of the debris and is a fusulinid packstone (figure 2.6 (C)), poorly sorted with some sparite, more mud and no quartz grains unlike the lower samples of the unit; contains *Parafusulina*, algae, brachiopods, few small foraminifers, and fewer algal coated grains. Rock sample WP-11 was taken from the uppermost part of the debris and is a fusulinid packstone very similar in texture to sample WP-10 only with less mud. The fusulinids (*Parafusulina* cf. *P. bösei* var. *attenuata* (Dunbar and Skinner, 1937)) are partially silicified (figure 2.6 (D)).

Unit 6 is a 4.3 meter thick partially covered siltstone with four thin to thick limestone beds; lower contact is irregular (figure 2.7). Siltstone weathers light grey with tan to somewhat orange patches within the upper part of the siltstone. The lowest limestone (sample WP-12) is a carbonate mudstone; brown

in the lower part and dark brown in the middle and upper parts, weathers grey; contains small foraminifers, silicified and un-silicified fusulinids (*Parafusulina*), sponge spicules, and ostracodes in the lower part; rock appears banded with

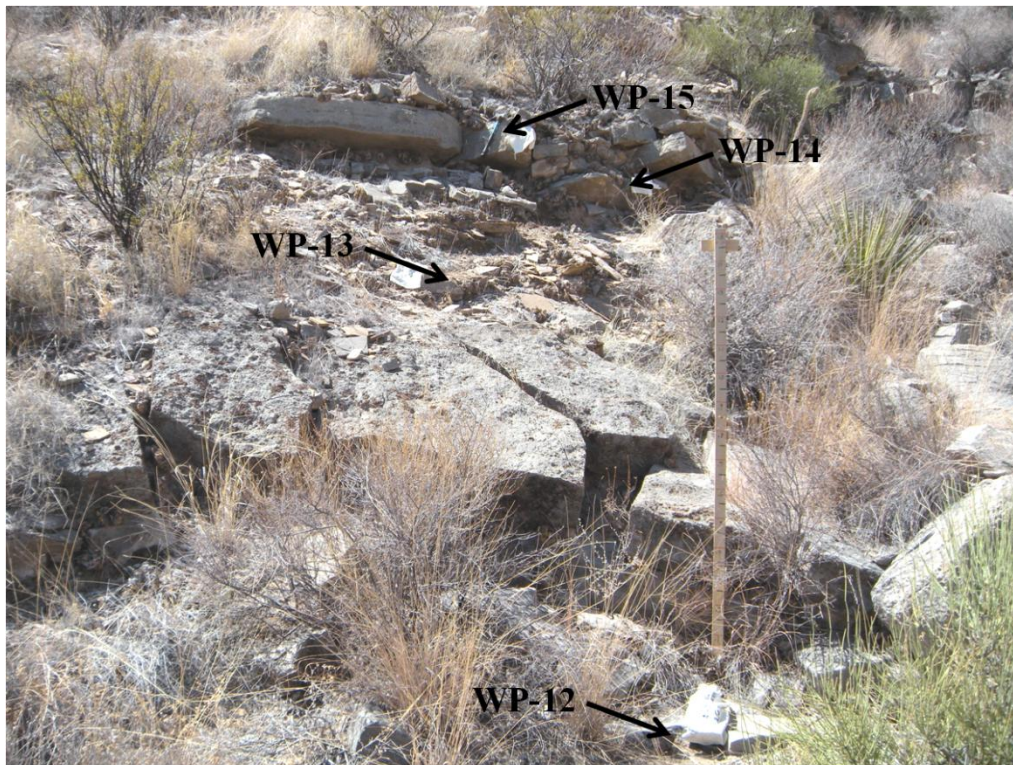


Figure 2.7: Photograph of Package A, unit 6; showing where samples WP-12 through WP-15 were collected.

scattered angular pyrite grains, and some sparite filled very coarse vugs. The second limestone (sample WP-13) is a fusulinid packstone; brown to grey, weathers grey; contains silicified and un-silicified *Parafusulina*, brachiopods, bryozoans, *Tubiphytes*, ostracodes, gastropods, and rounded to subrounded mudstone lithoclasts (figure 2.8 (A)). The third limestone sample (WP-14) is a packstone with some sparite; light brown, weathers grey to light brown;

lithoclasts are medium sized, subangular to angular; contains fusulinids (*Parafusulina*), small foraminifers (*Geinitzina*), bryozoans, brachiopods, ostracodes, *Tubiphytes*, and is pelletoid (figure 2.8 (B)). The fourth and top

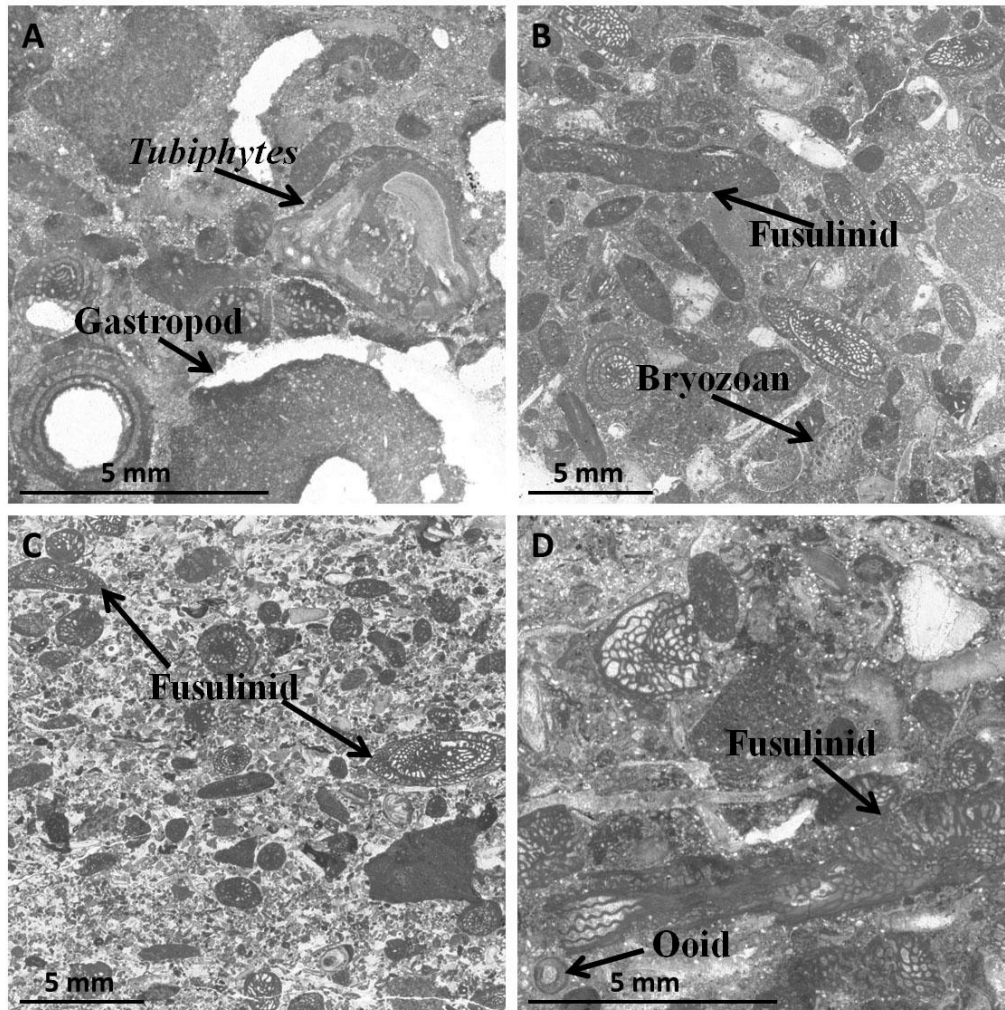


Figure 2.8: Thin sections of Package A, unit 6 (A) and (B); unit 7 (C) and (D) showing the texture of the rock samples. (A) is sample WP-13 of a fusulinid packstone with *Tubiphytes* and part of a large gastropod; (B) is sample WP-14 of a packstone with *Parafusulina* and other fossil fragments; (C) is sample WP-16A of a fusulinid packstone with a couple of oblique sections of *Parafusulina*; and (D) is sample WP-16D of a packstone with fusulinid fragments.

limestone in the unit (sample WP-15) is a fusulinid packstone with some silicification; grey, weathers light grey; contains *Parafusulina*, *Tubiphytes*, bryozoans, a few mollusk fragments, scattered ostracodes, and medium to coarse sized mudstone lithoclasts with pellets in some of the clasts; less than 5% quartz grains, medium to coarse-grained, very poorly sorted, angular quartz grains in lithoclasts.

Unit 7 is 2.7 meter thick with a lower 1.5 meter siltstone capped by an 80 cm limestone bed, overlain by siltstone with a medium limestone bed topping the



Figure 2.9: Photograph of Package A, unit 7; showing where samples WP-12 through WP-15 were collected.

unit; lower contact of the is sharp (figure 2.9). Siltstone is very fine-grained; weathers tan to light grey with a few very thin lenses of limestone in the upper part; weathers tan to light grey. The lowest part of the limestone bed (sample WP-16A) is a fusulinid packstone with little sparite; dark brown to grey, weathers grey; contains *Parafusulina*, echinoid spines, ostracodes, mollusks fragments, rare bryozoans, rare small ammonoids, subrounded to angular lithoclasts, and less than 5% quartz grains, medium to coarse-grained, poorly sorted, angular (figure 2.8 (C)). The lowest part of the limestone bed is overlain by debris with an irregular contact consisting of broken fossil fragments (sample WP-16B and 16C) (lower and upper part of the debris); dark brown to grey, weathers light grey; fines upward. Lower sample WP-16B of the debris contains medium to very coarse sized lithoclasts, fusulinids (*Parafusulina*), bryozoans, and brachiopods. Upper sample WP-16C of the debris has finer sized lithoclasts, fusulinids (*Parafusulina*), bryozoans, and scarce brachiopods. The upper limestone bed (sample WP-16D) topping the unit is a packstone; light brown to tan, weathers grey to light grey with scattered quartz grains; grades upwards into quartzose sandstone; the quartz grains are fine- to medium-grained, poorly to moderately sorted, subrounded to angular; contains fusulinids (*Parafusulina*), bryozoans, brachiopods, echinoid spines, scarce ooids, and medium to coarse sized subrounded to subangular lithoclasts (figure 2.8 (D)).

Unit 8 is a 3.5 meter thick partially siltstone and is interbedded in the lower part with thin to medium limestone beds; upper part has more siltstone with interbedded laminated limestone beds with a thick limestone bed in the upper part followed by more siltstone with more laminated interbedded limestone; lower contact is sharp (figure 2.10). Siltstone is very fine-grained; weathers light grey to tan. The lower two limestone beds were not sampled due to their similarity in the field to sample WP-17A. The limestone bed sample WP-17A is a wackestone;

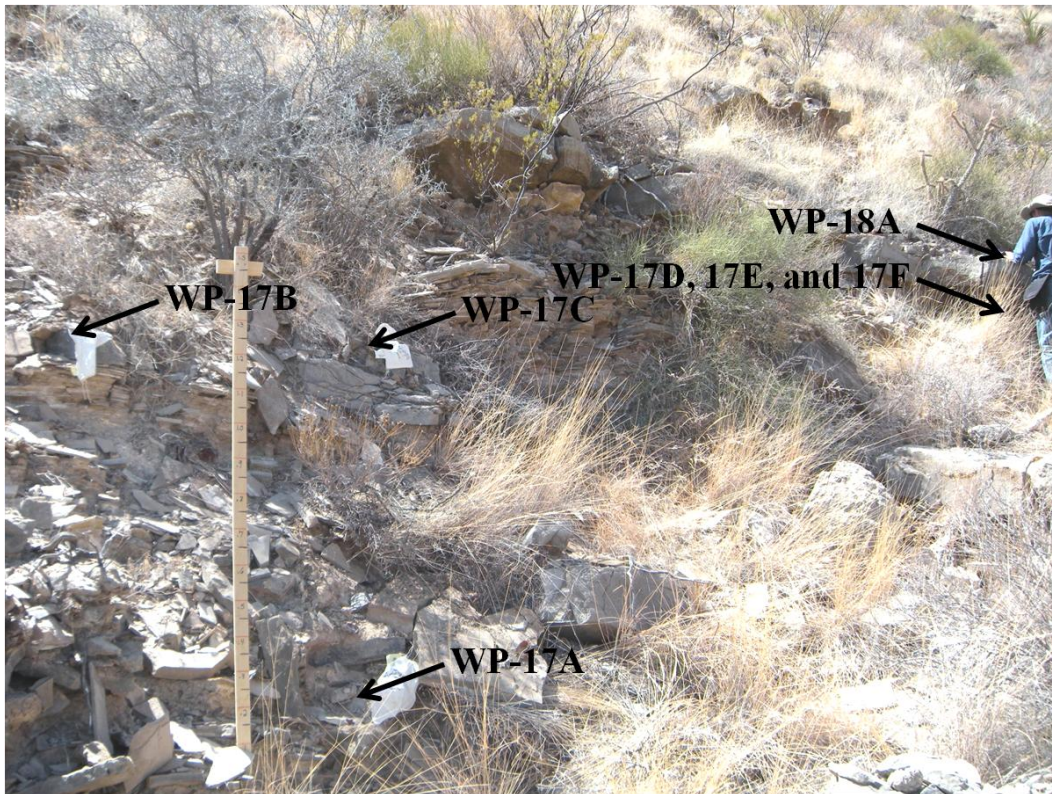


Figure 2.10: Photograph of Package A, unit 8; showing where samples WP-17A through 17F were collected. Unit 9 begins in the upper right-hand corner at sample WP-18A.

dark brown, weathers grey; contains *Parafusulina*, bryozoans, ostracodes, algae, mollusk fragments, medium sized lithoclasts, and less than 5% scattered quartz grains, medium- to coarse-grained, poorly sorted, angular. Mud matrix contains sponge spicules. Thick limestone bed (samples WP-17B and 17C) in the upper part of unit grades upward from a packstone (sample WP-17B) into a mudstone (sample WP-17C); dark brown to brown and weathers grey. The packstone (sample WP-17B) contains fusulinids (*Parafusulina*), bryozoans, brachiopods, scarce crinoids, algae, scarce rugose corals, and medium sized subrounded to angular lithoclasts (figure 2.11 (A)). The mudstone (sample WP-17C) grades with a sharp transition from dark brown to a light brown, sharp contrast of color (figure 2.11 (B)); lower and dark part of the sample contains sponge spicules, whereas the lighter upper part contains sponge spicules and rare ostracodes. The upper very thin limestone bed (sample WP-17D) is a mudstone, dark brown with light brown wavy laminations with sponge spicules, radiolarians, and less than 5% quartz grains, medium- to coarse-grained, very poorly sorted, angular; quartz grains are present in the light brown laminations. One of the sampled laminated limestone beds from the upper part of the unit is a wackestone (sample WP-17E) dark brown, weathers light grey; contains *Parafusulina*, brachiopods, rare small foraminifers, and medium sized lithoclasts. Second laminated limestone bed from the upper part of the unit is a fusulinid packstone (sample WP-17F) dark brown to brown, weathers light grey; contains *Parafusulina*, brachiopods, bryozoans,

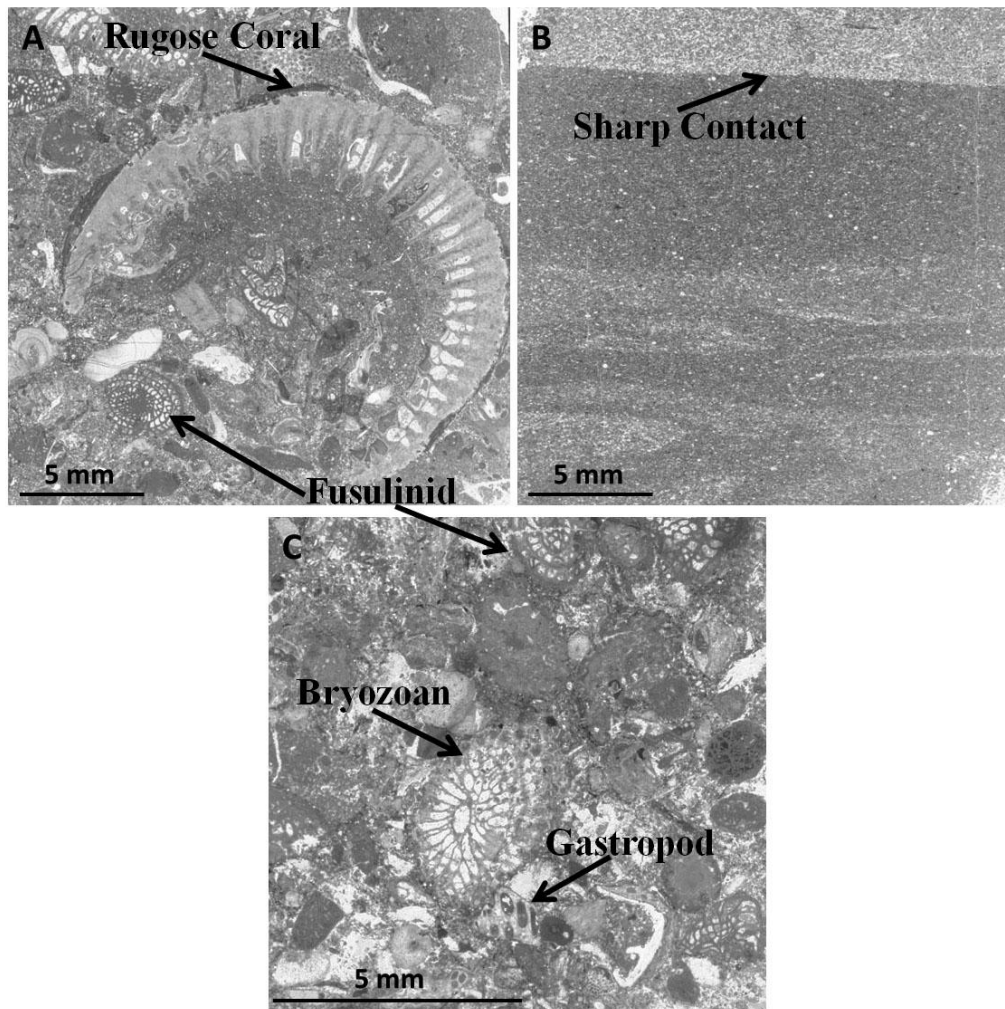


Figure 2.11: Thin sections of Package A, unit 8 (A), (B), and (C) showing the texture of the rock samples. (A) is sample WP-17B of a packstone with a rugose coral filled with micrite and other fossil fragments; (B) is sample WP-17C of a mudstone with a sharp contact; (C) is sample WP-17F of a fusulinid packstone with bryozoan and gastropod fragments and other fossil constituents.

Tubiphytes, echinoid spines, scarce gastropods, rare small foraminifers

(Palaeotextulariids), medium sized lithoclasts, and 5% quartz grains, medium- to coarse-grained, poorly sorted, angular (figure 2.11 (C)).

Unit 9 is 4.3 meter thick mostly siltstone with four medium to thick limestone beds; lower contact is sharp (figure 2.10 and 2.12). Siltstone weathers light grey when visible due to large pieces of rock debris and vegetation covering parts of the unit; upper siltstone is laminated and weathers tan with some thin limestone beds. Lowest limestone (sample WP-18A) is a 30 cm thick fusulinid wackestone/packstone; dark brown and weathers light grey with light brown

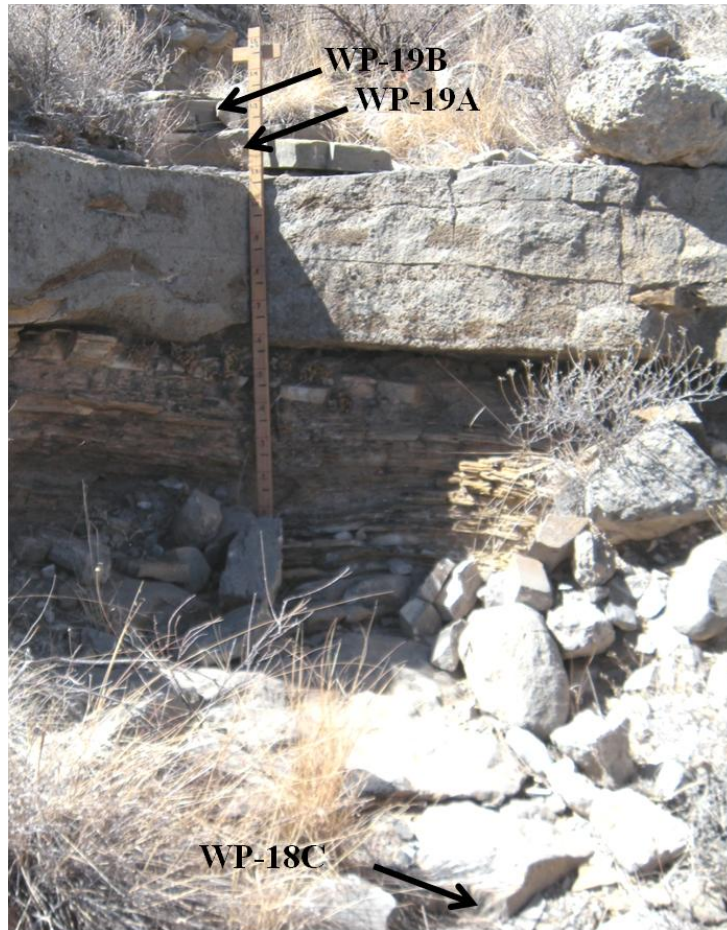


Figure 2.12: Photograph of Package A, unit 9; showing where samples WP-18B through 19B were collected from the upper part of the unit.

patches; contains *Parafusulina*, bryozoans, small foraminifers, rare *Tubiphytes*, ostracodes, scarce gastropods, very rare echinoid fragments, medium to coarse sized subrounded lithoclasts, and 5-10% quartz grains, fine- to medium-grained, poorly sorted, subrounded to angular (figure 2.13 (A)). The second limestone (sample WP-18B) is a pelletoid/fusulinid packstone, medium-bedded; dark brown and weathers light grey; contains *Parafusulina*, bryozoans, brachiopods, rare small foraminifers, scarce echinoid fragments, medium to coarse sized subrounded lithoclasts, and very few quartz grains, fine- to medium-grained, very poorly sorted, subrounded to angular (figure 2.13 (B)). The third limestone (sample WP-18C) is a coarse-grained wackestone, medium-bedded; dark brown to brown, weathers light grey; contains *Parafusulina*, bryozoans, brachiopod fragments, less than 5% pyrite, medium to very coarse sized subrounded to angular partially oriented lithoclasts, and less than 5% quartz grains, medium-grained, very poorly sorted, subrounded to angular. The fourth and top limestone in the unit (samples WP-19A and 19B) is 75 cm thick and samples were taken in the upper 30 cm; brown to light brown, weathers light grey to tan and then back to light grey. The lower part of the limestone bed is heavily weathered and difficult to sample; weathers light grey, bed has tan and light brown lithoclasts up to 35 cm across and up to 10 cm in height; some wavy bedding observed. The upper part (sample WP-19A) is a packstone; contains fusulinids (*Parafusulina*), brachiopods, bryozoans, *Tubiphytes*, echinoid spines, rare tiny foraminifers (Palaeotextularids),

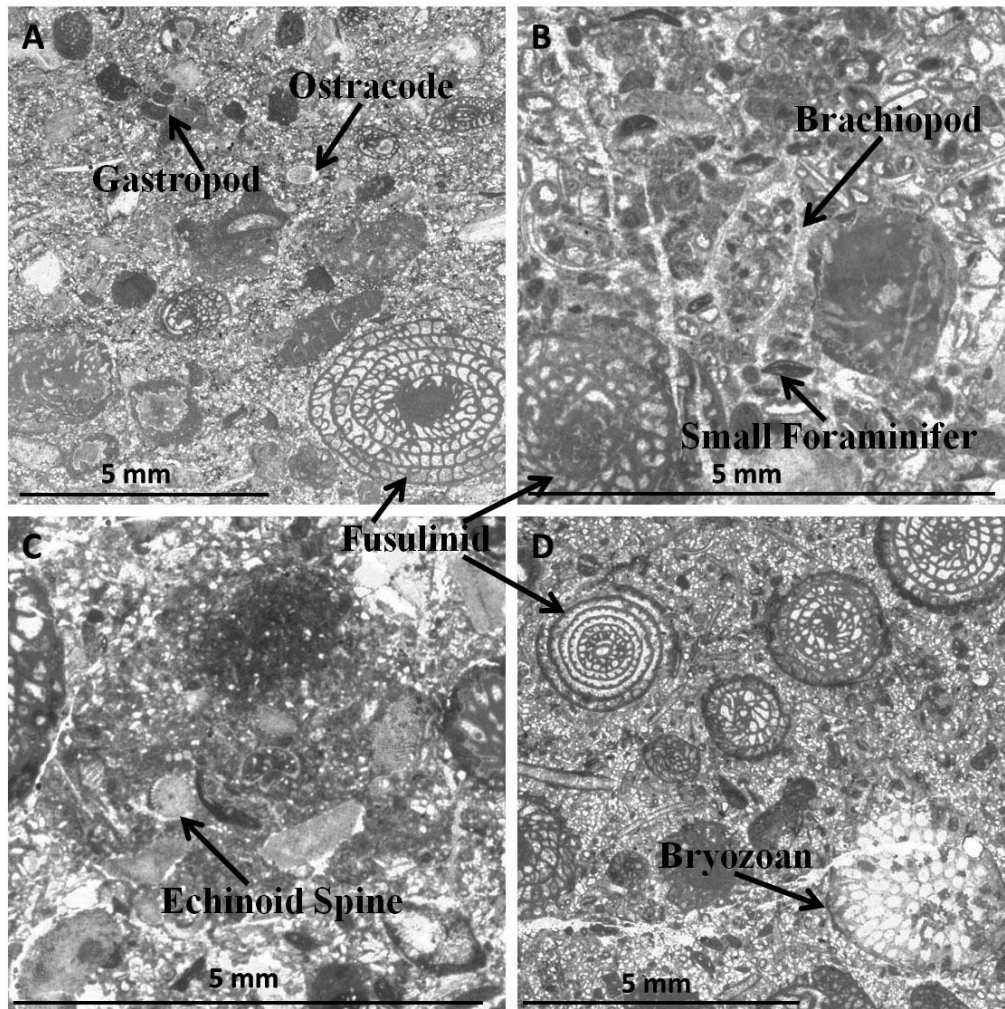


Figure 2.13: Thin sections of Package A, unit 9; (A), (B), and (C); unit 10 (D) showing the texture of the rock samples. (A) is sample WP-18A of a fusulinid wackestone/packstone with gastropod and ostracode labeled; (B) is sample WP-18B of a pelletoid/fusulinid packstone that has small foraminifers and brachiopod filled with micrite and pellets; (C) is sample WP-19A of a packstone with a section of a echinoid spine; and (D) is sample WP-21 of a quartzose fusulinid packstone with several equatorial sections of *Parafusulina* and bryozoan.

medium to very coarse sized subrounded to angular lithoclasts, and less than 5% quartz grains, medium-grained, very poorly sorted, subrounded to angular (figure 2.13 (C)). The uppermost part of the limestone (sample WP-19B) is a wackestone,

which fines upwards and sharply transitions into a mudstone with abundant very tiny foraminifers, sponge spicules, fusulinids (*Parafusulina*) in the lower part, brachiopods, rare bryozoans, and medium sized subrounded to angular lithoclasts.

Unit 10 is a 5.0 meter thick partially siltstone interbedded with multiple thin to medium limestone beds and a thin limestone bed capping the unit; lower contact of the unit is sharp (figure 2.14). The siltstone is very fine-grained;



Figure 2.14: Photograph of Package A, unit 10; showing where sample WP-20 was collected from the lower part of the unit. Lithology of the unit is of a siltstone interbedded by limestone that is similar throughout as the photograph presented.

weathers tan to light grey with some visible quartz grains in the lower part of the siltstone of the unit. Limestone beds were sampled in the lower, middle, and upper part of the unit. The lowermost limestone (sample WP-20) is a pelletoid

packstone; light brown to brown, weathers light grey; contains fusulinids (*Parafusulina*), bryozoans, small foraminifers, brachiopods, and medium sized subrounded lithoclasts. The middle limestone (sample WP-21) is a quartzose fusulinid packstone; light brown, weathers light grey; fine grades upwards; contains *Parafusulina*, mollusk fragments, brachiopods, gastropods, bryozoans, scarce small foraminifers, medium sized subrounded to angular lithoclasts, and 15-20% quartz grains, medium- to coarse-grained, moderate to well sorted, subrounded to angular (figure 2.13 (D)). The uppermost limestone (sample WP-22) is a quartzose packstone; light brown and weathers light grey; fines upwards; contains pellets, fusulinids (*Parafusulina*), mollusk fragments, few small foraminifers, scarce echinoid spines, medium sized subrounded to angular lithoclast, and 40% quartz grains, medium- to coarse-grained, moderate to well sorted, subrounded to angular.

Unit 11 is a 5.0 meter thick mostly siltstone partially covered with vegetation and rock debris with four medium to thick beds in the upper part; lowermost bed is a limestone and the upper three beds are sandstone with the uppermost sandstone topping the unit; lower contact of the unit is sharp (figure 2.15). Siltstone is very fine-grained and weathers tan with the lower part showing laminations. The lowest limestone(sample WP-23) is a quartzose packstone with some sparite; contains brachiopod and mollusk fragments, pellets, fusulinids (*Parafusulina*), scarce small foraminifers, few echinoid spines, scarce bryozoans,

medium to coarse sized subrounded to angular lithoclasts, and 30% quartz grains, medium to coarse-grained, moderate to well sorted, subrounded to angular (figure 2.16 (A)). The upper three beds are sandstone; weather tan and no samples were taken.

Unit 12 is 1.8 meter thick with a 30 cm thick siltstone in the lowermost part capped by a 1.5 meter thick limestone; lower contact of the unit is irregular



Figure 2.15: Photograph of Package A, unit 11 upper part; showing where sample WP-23 was collected. Samples WP-24 and 25 were collected from unit 12.

(figure 2.15). Siltstone is very fine- to fine-grained; weathers tan. The rock samples WP-24 was taken in the lower part of the limestone and is a quartzose wackestone; light brown, weathers light grey; grades upward with more mud in

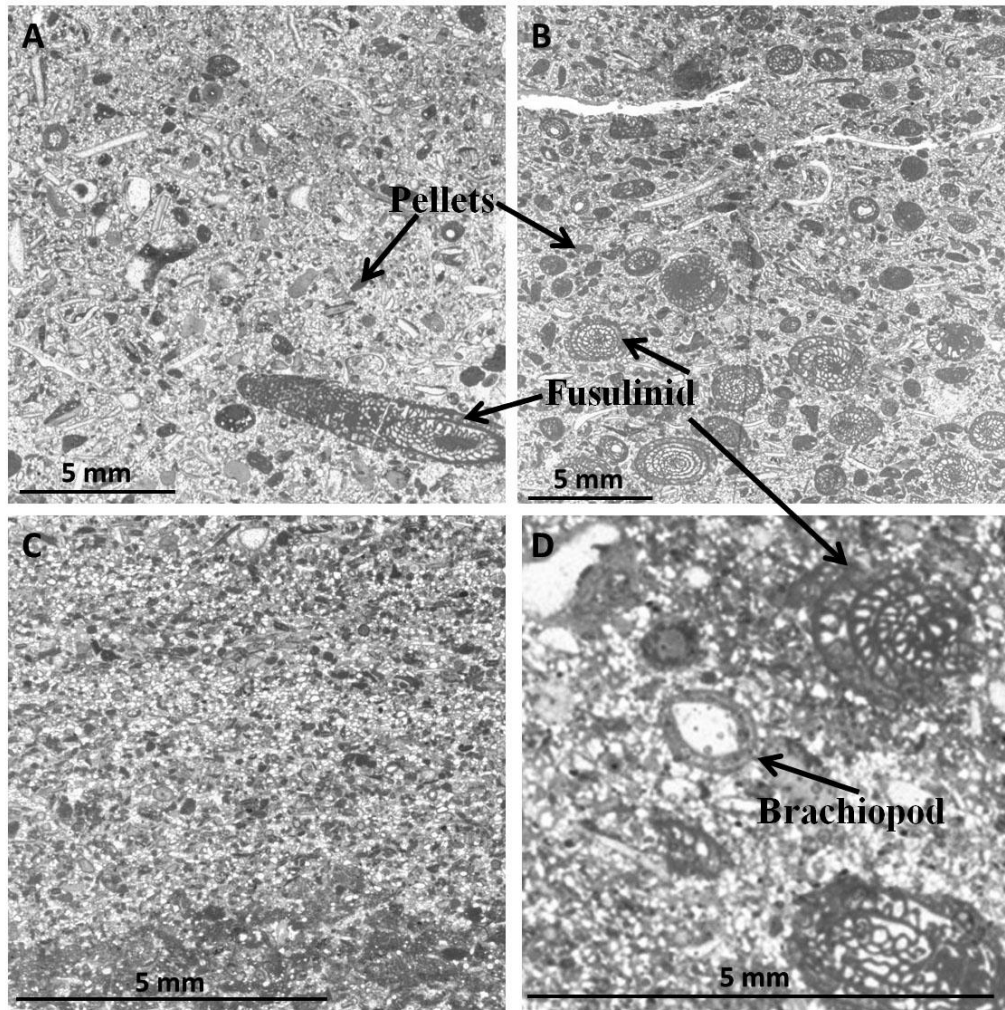


Figure 2.16: Thin sections of Package A, unit 11 (A); unit 12 (B) and (C); and unit 13 (D) showing the texture of the rock samples. (A) is sample WP-23 of a quartzose packstone with pellets and fusulinids; (B) is sample WP-25 of a quartzose fusulinid packstone that has abundant *Parafusulina*; (C) is sample WP-27 of a quartzose pelletoid packstone with a lamination transition in the lower part; and (D) is sample WP-28B of a wackestone with brachiopod that has an algal coating.

the lower part; contains scarce fragments of fusulinids (*Parafusulina*), more pellets in the lower part, medium sized subrounded to subangular lithoclasts, and 30-40% quartz grains, medium- to coarse-grained, moderate to well sorted, subrounded to angular. The rock sample WP-25 was taken in the upper part of the limestone and is a quartzose fusulinid packstone; light brown to light grey, weathers light grey; contains *Parafusulina*, pellets, brachiopod and mollusk fragments, small foraminifers, few echinoid spines, scarce crinoid fragments, medium to coarse sized rounded to angular lithoclasts, and 20-30% quartz grains medium- to coarse-grained, moderately sorted, subrounded to angular (figure 2.16 (B)).

Unit 13 is 2.8 meter thick mostly siltstone with two thin to medium limestone beds in the middle part of the unit separated by a 30 cm siltstone; unit is topped by a medium limestone bed; lower contact of the unit is irregular (figure 2.17 (A) and (B)). Siltstone is fine-grained; weathers light grey with silty platy laminations that weather tan. The lower limestone (sample WP-26) is a light brown quartzose pelletoid packstone with dark brown bands, carbonate packstone to wackestone; highly quartzose between the dark layers; weathers light grey to grey and is laminated; dark laminations contain small foraminifers and fragments of fusulinids, sponge spicules, ostracodes, scarce mollusk fragments, scarce medium sized angular lithoclasts, interlayer's contain 30-40% quartz grains, fine- to medium-grained, poorly to moderately sorted, rounded to subangular. The

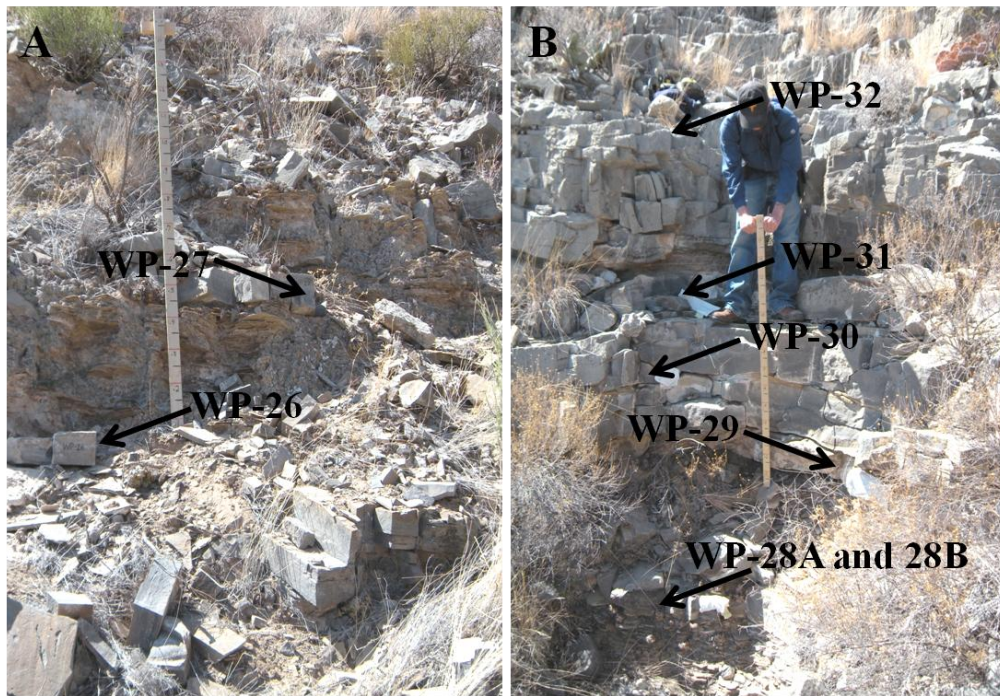


Figure 2.17: Photograph of Package A, unit 13 upper part; showing where samples WP-18A and 18B were collected, and the lower part of unit 14 (FR unit) where samples WP-29 through 32 were collected.

middle limestone (sample WP-27) is similar in texture to the lower sample WP-26 except it does not contain as many lithoclasts (figure 2.16 (C)). The bed topping the unit (samples WP-28A and 28B) in the lower part is approximately 5 cm thick quartzose sandstone; weathers tan; fine- to medium-grained, very well sorted with very few medium sized subrounded to subangular lithoclasts. Overlying with an irregular transitional contact is a 15 cm thick wackestone; dark brown, weathers grey; contains *Parafusulina*, silicified and non-silicified bryozoans fragments, scarce mollusk and brachiopod fragments, *Tubiphytes*, echinoid spines, rare crinoid fragments, medium sized subrounded to angular lithoclasts, and 10-15%

quartz grains, medium-grained, poorly to moderately sorted, subrounded to angular (figure 2.16 (D)).

Unit 14 is a 7.0 meter thick and tops Package A; unit is mostly limestone and informally named the FR unit with abundant visible fusulinids (*Parafusulina*). The unit begins with a 60 cm siltstone followed by a 1.1 meter limestone bed overlain by a 20 cm siltstone, and then topped by a 5.1 meter limestone; lower contact of the unit is sharp (figures 2.17 and 2.18). Both siltstone beds are fine-grained, weather light grey with containing some very thin beds of limestone; no samples taken. The lowermost part of the lower limestone bed (sample WP-29) is part wackestone/packstone in its lower part with an irregular transition into a mudstone; brown to dark brown, weathers tan to grey. The wackestone/packstone part contains fusulinids (*Parafusulina*), bryozoans, *Tubiphytes*, few echinoid spines, scarce crinoid fragments, medium to very coarse sized subangular to angular lithoclasts, and less than 5% quartz grains, medium- to coarse-grained, very poorly sorted, subrounded to angular. The mudstone part of rock sample WP-29 contains abundant sponge spicules and some quartz grains, medium-grained, very poorly sorted, subrounded to angular. The middle part of the lower limestone (sample WP-30) is a quartzose pelletoid packstone, quartz grains have a thin oolitic coating; brown, weathers grey; contains fusulinids (*Parafusulina*), few gastropods, scarce echinoid spines, medium sized subrounded to angular lithoclasts, and 10% quartz grains, medium- to coarse-grained, poorly

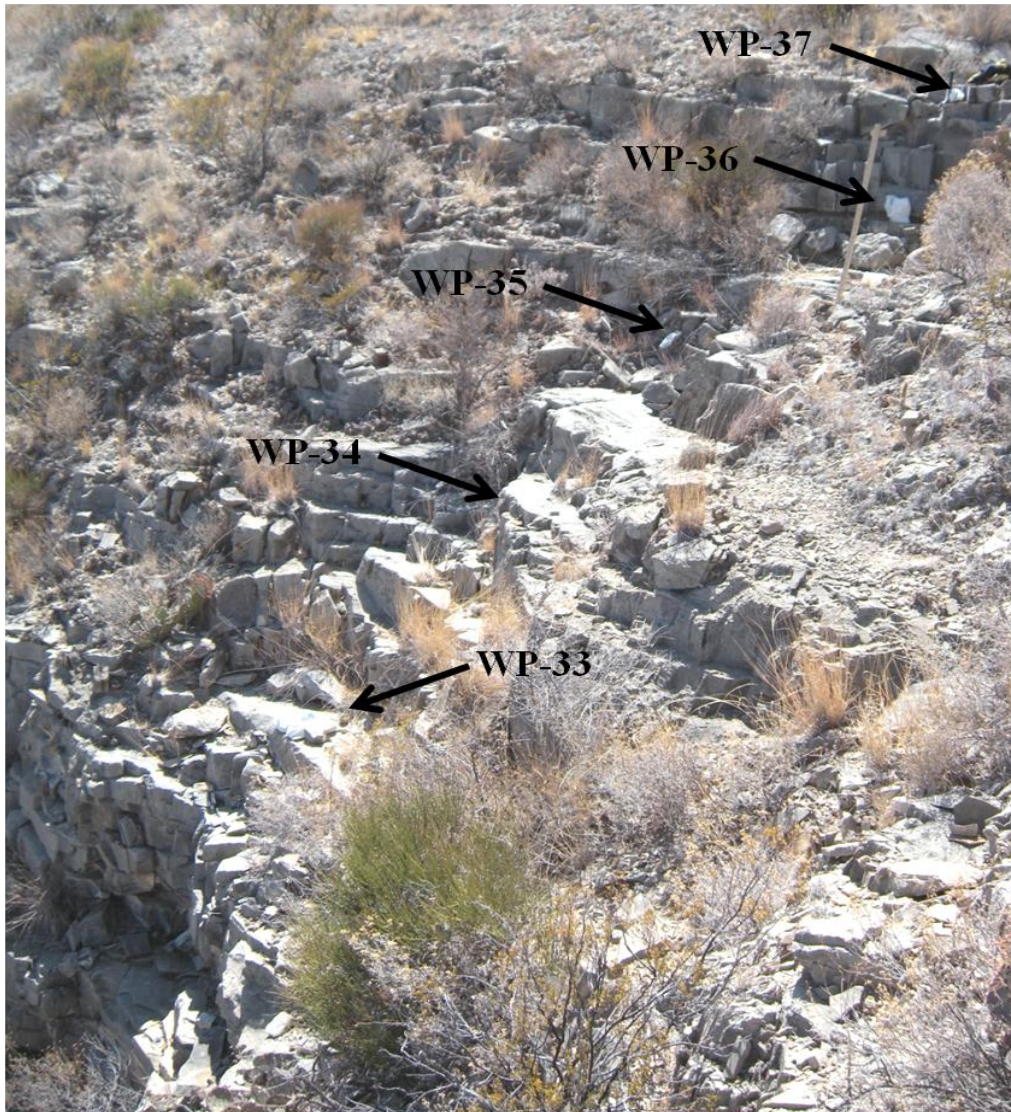


Figure 2.18: Photograph of Package A, unit 14 (FR unit), upper part; showing where samples WP-33 through 37 were collected; unit topping Package A.

to moderately sorted, subrounded to angular (figure 2.19 (A)). The upper part of the lower limestone (sample WP-31) is a pelletoid packstone; brown, weathers grey with small ooids, few small foraminifers, scarce fragments of fusulinids (*Parafusulina*), and less than 5% quartz grains, medium-grained, poorly sorted,

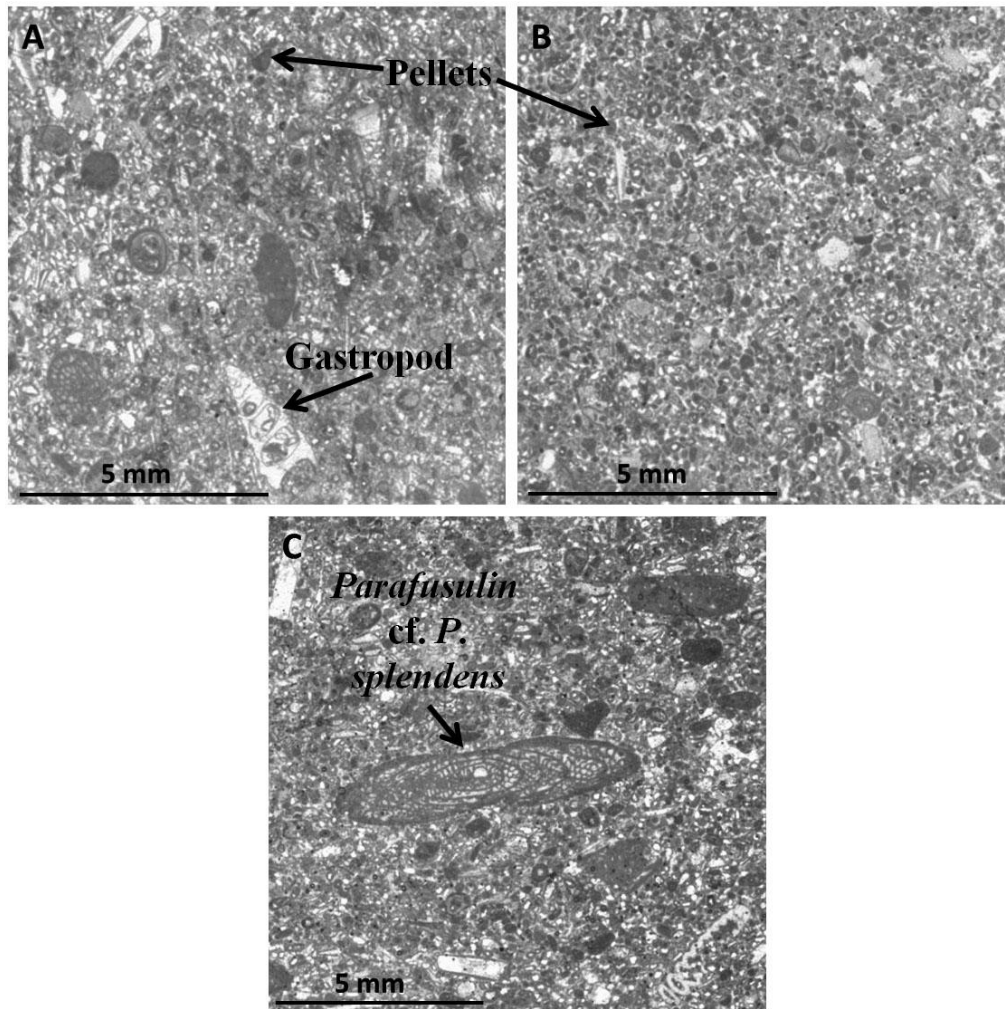


Figure 2.19: Thin sections of Package A, unit 14 (FR unit) (A), (B), (C) showing the texture of the rock samples. (A) is sample WP-30 of a quartzose pelletoid packstone with a small gastropod; (B) is sample WP-31 of a pelletoid packstone; and (C) is sample WP-32 of a quartzose pelletoid packstone with an oblique section of the fusulinid species *Parafusulina cf. P. splendens*.

subangular to angular (figure 2.19 (B)). Six samples were taken from the upper limestone sequence. The first sample WP-32 is similar in texture to sample WP-30 except it has less quartz grains, also contains mollusk fragments, and the fusulinid species *Parafusulina cf. P. splendens* (Dunbar and Skinner, 1937). The

quartz grains are coated and form the centers of ooids (figure 2.19 (C)). The second limestone sample WP-33 is a pelletoid packstone, some of the quartz grains are thinly coated; brown to light brown, weathers grey to light grey with very few small foraminifers, and less than 5% quartz grains, fine- to medium-grained, poorly sorted, subangular to angular. The third limestone sample WP-34 is similar in texture to sample WP-33 except it is light brown with scarce partially silicified and non-silicified fragments of fusulinids (*Parafusulina*). Quartz grains are slightly coated. The fourth limestone sample WP-35 is a sponge spicule rich carbonate mudstone; dark brown to brown to light brown, weathers dark grey to grey with some siliceous vugs near the bottom and has a dark brown band at the top containing small foraminifers (figure 2.20 (A)). The fifth limestone sample

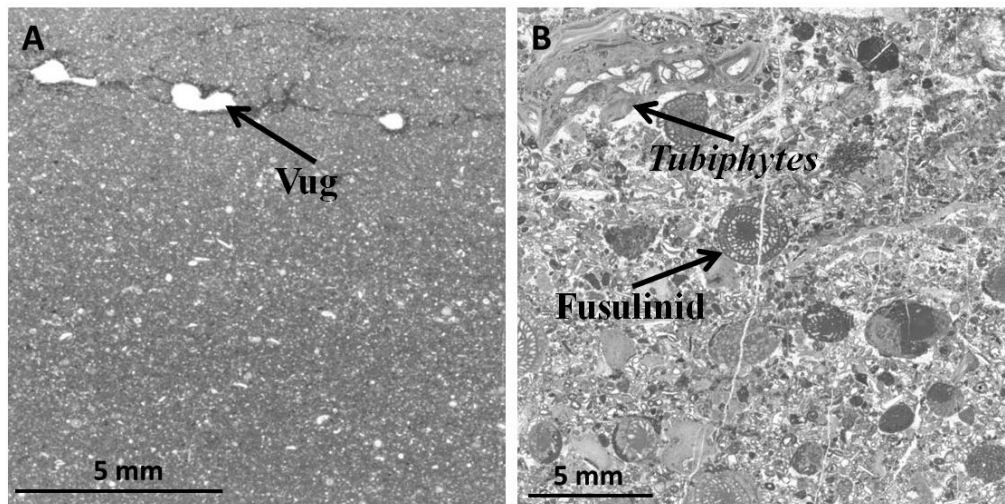


Figure 2.20: Thin sections of Package A, unit 14 (FR unit) (A) and (B) showing the texture of the rock samples. (A) is sample WP-35 of a sponge spicule rich carbonate mudstone with a sparite filled vugs; and (B) is sample WP-37 of a very coarse packstone with fusulinids, *Tubiphytes*, and other constituents.

WP-36 is a wackestone; dark brown, weathers grey; contains pellets, abundant small foraminifers, ostracodes, *Tubiphytes*, brachiopod fragments, medium to coarse sized subrounded to subangular and very dark brown lithoclasts, and less than 5% quartz grains not coated, fine- to medium-grained, very poorly sorted, subangular to angular. The uppermost limestone sample WP-37 is a very coarse packstone; brown to light brown, weathers grey to light grey; contains fusulinids (*Parafusulina*), bryozoans, *Tubiphytes*, mollusk and brachiopod fragments, and medium to very coarse subrounded to angular lithoclasts; some fragments are partially silicified (figure 2.20 (B)).

2.6 Package B

Unit 1 of Package B is a 5.7 meter thick mostly siltstone with a 20 cm thick limestone bed capping the unit; lower contact of the unit is sharp (figure 2.21). The siltstone is very fine- to fine-grained; weathers tan with some laminated silty limestone interbedded; partially covered by vegetation and rock debris. The capping limestone (sample WP-38) is a spiculitic carbonate mudstone with a top thin layer of quartzose grainstone (figure 2.22 (A)), medium- to coarse-grained, well sorted in thin layer, subangular to angular, and is 50% quartz grains and 50% carbonate fragments; brown to tan, weathers grey to light grey; contains scarce ostracodes and very rare quartz grains in the mudstone.

Unit 2 is a 2.3 meter thick mostly siltstone with three medium to thick limestone beds in the upper part of the unit with the uppermost limestone bed

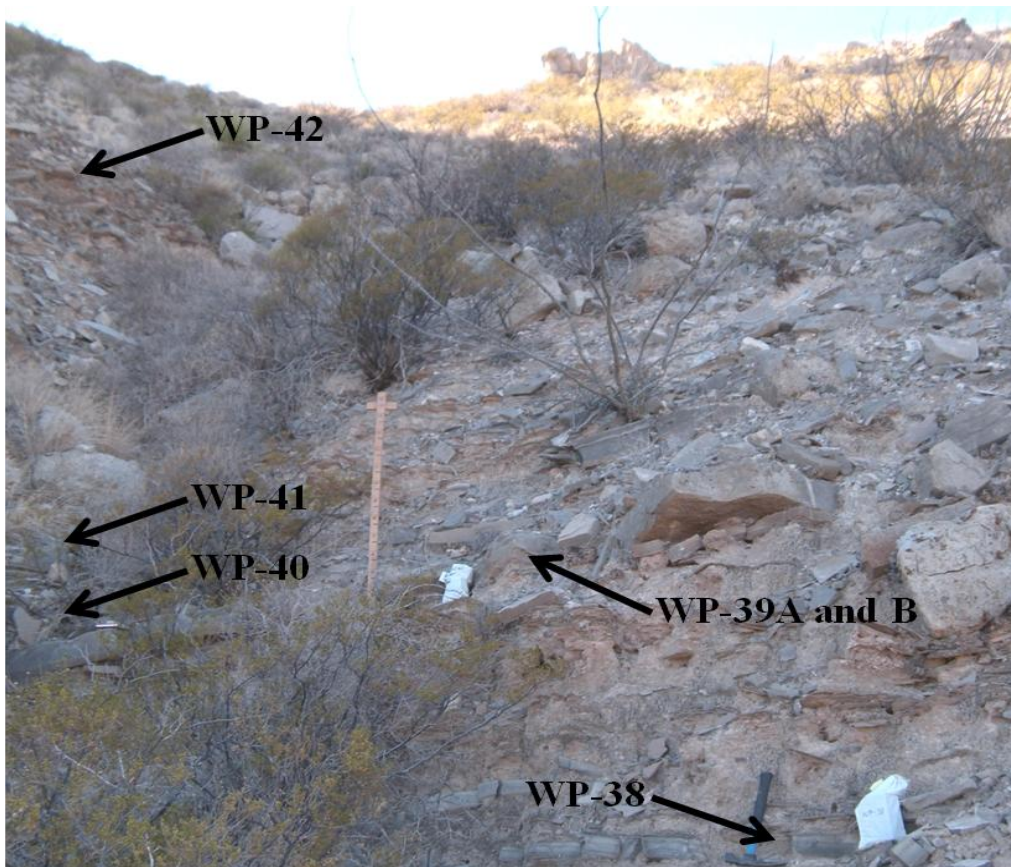


Figure 2.21: Photograph of Package B, unit 1 upper-most part; showing where sample WP-38 was collected. Samples WP-39A through 41 were collected from unit 2 and sample 42 from the middle of unit 3.

topping the unit; lower contact of the unit is sharp (figure 2.21). Siltstone is very fine- to fine-grained; weathers tan with some laminated silty limestone interbedded in the lower part with more laminated silty limestone in the upper part; partially covered by vegetation and rock debris in the lower part. The lower limestone (samples WP-39A and 39B) is a wackestone in the lower part and transitions into a packstone in the upper part; brown to dark brown, weathers light brown to grey with light grey pebbles in the upper part. The wackestone (sample

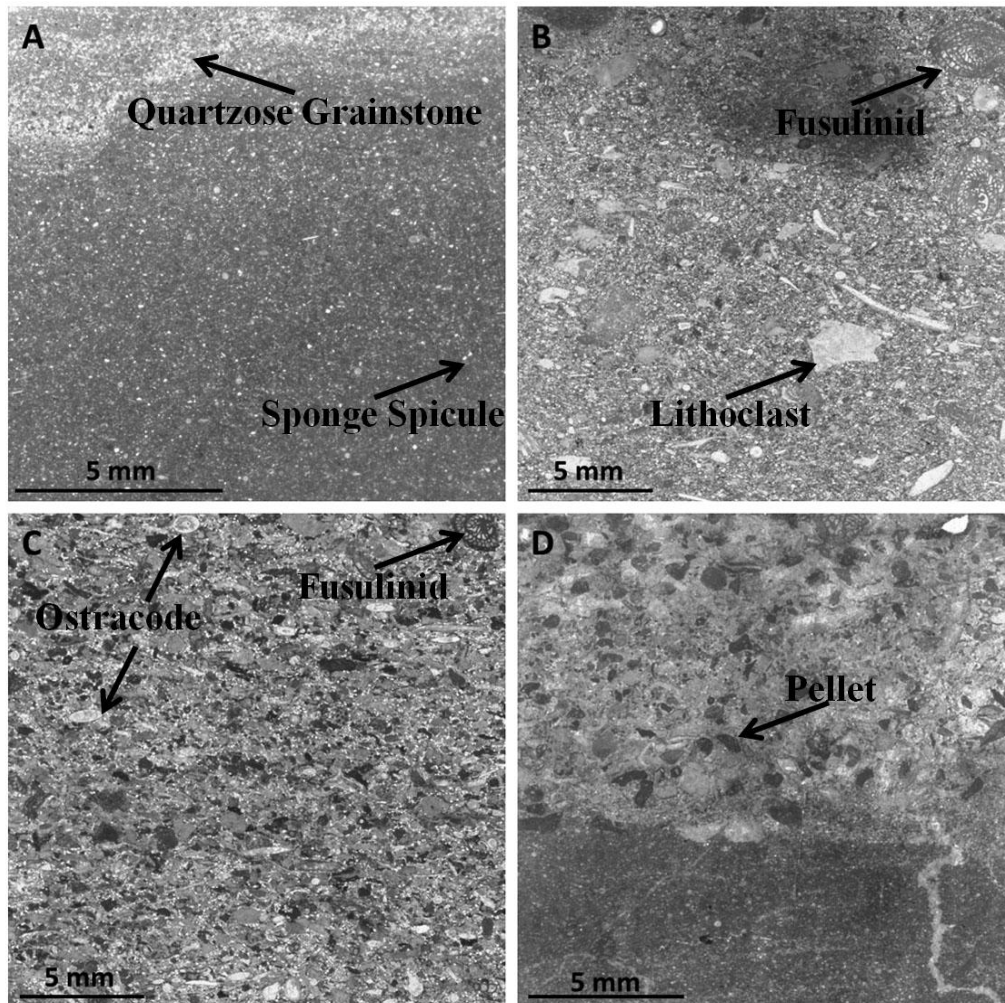


Figure 2.22: Thin sections of Package B, unit 11 (A); unit 2 (B), (C), and (D) showing the texture of the rock samples. (A) is sample WP-38 of a spiculitic carbonate mudstone with a top thin layer of quartzose grainstone; (B) is sample WP-39A of a wackestone with *Parafusulina* and lithoclasts; (C) is sample WP-39B of a wackestone with ostracodes and fusulinids; and (D) is sample WP-41 of a mudstone with a band of packstone that contains pellets.

WP-39A) coarsens upwards; contains fusulinids (*Parafusulina*), sponge spicules, ostracodes, brachiopod and bryozoan fragments, medium to coarse sized subrounded to angular lithoclasts, some secondary silicification, and less than 5% quartz grains, coarse-grained, very poorly sorted, rounded to subangular (figure

2.22 (B)). The packstone (sample WP-39B) coarsens upwards with grains oriented (figure 2.22 (C)); contains fewer fusulinids (*Parafusulina*), ostracodes, bryozoans, mollusk and brachiopod fragments, medium to pebble sized subangular to angular lithoclasts, and less than 5% quartz grains, fine- to medium-grained, poorly sorted, subrounded to subangular. The middle limestone (sample WP-40) is a wackestone; dark brown to light brown, weathers light brown to light grey; contains fusulinids (*Parafusulina*), *Tubiphytes*, rare bryozoans, scarce gastropods, mollusk and brachiopod fragments, medium to coarse sized subrounded to angular lithoclasts, some pelletoid, and less than 5% quartz grains, fine-grained, very poorly sorted, subrounded to subangular. The limestone (sample WP-41) topping the unit is a mudstone with wavy irregular transitions between bands of packstone (figure 2.22 (D)); brown to dark brown, weathers light brown to light grey and is wavy bedded; mudstone contains sponge spicules; packstone contains pellets, *Tubiphytes*, fusulinids (*Parafusulina*), rare small foraminifers, scarce crinoid fragments, medium to coarse sized subrounded to angular lithoclasts, and less than 5% quartz grains, medium- to coarse-grained, very poorly sorted, subrounded to angular.

Unit 3 is a 5.4 meter thick mostly siltstone with a varying thin- to medium-bedded limestone in the middle part of the unit (figure 2.21); lower contact is wavy. The siltstone is very fine- to fine-grained, weathers tan with interbedded very thin laminated limestone beds. The limestone (sample WP-42) is

a pelletoid packstone with a irregular transition into a 1 cm mudstone at the top; packstone contains fragments of *Tubiphytes*, brachiopods, mollusks, scarce small foraminifers, few ostracodes, medium to coarse sized subrounded to subangular lithoclasts, some secondary silicification, and less than 5% quartz grains, fine-grained, very poorly sorted, subrounded to subangular (figure 2.23 (A)).

Unit 4 is 5.2 meter thick partial siltstone interbedded with thin to medium limestone beds. Three samples taken in the lower part and one at the top; lower contact of the unit is sharp (figures 2.24 and 2.25). Siltstone is very fine- to fine-grained, weathers tan with laminated to very thin beds of silty limestone. The lowermost limestone (sample WP-43) is a sponge spicule rich mudstone; dark brown, weathers light brown in the lower part and light grey in the upper part where it was sampled (figure 2.23 (B)). The second medium sized limestone (sample WP-44) is a packstone that fines upwards with oriented grains; brown to light grey to grey, weathers light brown to tan; contains pellets, sponge spicules, small fragments of brachiopods, mollusks and bryozoans, scarce small foraminifers, medium to coarse sized subrounded to angular lithoclasts, and less than 5% quartz grains, fine-grained, very poorly sorted, rounded to subangular. The third medium sized limestone (sample WP-45) in the lower part of the unit is a sponge spicule mudstone; dark brown, weathers tan to light grey with faint laminations (figure 2.23 (C)); contains rare ostracodes, and a very thin lighter

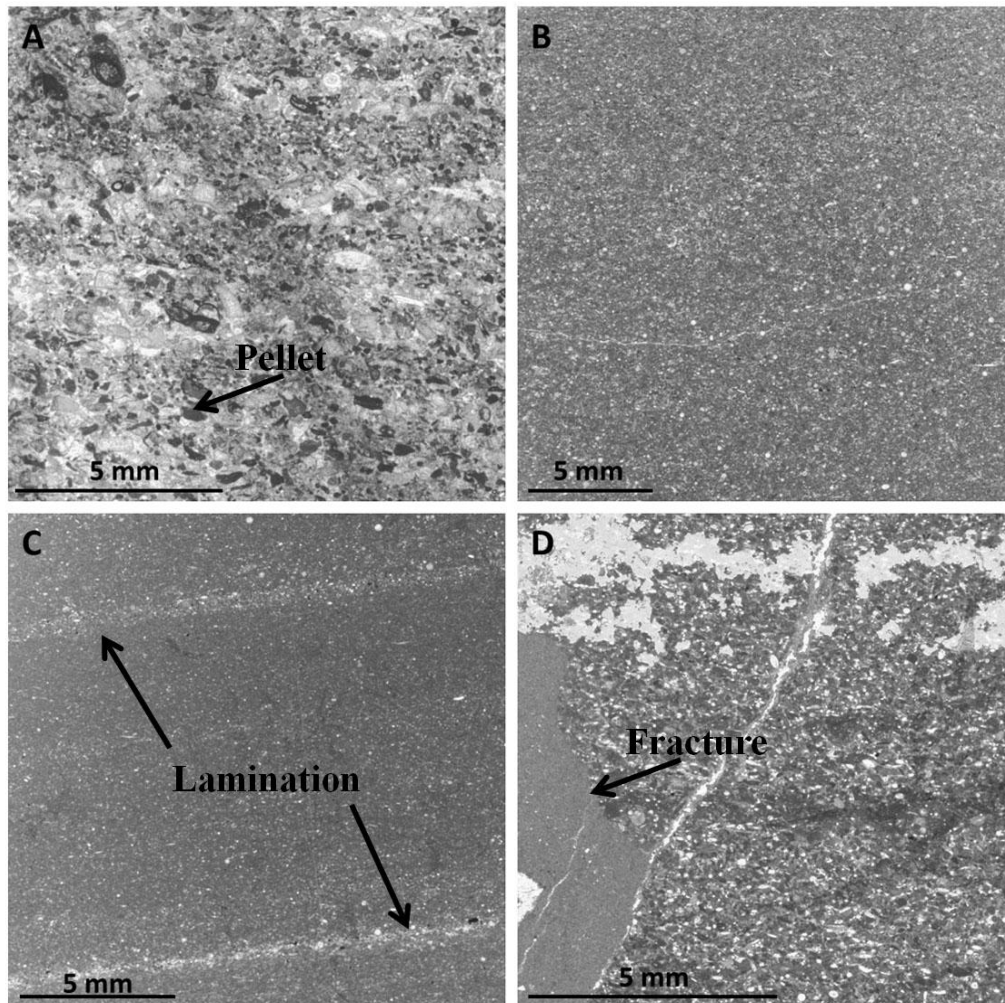


Figure 2.23: Thin sections of Package B, unit 3 (A); unit 4 (B), (C), and (D) showing the texture of the rock samples. (A) is sample WP-42 of a pelletoid packstone; (B) is sample WP-43 of a sponge spicule rich mudstone; (C) is sample WP-45 of a sponge spicule mudstone with faint laminations; and (D) is sample WP-46 of a fine-grained pelletoid packstone with a large mud filled fracture.

band with a few quartz grains in it, which are fine-grained, very poorly sorted, subrounded to subangular. The uppermost limestone (sample WP-46) topping the unit is a fine-grained pelletoid packstone; light brown, weathers light grey; contains tiny foraminifers, mollusk fragments, medium sized subrounded to

subangular lithoclasts, and tan mud filled fractures with some sparite (figure 2.23 (D)).

Unit 5 is a 13.0 meter thick siltstone; partly covered and its lower contact obscured. Abundant vegetation covers nearly the entire unit with some rock debris. This part of the WP-section is very steep. The overlying limestone units(6-8) were named the C-debris, due to its massive size totaling 11.5 meters with two major parts being conglomeratic with up to boulder sized lithoclasts.



Figure 2.24: Photograph of Package B, unit 4 lower part; showing where samples WP-43 through WP-45 were collected from the unit.

Unit 6 of the C-debris is a 4.5 meter thick limestone capped by a conglomeratic limestone up to 1.6 meter thick with up to boulder sized lithoclasts;

lower contact is obscured by vegetation and rock debris (figure 2.25). The lowermost part of the limestone (sample WP-47) is a pelletoid packstone; brown, weathers light grey; contains small foraminifers, some coated, ooids, and medium

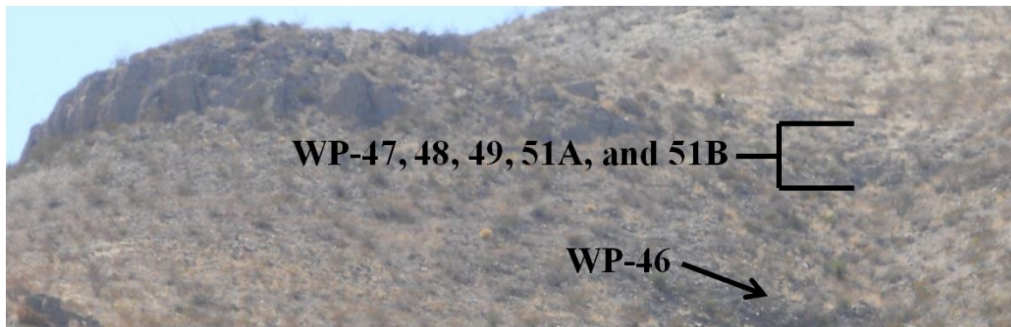


Figure 2.25: Photograph of Package B, unit 4 uppermost part; showing where sample WP-46 was collected. Unit 6, 7, and 8 (C-debris) is between where samples WP-47 through 51B were collected; also the unit topping Package B.

sized, subrounded to subangular lithoclasts (figure 2.26 (A)). The upper part of the limestone (sample WP-48) below the debris is a similar in texture to sample WP-47. The overlying conglomeratic limestone is highly weathered and difficult to sample. Upper part of the conglomeratic limestone (sample WP-49) is a pelletoid packstone with large brachiopod fragments, small foraminifers, and less ooids than the previous two (samples WP 47 and 48), and medium to coarse sized subrounded to subangular lithoclasts (figure 2.26 (B)).

Unit 7 of the C-debris is 2.1 meter thick limestone wedged between two conglomeratic limestone beds; lower contact of unit is irregular (figure 2.25). The lower part of the limestone (sample WP-50) is a foraminifer rich packstone; light brown to brown, weathers light grey; contains pellets, small foraminifers,

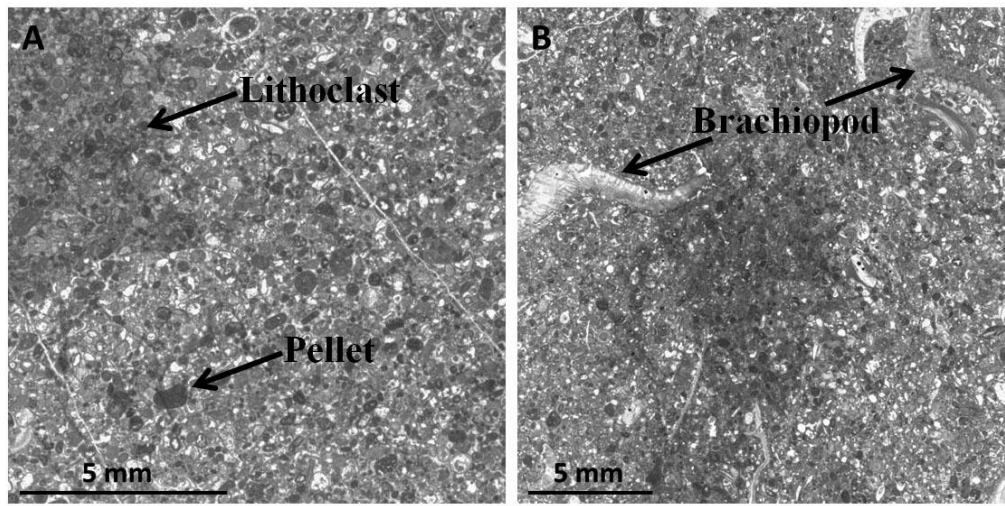


Figure 2.26: Thin sections of Package B, unit 6; (A) and (B) showing the texture of the rock samples. (A) is sample WP-47 of a pelletoid packstone with pellets and part of a mudstone lithoclast; (B) is sample WP-49 of a pelletoid packstone with brachiopod fragments.

fusulinids species (*Leëlla fragilis*) and *Parafusulina* cf. *P. deliciosensis* (Dunbar and Skinner, 1937; Dunbar, 1944), *Tubiphytes*, brachiopods, scarce echinoid spines, medium sized subrounded to subangular lithoclasts. The unit marks the first occurrence of the fusulinid species *Leëlla fragilis* in the WP-section (figure 2.27 (A)).

Unit 8 of the C-debris is 4.9 meter thick debris with an irregular contact with the overlying limestone that tops Package B; lower contact of the unit is also irregular (figure 2.25). The debris unit is highly weathered and difficult to sample; two samples were taken from the uppermost part. The overlying limestone is partially covered and was not sampled. The upper sample of the debris (sample WP-51A) is very coarse packstone; light grey, weathers tan; contains *Tubiphytes*,

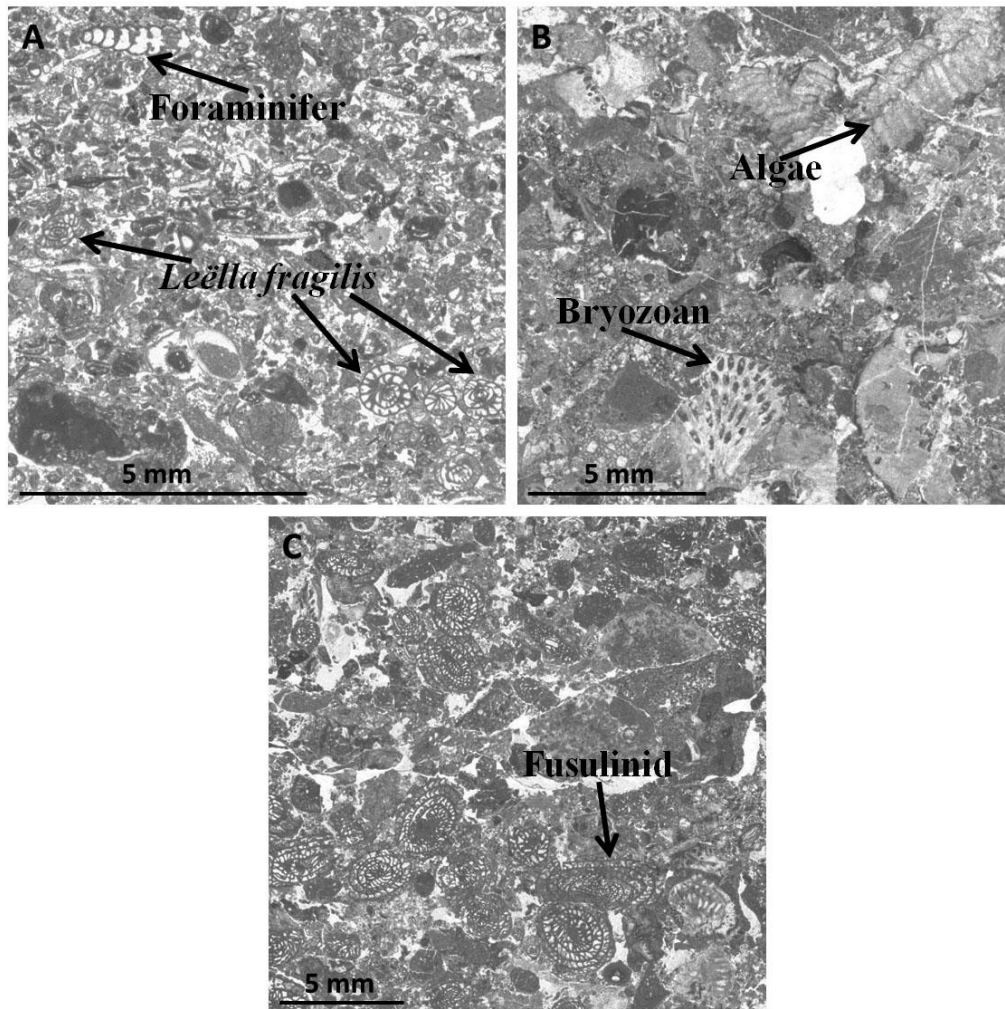


Figure 2.27: Thin sections of Package B, unit 7 (A); unit 8 (B) and (C) showing the texture of the rock samples. (A) is sample WP-50 of a foraminifer rich packstone with (left to right) oblique, axial, and equatorial section of fusulinid species *Leëlla fragilis*; (B) and (C) are part of a debris, where (B) is sample WP-51A of a coarse packstone with a bryozoan and algae, and (C) is sample WP-51B of a coarse lithoclastic packstone with fusulinids *Parafusulina*.

algae, bryozoan and brachiopod fragments, medium to very coarse subrounded to angular lithoclasts (figure 2.27 (B)). The uppermost part of the debris (sample WP-51B) is a coarse lithoclast packstone; grey, weathers light grey to tan;

contains abundant fusulinids (*Parafusulina*) and medium to coarse subrounded to subangular lithoclasts (figure 2.27 (C)).

2.7 Package C

Unit 1 of Package C is a 7.2 meter thick mostly siltstone with three thin to thick limestone beds; a lower, middle, and one at the top; lower contact is obscured by abundant vegetation and some rock debris. The siltstone is very fine- to fine-grained, weathers tan and is partially obscured by rock debris (figure 2.28). The lower limestone (sample WP-52) is a pelletoid packstone, and is partially covered; brown, weathers grey; contains small foraminifers (*Geinitzina*), ooids, some ostracodes, scarce echinoid spines, rare small ammonoids, medium sized subrounded to subangular lithoclasts, and less than 5% quartz grains, some thinly coated, fine- to medium-grained, very poorly sorted, subrounded to angular (figure 2.29 (A)). The middle limestone(sample WP-53) is a packstone, with some quartz grains that have a thin coating on them; dark brown to brown, weathers grey to light grey; coarsens upwards; contains pellets, small foraminifers, fusulinid species *Leëlla fragilis* and *Parafusulina* cf. *P. lineate* (Dunbar and Skinner, 1937), brachiopod and mollusk fragments, *Tubiphytes*, rare crinoids, medium sized subrounded to subangular lithoclasts, some pelletoid, and 5-10% quartz grains, medium-grained, poorly to moderately sorted, subrounded to subangular (figure 2.29 (B)). The thick limestone (sample WP-54A-C) at the top of the unit fines upwards from debris in the lowermost part into a fine-grained



Figure 2.28: Photograph of Package C, unit 1 upper part; showing where samples WP-53 through WP-54C were collected from the unit.

fusulinid rich packstone at the top; light brown to brown, weathers tan to light grey. The first sample WP-54A is a debris; contains fusulinids (*Parafusulina* and scarce *Leëlla*), brachiopod fragments, *Tubiphytes*, rare bryozoans, scarce echinoid spines, rare small foraminifers, medium to very coarse sized subrounded to angular lithoclasts, some filled with pellets, secondary silicified vugs, some quartz grains, very fine- to fine-grained, very poorly sorted, subrounded to subangular

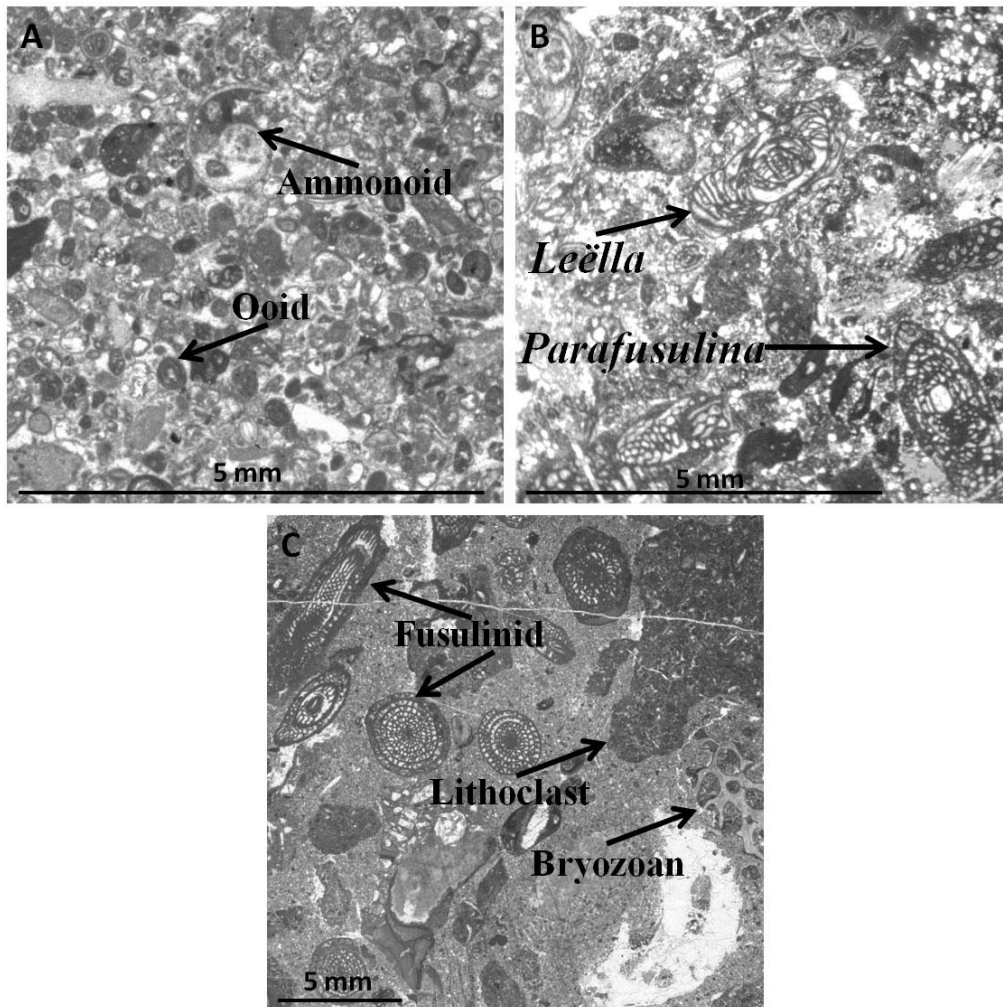


Figure 2.29: Thin sections of Package C, unit 1; (A), (B), (C), and (D) showing the texture of the rock samples. (A) is sample WP-52 of a pelletoid packstone with a rare small ammonoid and an ooid; (B) is sample WP-53 of a packstone with fusulinids species *Leëlla fragilis* and *Parafusulina* cf. *P. lineata*; (C) is sample WP-54A of a debris with *Parafusulina*, lithoclasts and bryozoans fragment.

(figure 2.29 (C)). The second sample WP-54B is a fusulinid packstone that fines upwards; contains *Parafusulina* and *Leëlla*, small foraminifers, brachiopod and mollusk fragments, rare bryozoans, and medium to coarse sized subrounded to subangular lithoclasts. The third sample WP-54C is a fine-grained fusulinid

packstone; contains fusulinid species *Leëlla fragilis* and *Parafusulina* cf. *P. rothi* (Dunbar and Skinner, 1937), small foraminifers, *Tubiphytes*, brachiopod and mollusk fragments, bryozoans, scarce crinoid fragments, medium sized subrounded to subangular lithoclasts, some pelletoid, and some quartz grains, very fine-grained, very poorly sorted, subrounded to subangular (figure 2.30).

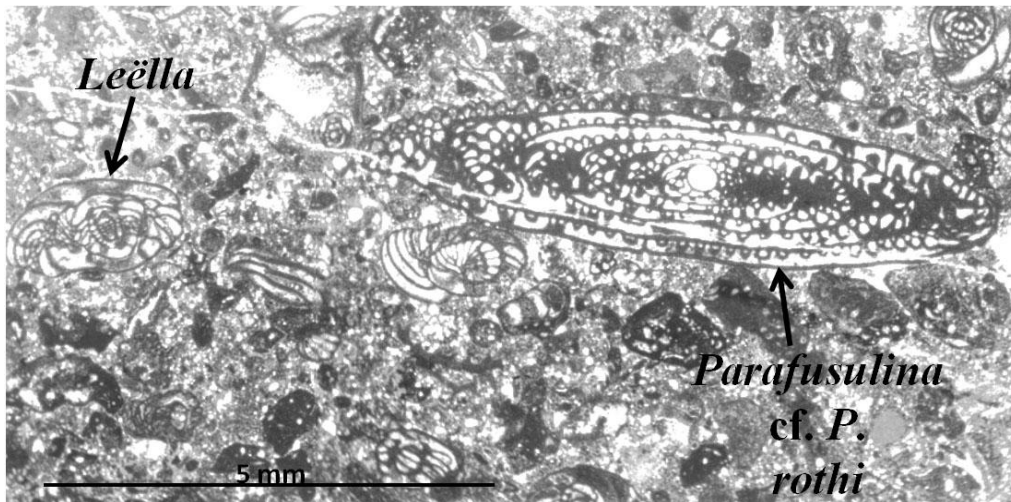


Figure 2.30: Thin section of Package C, unit 1 (sample WP-54C) showing the texture of a fine-grained fusulinid packstone containing the species *Leëlla fragilis* and *Parafusulina* cf. *P. rothi*.

Unit 2 is a 5.5 meter thick mostly siltstone with three thin to medium limestone beds in the upper part with the uppermost limestone topping the unit; lower contact of the unit is sharp (figure 2.31). The siltstone is very fine- to fine-grained; weathers tan; with few very thin limestone beds and is partially covered by vegetation and rock debris. The lower part of the siltstone is 3.1 meters, followed by a 10-15 cm thick silty limestone that weathers tan. The middle limestone (sample WP-55) is a mudstone; tan to light grey, weathers tan to light



Figure 2.31: Photograph of Package C, unit 2 upper part; showing where sample WP-55 was collected.

grey and is laminated (figure 2.32 (A)); contains rare medium sized subangular lithoclasts and less than 5% quartz grains, very fine- to fine-grained, very poorly sorted, rounded to subrounded. The uppermost limestone is similar in appearance in the field to the middle limestone; no sample was taken.

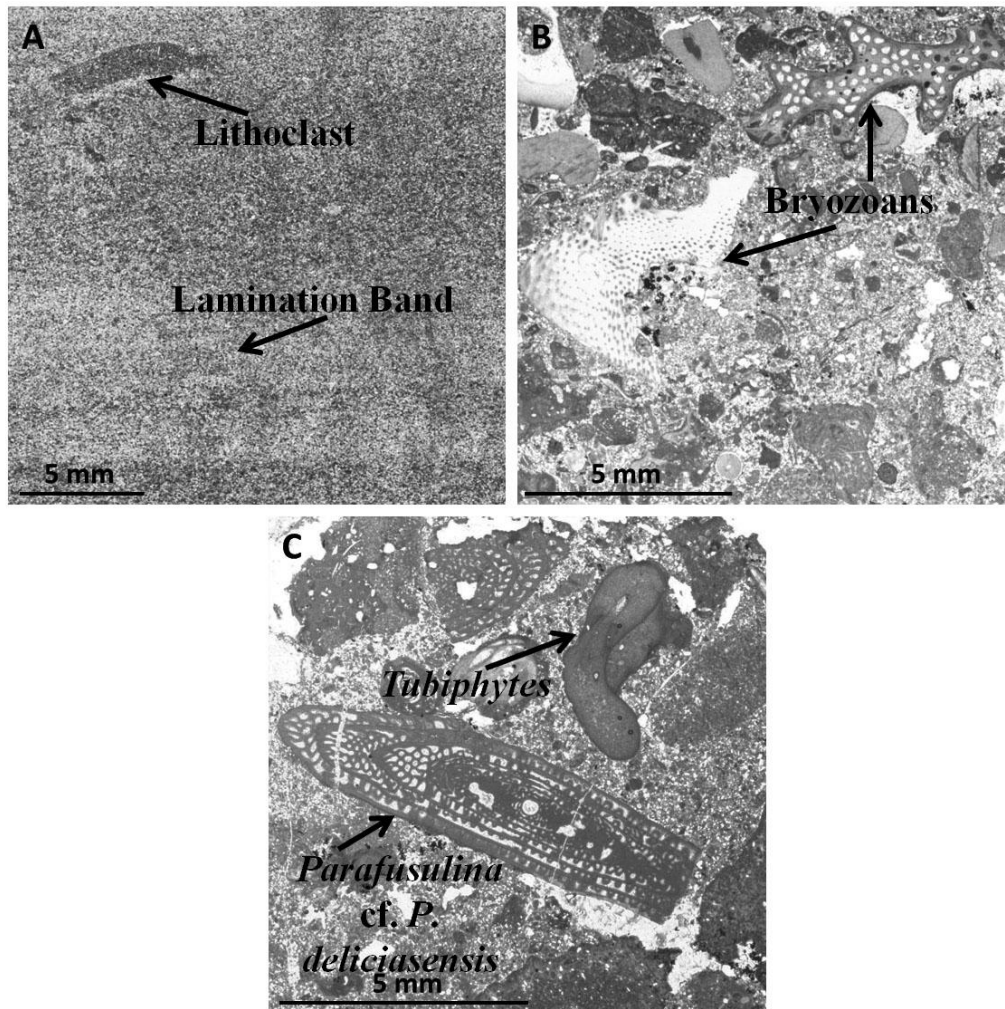


Figure 2.32: Thin sections of Package C, unit 2 (A); unit 4 (B) and (C) showing the texture of the rock samples. (A) is sample WP-55 of a mudstone with a lithoclast and lamination band; (B) is a section of sample WP-56 of a packstone with two different types of bryozoans (C) is a second section of the sample of WP-56 with *Tubiphytes* and equatorial sectional fragment of *Parafusulina* cf. *P. deliciosensis*.

Unit 3 is a 7.5 meter thick siltstone with its lower sharp contact; unit also includes very thin limestone beds; no samples were taken. Siltstone is very fine- to fine-grained, weathers tan in the lower part and light grey to greenish grey in

the upper part. Unit 3 of the WP-section is very steep and partially covered by silt and rock debris.

Unit 4 is 1.2 meter thick and has a 40 cm thick limestone in the lowermost part followed by 60 cm thick sandstone and is topped by a thin limestone bed; lower contact of the unit is sharp (figure 2.33). The lowermost limestone (sample WP-56) is a packstone with an irregular transition into a wackestone; dark brown



Figure 2.33: Photograph of Package C, unit 4; showing where sample WP-56 was collected from the unit.

to brown, weathers light grey; packstone contains fragments of *Parafusulina* and few *Leëlla*, *Tubiphytes*, bryozoan and brachiopod fragments, pellets, scarce small foraminifers, some secondary silicification, medium sized subrounded to subangular lithoclasts, some with pellets in them, and less than 10% quartz grains, very fine- to medium-grained, poor to moderately sorted, subrounded to subangular (figures 2.32 (B) and (C)); wackestone contains small fragments of ostracodes, mollusks, pellets, and medium sized subrounded to subangular lithoclasts. Sandstone is laminated with very thin limestone beds less than 1 cm thick, weathers tan to light grey to greenish grey and is brachiopod rich. The 5-10 cm thick limestone topping the unit weathers light grey, is wavy and was not sampled.

Unit 5 is a 7.1 meter thick siltstone with its upper part more weather resistant and of a sandy texture, but still dominantly a siltstone; lower contact of the unit is irregular. The siltstone is very fine- to fine-grained, weathers light grey to tan to greenish grey with some very thin limestone beds. The upper part of the unit is ammonoid rich with some brachiopods. Unit is partially covered by vegetation and abundant rock debris; no samples were taken.

Unit 6 is a 2.7 meter thick sandy siltstone similar in texture to the upper part of unit 5 previously discussed; unit has two medium limestone beds, one at the base and one at the top of the unit; lower contact of the unit is wavy. The sandy siltstone is fine-grained, weathers light grey to tan to greenish grey with

some very thin limestone beds and is ammonoid rich with some brachiopods. The lower limestone (sample WP-57) is a laminated carbonate mudstone; light brown to brown, weathers light grey; contains scarce sponge spicules, medium sized subrounded to subangular lithoclasts, scarce quartz grains, very fine- to fine-grained, very poorly sorted, subrounded to subangular (figure 2.34 (A)). The top limestone (sample WP-58) is a packstone; light brown, weathers light grey and is wavy bedded; contains *Tubiphytes*, pellets, mollusk and brachiopod fragments, fusulinids (*Leëlla* and fragments of *Parafusulina*), some ooids, scarce small foraminifers, some secondary silicification, medium to coarse sized subangular to angular lithoclasts, some with pellets in them (figure 2.34 (B)).

Unit 7 is 6.0 meter thick with a 1.6 meter thick siltstone in the lower part and a massive 4.4 meter thick laminated limestone at the top; lower contact of the unit is irregular (figure 2.35 (A)). The siltstone is fine-grained, weathers tan to greenish grey and is partially covered by vegetation and rock debris. The massive limestone contains many 2-5 cm thick beds with interbedded thin siltstone; weathers light grey to grey and is greenish grey in the upper part. The lowermost bed (sampled WP-59) is a fine-grained carbonate mudstone, light brown, weathers grey to light grey; contains sponge spicules and scarce medium sized subrounded to subangular lithoclasts (figure 2.34 (C)).

Unit 8 is 3.5 meter thick partially siltstone in the lower part and is topped by a very thick debris; lower contact of the unit is wavy (figure 2.35 (B)). The

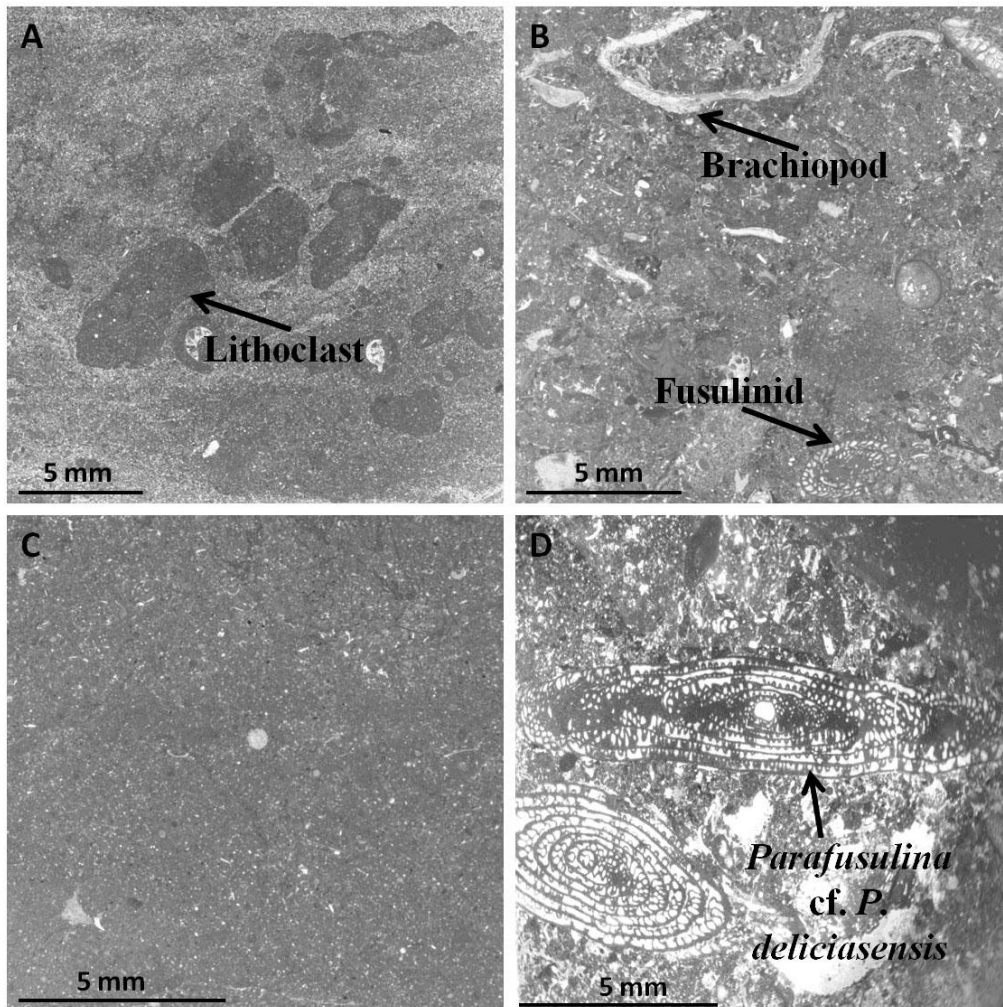


Figure 2.34: Thin sections of Package C, unit 6 (A) and (B); unit 7 (C); and unit 8 (D) showing the texture of the rock samples. (A) is sample WP-57 of a laminated carbonate mudstone with lithoclasts; (B) is sample WP-58 of a packstone with brachiopod fragments and fusulinid genus *Parafusulina*; (C) is sample WP-59 of a fine-grained carbonate mudstone; and (D) is sample WP-60 of a packstone with an equatorial section of the fusulinid species *Parafusulina* cf. *P. deliciosensis*.

siltstone is quartzose; fine-grained and weathers tan to light grey; partially covered by vegetation and rock debris. The debris weathers light grey to light brown and has lithoclasts up to pebble size in the lower part and fines upwards. In the upper part of the debris a random rock was selected; sample WP-60 is a

packstone; light brown, weathers light grey and fines upwards; contains pellets, bryozoans, fusulinid species *Parafusulina* cf. *P. deliciosensis*, brachiopod and mollusk fragments, small foraminifers, *Tubiphytes*, scarce echinoid spines, medium to coarse sized subrounded to subangular lithoclasts, some secondary silicification, and less than 5% quartz grains, fine- to medium-grained, very poorly sorted, subrounded to subangular (figure 2.34 (D)).

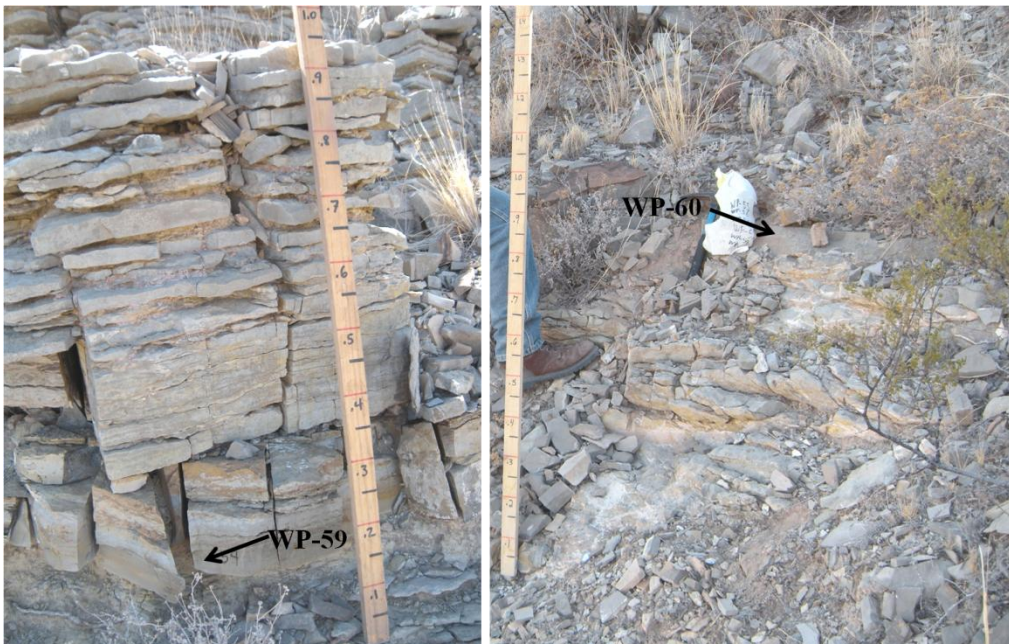


Figure 2.35: Photograph of Package C, unit 7 middle part; (A) showing where sample WP-59 was collected and (B) of unit 8 where sample WP-60 was collected; also the topping unit of the Package C.

2.8 Package D

Unit 1 of Package D is an 8.5 meter thick covered interval with its lower contact obscured by vegetation and some rock debris. The unit in the field is not steep; therefore there may be weather resistant beds hidden by the vegetation.

Unit 2 is 4.0 meter thick; three thick to very thick limestone beds with siltstone in between; the first limestone is 70 cm thick, second is 2.0 meter thick, and the third limestone topping the unit is 70 cm thick; lower contact of the unit is obscured (figure 2.36). The siltstone is very fine- to fine-grained, weathers light



Figure 2.36: Photograph of Package D, unit 2 lower part; showing where sample WP-61 was collected.

grey. The lower limestone (sample WP-61) is a pelletoid packstone that contains finer grained bands with some medium lithoclasts floating in the matrix, very small peloids and sponge spicules; light brown, weathers grey to light grey; contains small foraminifers, brachiopod and mollusk fragments, small unidentified fusulinids of *Staffella* type, crinoid fragments, echinoid spines, some

Tubiphytes, scarce bryozoan fragments, some secondary silicification, and medium to pebble sized subrounded to subangular lithoclasts, some pelletoid (figure 2.37 (A)). The lower part of the middle limestone (sample WP-62) is a

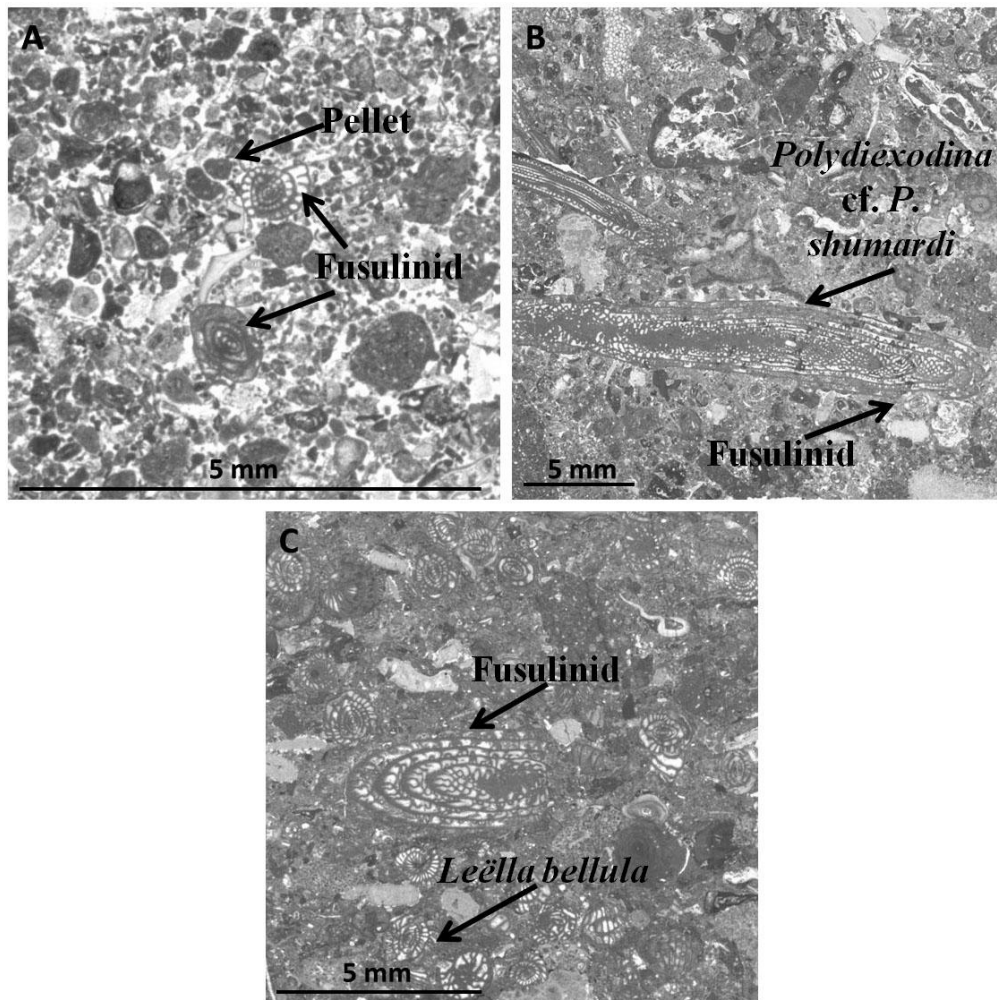


Figure 2.37: Thin sections of Package D, unit 2; (A), (B), and (C) showing the texture of the rock samples. (A) is sample WP-61 of a pelletoid packstone with unidentified *Staffella* type fusulinids; (B) is sample WP-63 of a fusulinid packstone with unidentified *Staffella* type fusulinids, and an oblique section of the fusulinid genus *Polydiexodina*; (C) is sample WP-64 of a wackestone with equatorial section of a fusulinid species *Leëlla bellula* and a fragment of *Polydiexodina* cf. *P. shumardi*.

laminated carbonate mudstone; brown to light brown, weathers grey to light grey with brown fine-grained bands and light brown very fine-grained bands; contains sponge spicules. The upper part of the middle limestone (sample WP-63) is a fusulinid packstone; light brown to brown, weathers light grey to grey; contains the fusulinid species *Polydiexodina* cf. *P. shumardi* and small unidentified fusulinids of *Staffella* (Dunbar and Skinner, (1937), pellets, small foraminifers, bryozoans, brachiopod and mollusk fragments, *Tubiphytes*, echinoid spines, crinoids, rare ostracodes, scarce ammonoids, some secondary silicification, and medium sized subrounded to subangular lithoclasts (figure 2.37 (B)). The upper part of the middle limestone marks the first occurrence of fusulinid genus *Polydiexodina* in the WP-section. The upper limestone (sample WP-64) is a wackestone that fines upwards into a carbonate mudstone with a sharp transition; light brown, weathers light grey; wackestone contains abundant fusulinids *Polydiexodina*, and species *Leëlla bellula* (Dunbar and Skinner, 1937), *Tubiphytes*, ooids, small foraminifers, bryozoans, brachiopod fragments, and medium sized subrounded to subangular lithoclasts; carbonate mudstone contains sponge spicules (figure 2.37 (C)). The lower part of the limestone (sample WP-64) within the wackestone marks the first occurrence of *Leëlla bellula* in the WP-section.

Unit 3 is 2.5 meter thick with the lower part being a 1.1 meter thick siltstone partially covered by vegetation and rock debris, and capped by a 1.4

meter thick limestone; the lower contact is sharp. The siltstone is very fine- to fine-grained, weathers light grey and partially covered by vegetation. The limestone sampled in the lower part (sample WP-65) is a fusulinid packstone that fines upwards into a wackestone; brown to dark brown, weathers light grey to grey; fusulinid packstone contains pellets, abundant *Codonofusiella paradoxica* and *Leëlla* (Dunbar and Skinner, 1937), brachiopod and mollusk fragments, small foraminifers, some ostracodes, scarce *Tubiphytes*, medium sized subrounded to subangular lithoclasts; wackestone contains sponge spicules, pellets, and brachiopod fragments (figure 2.38 (A)). The lower part of the limestone (sample WP-65) marks the first occurrence of *Codonofusiella paradoxica* in the WP-section.

Unit 4 is a 3.8 meter thick mostly siltstone with a 40 cm thick limestone bed in the middle part of the unit; the lower contact of the unit is sharp. The siltstone is very fine- to fine-grained, weathers light grey to tan and is partially covered by vegetation and rock debris. The limestone (sample WP-66) is a pelletoid packstone; dark brown, weathers grey; contains fusulinids (*Leëlla*), small foraminifers, *Tubiphytes*, mollusk and brachiopod fragments, scarce echinoid spines, and medium sized subrounded to angular lithoclasts (figure 2.38 (B)).

Unit 5 is a 3.2 meter thick siltstone interbedded with multiple thin to medium limestone beds and a 20 cm limestone capping the unit; lower contact of the unit is sharp. The siltstone is very fine-grained; weathers tan to light grey.

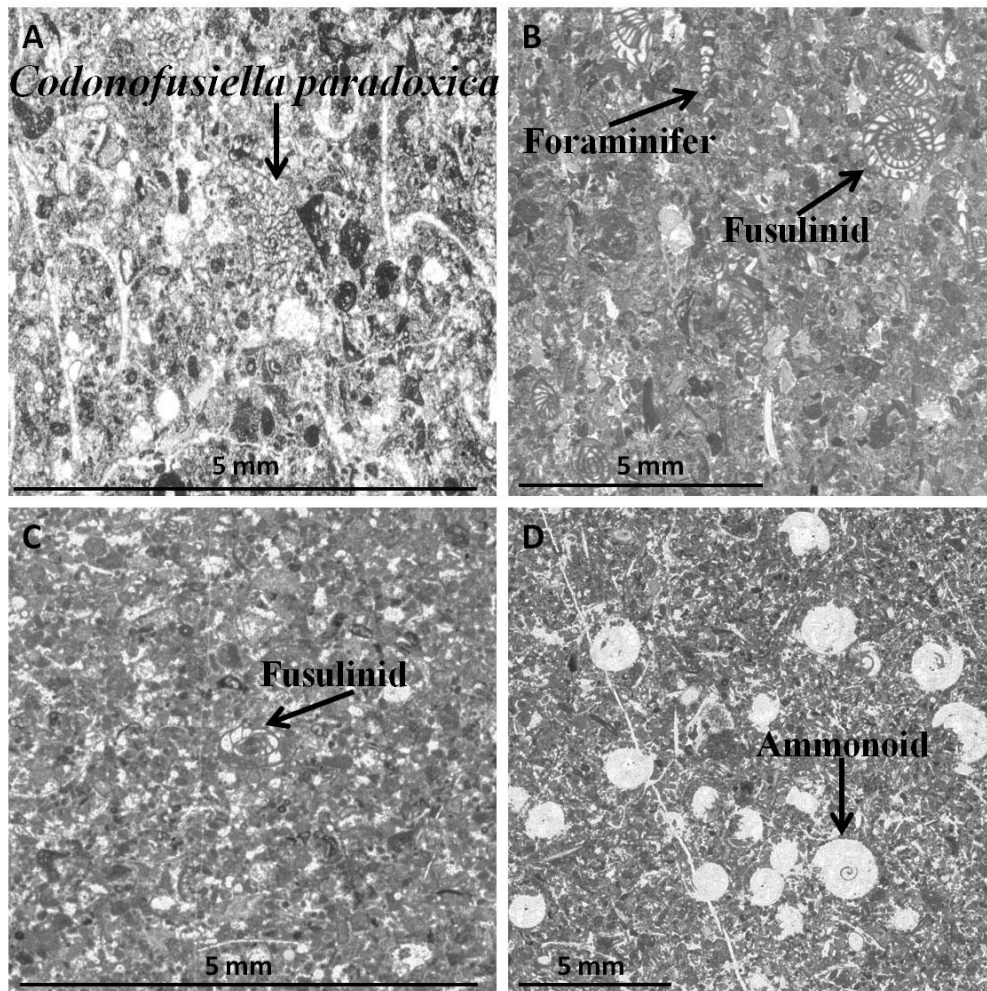


Figure 2.38: Thin sections of Package D, unit 3 (A); unit 4 (B); unit 5 (C) and (D) showing the texture of the rock samples. (A) is sample WP-65 of a fusulinid packstone with brachiopod fragments and an equatorial section of fusulinid species *Codonofusiella paradoxica*; (B) is sample WP-66 of a pelletoid packstone with foraminifers and fusulinids *Leëlla*; (C) is sample WP-67 of fine-grained packstone with a *Leëlla*; and (D) is sample WP-68 of a quartzose sponge spicule packstone with abundant ammonoids.

Limestone beds were sampled in the middle part and the upper-most part. The middle limestone (sample WP-67) is a fine-grained packstone; dark brown to brown, weathers grey with some laminations; contains pellets, abundant small foraminifers, sponge spicules, brachiopod fragments, some ostracodes, very scarce fusulinids (*Leëlla*), and medium sized subrounded to subangular lithoclasts (figure 2.38 (C)). The limestone (sample WP-68) tops the unit. The lower part is a packstone with pellets; dark brown, weathers grey; contains abundant small foraminifers, fusulinids (*Codonofusiella*), ostracodes, medium sized subrounded to subangular lithoclasts with secondary silicification; the upper part is a quartzose sponge spicule packstone with abundant ammonoids, and less than 5% quartz grains, medium- to coarse-grained, poorly to moderately sorted, subrounded to angular (figure 2.38(D)).

Unit 6 is 5.2 meters thick and mostly covered with two medium thick limestone beds; one in the middle part and one topping the unit; lower contact of the unit is sharp. The covered parts are obscured by vegetation and rock debris. The middle limestone was not sampled, but was similar in texture to the limestone topping the unit. The topping limestone (sample WP-69) is a wackestone; dark brown to brown, weathers grey with some laminations; contains pellets, small foraminifers, sponge spicules, brachiopod fragments, some ostracodes, and medium sized subrounded to subangular lithoclasts (figure 2.39 (A)).

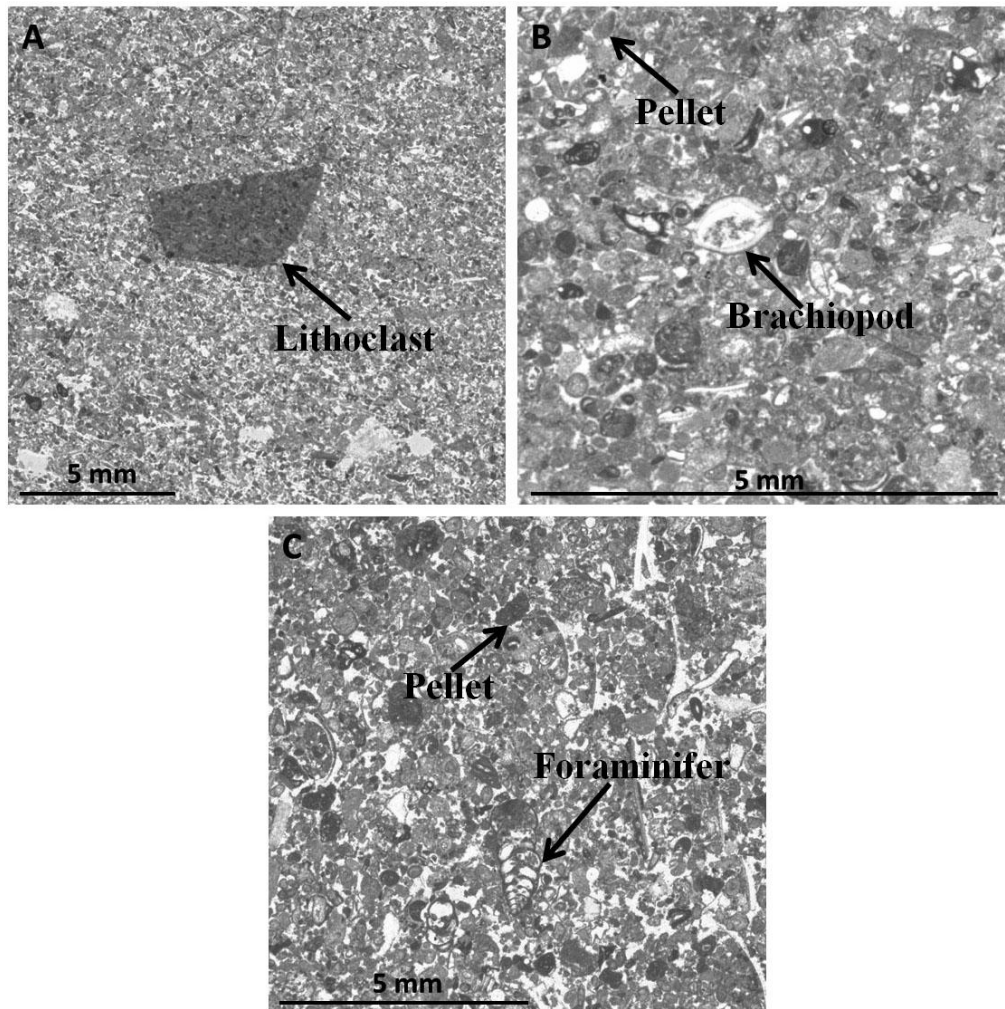


Figure 2.39: Thin sections of Package D, unit 6 (A); unit 7 (B); unit 8 (C) showing the texture of the rock samples. (A) is sample WP-69 of a wackestone with a mudstone lithoclast; (B) is sample WP-70 of a pelletoid packstone containing a brachiopod filled with micrite at the base and sparite in the upper part; (C) is sample WP-71 of pelletoid packstone with foraminifers.

Unit 7 is 2.8 meters thick with a 40 cm thick siltstone capped by a 2.4 meter thick limestone; lower contact of the unit is sharp. The siltstone is very fine- to fine-grained, weathers light grey to tan. The massive overlying limestone was sampled in the middle of the bed. Limestone (sample WP-70) is a pelletoid

packstone; dark brown to brown, weathers grey to light grey; contains small foraminifers, brachiopod fragments, ostracodes, some secondary silicification, few ooids, scarce *Tubiphytes*, medium sized subrounded to subangular lithoclasts (figure 2.39 (B)).

Unit 8 is 4.0 meters thick, mostly a megabreccia, named the B-debris as originally described by Kennedy (2009); the unit is topped by a 20 cm thick limestone; lower contact of the unit is irregular. The B-debris was not sampled because of it being deeply weathered. Kennedy's (2009) simple description of the B-debris is that it is composed of a conglomerate or breccia with larger sized allochthonous clasts; debris was probably derived from a nearby shelf edge containing back reef, reef, and fore reef carbonate facies. He further divided the B-debris into three zones the lower, middle, and upper (figure 2.40). The lower part of the B-debris contains fusulinids (*Polydiexodina*, *Leëlla*, and *Codonofusiella*), brachiopods, mollusks, and *Tubiphytes*, and contains very large lithoclasts roughly of the same size, whereas the middle part contains smaller lithoclasts with seldom oversized floating clasts embedded in a slurry-like deposit of carbonate mud, and the upper part contains a rapid transition from lithoclasts over 5 cm to less than 1 cm across (Kennedy, 2009). The lower part of the B-debris is a carbonate megabreccia; dark grey, weathers grey with randomly oriented lithoclasts; contains pellets, small foraminifers, fusulinids, bryozoans, sponge spicules, ostracodes, echinoid spines, crinoids, medium to boulder sized

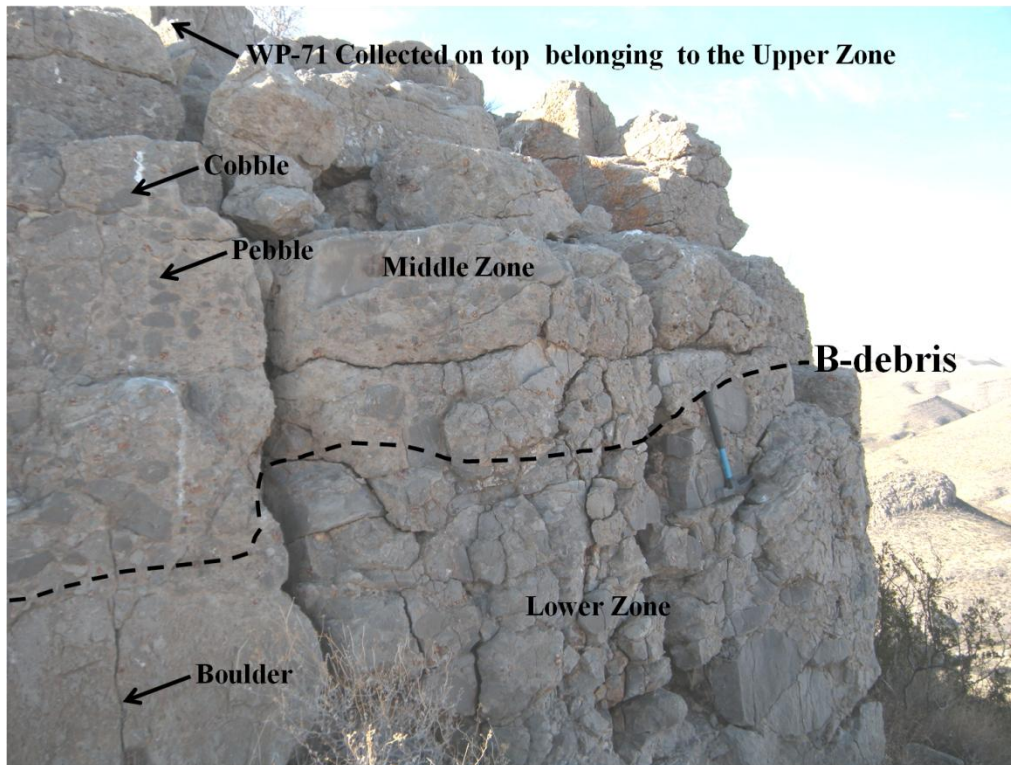


Figure 2.40: Photograph of part of the B-debris on the south side of the WP-section near the top of the ridge showing a black dotted line separating the lower and middle zone of the debris with a few clasts distinguished between them. The sample WP-71 was collected from the top of the B-debris topping the ridge.

lithoclasts, and quartz grains, very fine- to coarse-grained. The middle part of the B-debris is a carbonate breccia; grey to tan, weathers grey to light grey with some lithoclasts appearing to be oriented; contains similar fossil constitutes as the lower part of the B-debris. The upper part of the B-debris is a wackestone to a carbonate mudstone; light grey, weathers light grey fines upwards; contains similar fossil constitutes as the previously described in the lower and middle part of the B-debris. The topping limestone (sample WP-71) of the unit is a pelletoid

packstone; brown to dark brown, weathers light grey with a thin dark band in the middle part of the sample; contains small foraminifers (figure 2.39 (C)).

Chapter 3

MAPPING

3.1 Introduction

The B-debris originally described by Kennedy (2009) in a road cut along Texas FM road 2185 (figure 1.6) has been traced and mapped in the study area on foot north-northwest into the southern part of the Delaware Mountains to determine the extent of its exposure in the area. Several miles to the west of the highway the B-debris caps Package D in the WP-section (figure 2.1), and it was mapped from this point in all directions using a Garmin Rhino 120 GPS receiver. The GPS unit was set to take a tracking point every minute while hiking along the upper exposed part of the exposure of the unit. Each waypoint taken with the Garmin Rhino 120 GPS was used to mark the measured variable thickness changes and to recognize any faults. The area covered was primarily from the WP-section east to the original road cut of the B-section (figure 1.6) on Texas FM road 2185 and points to the north (figure 1.7). Two other prominent resistant limestone units were also noted if exposed and recognizable while hiking along the B-debris. These units, as described in the WP-section, are the FR unit topping Package A and the C-debris topping Package B (figure 2.1).

3.2 Study Area

The mapped study area is roughly 6x7 miles (~9.7x11.3 kilometers) and is outlined in the black box in a topographic map of the southern part of the

Delaware Mountains (figure 1.7). The study area is covered by parts of four USGS 1:24,000 quadrangles: NE Delaware Ranch, SE Seven Heart Gap, SW Square Mesa, and NW Seven Heart Gap. Most of the area mapped is shown in figure 3.1, where exposures of the FR unit are marked in red, C-debris in green, and the B-debris in blue; also noted are some of the major faults identified in the field or inferred from King (1948 and 1949) and McNutt (1948).

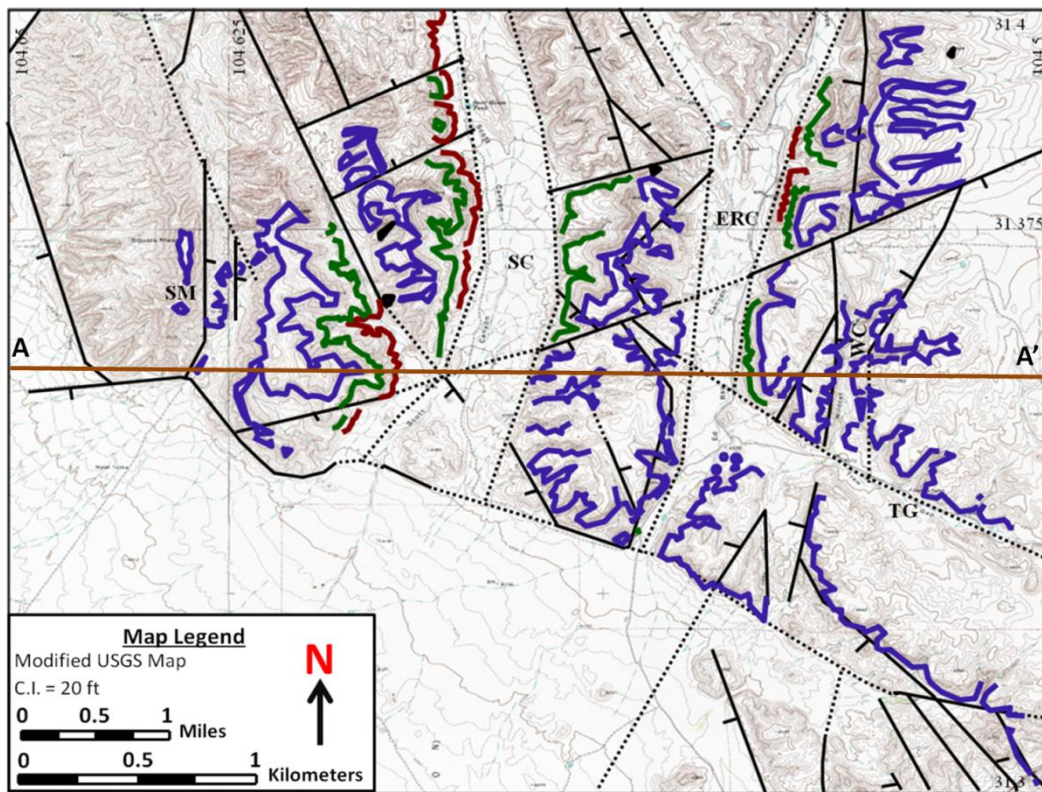


Figure 3.1: Topographic map showing the three main debris flows traced in the study area, where exposures of the FR unit are marked in red, C-debris in green, and the B-debris in blue; faults are marked in black with tick marks in the direction of the down side, solid lines are identified faults, and the dotted lines are covered faults. For label details refer to figure 1.5 and cross-section A-A' refer to figure 3.2.

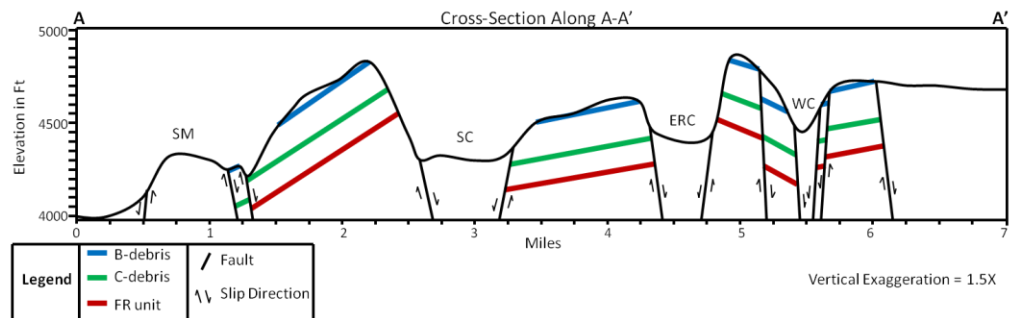


Figure 3.2: Cross-section along A-A' (west to east) marked on figure 3.1 in the southern part of the Delaware Mountains showing the general structural complexity along with the three units mapped from surface exposures that are not to scale and have vertical exaggeration in the dip. For label details refer to figure 1.5.

3.3 B-Debris Map

The B-debris was traced out in the study area by hiking along its exposed upper edge and collecting latitude and longitude coordinates data every minute, plus surface elevation data at every waypoint manually taken. The unit mostly caps the ridges in this area and is outlined in blue, showing its extent from Square Mesa on the west successively to the ridges of Scott Canyon (SC), Ed Ray Canyon (ERC), Wildcat Canyon (WC), and Trew Gap (TG) to the east in the southern part of the Delaware Mountains (figure 1.7). The B-debris can also be identified in some of the uplifted blocks south of Trew Gap northwest of the road cut along Texas FM road 2185 in the southeastern corner of the study area (figure 3.1). Faults have been noted on the topographic map (figure 3.1) in black, either from being directly identified in the field or inferred from King's (1948 and 1949) and McNutt's (1948) studies of the area. Most of the faults are noted (figure 3.1)

by giving the direction of the down side and upside of the faults to illustrate the complexity of the faulting in the area. The extreme western side and the south-southwestern part of the topographic map (figure 3.1) is younger in age and belongs to either the Salt Flats as noted in figure 1.2 or is Quaternary alluvium, where faults are unrecognizable or are covered by alluvium deposits.

3.4 Extent of Exposure

As noted above, the extent of the B-debris exposures in the study area is portrayed in figure 3.1, where the blue lines are the exposed edges of the B-debris

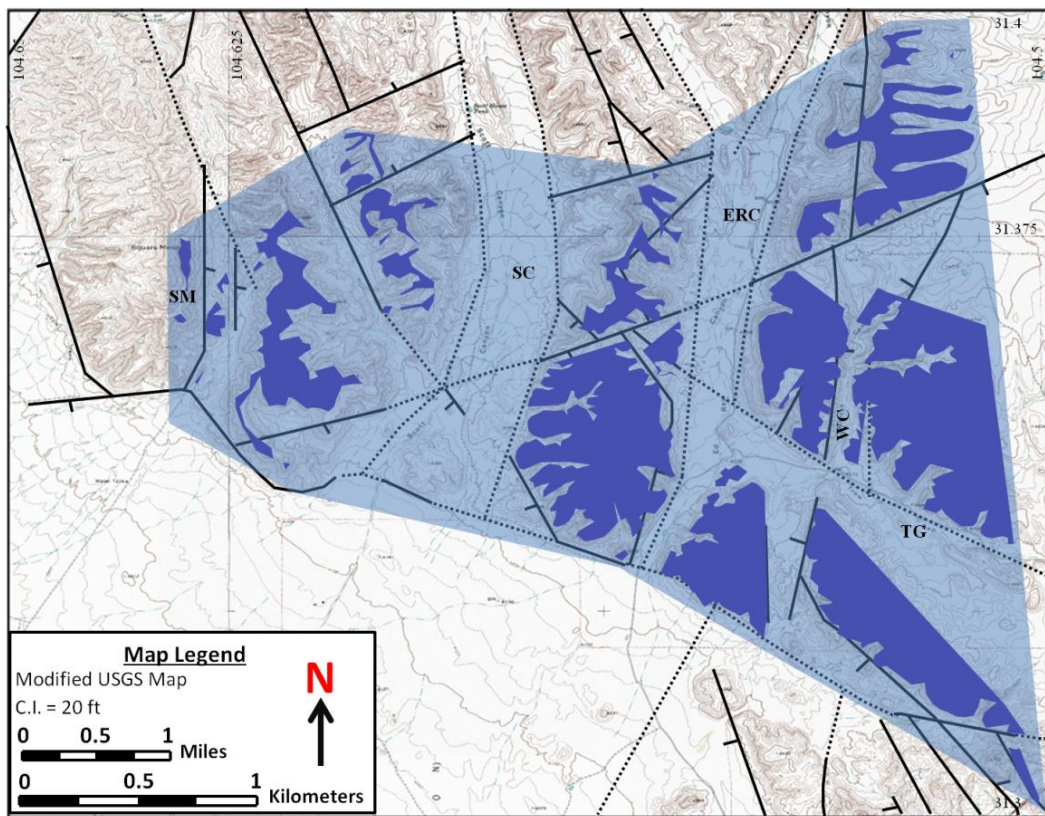


Figure 3.3: Outcrop map of the extent of the B-debris in the study area, where the present deposition of the debris in area is shaded in dark blue and the rough estimate of the minimum extent the debris covered is shaded light blue.

overlain on a USGS topographic map. In figure 3.3 of the study area, the blue outlined B-debris noted in figure 3.1 has been made into enclosed polygons, straight lined when needed to close a polygon, and shaded dark blue to show the direct extent of area that the B-debris encompasses. Using the same concept, a straight lined polygon shaded light blue (figure 3.3) was created to give a rough estimate of the minimum extent of the B-debris deposition as observed in the study area. The total area of the light blue shaded polygon encompasses 19 mi² (~30.5 km²). The faults previously mentioned in figure 3.1 have also been noted in figure 3.3. Other adjacent areas in and around the study area were also explored, but no other indications of the B-debris were evident.

Chapter 4

STRUCTURE

4.1 Introduction

The Delaware Basin is described by Garber et al. (1989) to be an asymmetric block-faulted basin with its axis parallel to the western edge of the Central Basin Platform. The Delaware Mountains are located in the uplifted western part of the Delaware Basin (figure 1.2) with exposed basinal strata belonging to the Delaware Mountain Group deposited during the Guadalupian of the Middle Permian (King, 1942). Near the end of the Pennsylvanian time, subsidence of the Delaware Basin began as monoclinical structures (figure 1.4) that were activated along the Bone Spring, Babb, and Victorio flexures (King, 1942; McNutt, 1948). During the Middle Tertiary extension, uplift and tilting of Delaware Basin began near the end of the Laramide phase (Horak, 1985; Hills, 1963, 1984). During the Late Tertiary, the main uplift and exposure of the Delaware Mountains occurred during the Basin and Range uplift phase (Horak, 1985) of the Guadalupe, Apache, and Glass Mountains (figure 1.2) (King, 1948).

Major faults in the study area have been either directly identified or inferred from King's (1948) and McNutt's (1948) studies and have been noted on the map in black in figure 3.1. There are clearly more faults in the study area, but those noted on the map (figure 3.1) are the major ones observed. These faults on the map (figure 3.1) illustrate the complexity of the faulting in the area and aid in

understanding some of the problems encountered while mapping the B-debris in the study area.

While mapping the B-debris, a major issue encountered was the repeated faulted block sections that can be seen at different elevations along the ridges of the canyons in the study area, especially in the Ed Ray Canyon area in the east central part of the southern Delaware Mountains. Kennedy (2009) presented a photograph (figure 4.1) showing very similar debris sections within several meters of each other, but at different elevations and forming prominent cliffs along the western flank of Ed Ray Canyon. These debris deposits were not analyzed in detail in his study. An example of this problem is illustrated in the photograph in figure 4.1 where two sections of debris can be identified as belonging to offset parts of the same unit of the B-debris. Many other sections in the study area also display the same features.



Figure 4.1: Arrows point to the B-debris of the western flank of Ed Ray Canyon, where the problem of down faulted blocks form repeated sections of the debris along the flanks of the canyons in the study area (Kennedy, 2009).

King (1948, 1949) interpreted these offset features of units in the Trans-Pecos area and determined them to be of linear scraps within the larger canyons, later named graben-boundary faults by Smith (1978). A graben-boundary fault is interpreted to be the result of a down-dropped faulted graben that results in closely spaced sets of normal faults that tier and collapse parts of the footwall downward into the graben. This interpretation may also be applied to half-grabens (figure 4.2). Some of the canyons in the study area have already been interpreted

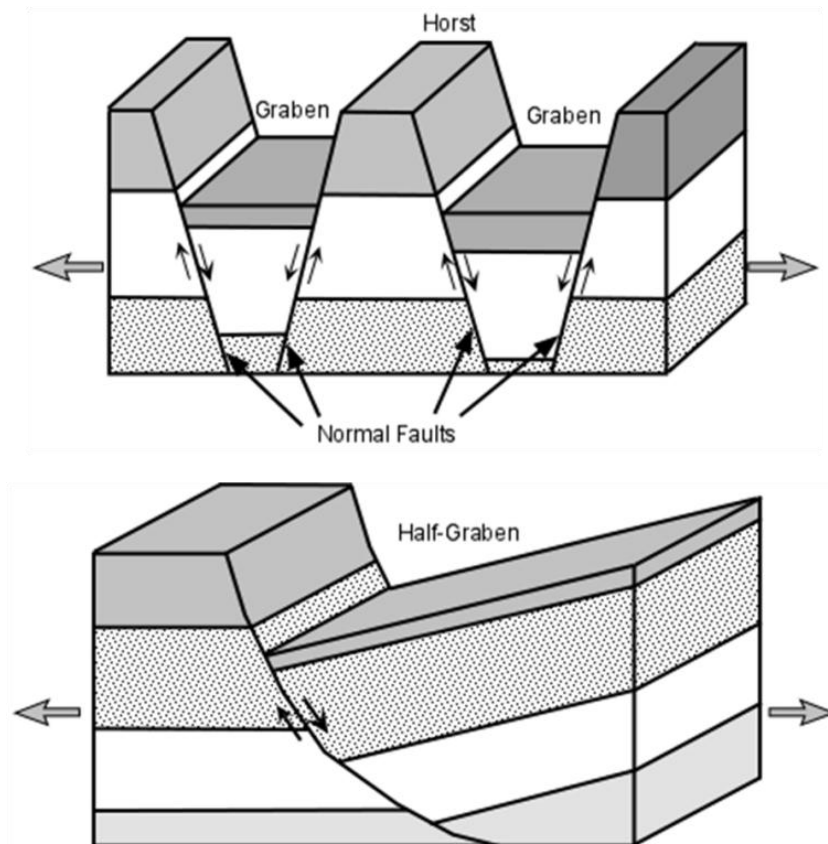


Figure 4.2: Illustrations of the structural dynamics under extensional stress showing normal faults associated with grabens, horsts, and half-grabens. (<http://earthsci.org/education/teacher/basicgeol/deform/deform.html>, image is available via the Earth Science Australia website).

to be as graben-boundary faults, such as two of the larger canyons Scott and Ed Ray (King, 1948, 1949). As can be seen in figure 4.1, the B-debris has been faulted in many places by the close proximity of normal faults that show tiered blocks located downward towards the graben.

4.2 Structural Interpretation

Displacement of significant sections of the B-debris at a number of places within the study area can be seen in figure 4.1. Starting on the western side of the study area and following along the cross-section A-A' in figure 3.2 just to the north of the cross-section, the ridge of Square Mesa is capped by the B-debris (figure 3.1), but directly to the east and several hundred meters down from the top of Square Mesa on its eastern flank is a downed section capped by the B-debris, bounded by a normal fault running south to north along the flank of Square Mesa (figure 4.3 (A)). To further illustrate the repetition of the pattern of normal faults is three tiered sections of the B-debris that can be seen in figure 4.3 (A) and 4.3 (B). The B-debris can be seen near the top of the canyon, and in the middle of the side of the canyon (figure 4.3 (A)). Also, directly below the northern most part of the down-dropped block shown in figure 4.3 (A) there is a small section of the B-debris (figure 4.3 (B)) where a normal fault can be seen on the right (west) side of the block separating it from older deposited beds of the eastern flank. On the western flank of Scott Canyon on its highest ridge capped by the B-debris in the

middle part (figure 3.1) there is also a downed tiered section that has sunk towards the canyon (figure 4.4).

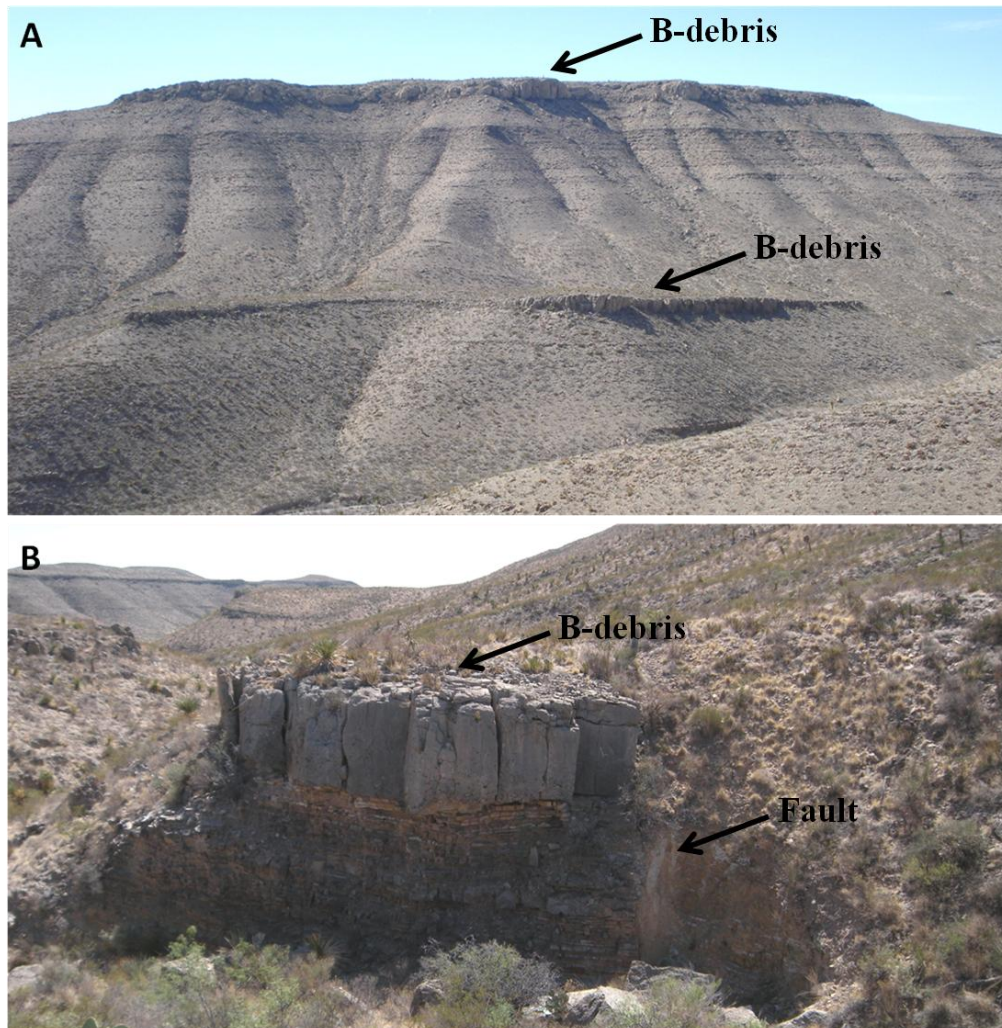


Figure 4.3: Photographs (A) and (B) of the eastern flank of Square Mesa on the westernmost ridge of the study area. (A) B-debris caps the top of the ridge with a second section of the debris down faulted several hundred meters below. (B) Third faulted block of the B-debris and underlying strata in the lowermost part of the canyon with a visible fault gauge on the right side.

Another angle of view of a downed tiered section of the B-debris is that of a photograph taken between two sections with seven meters of displacement on

the western flank of Ed Ray Canyon (figure 4.5 (A)). This site can be seen in Kennedy's (2009) original photograph (figure 4.1). The top part of the upper section of the B-debris near its edge (figure 4.5 (B)) shows joint fractures from

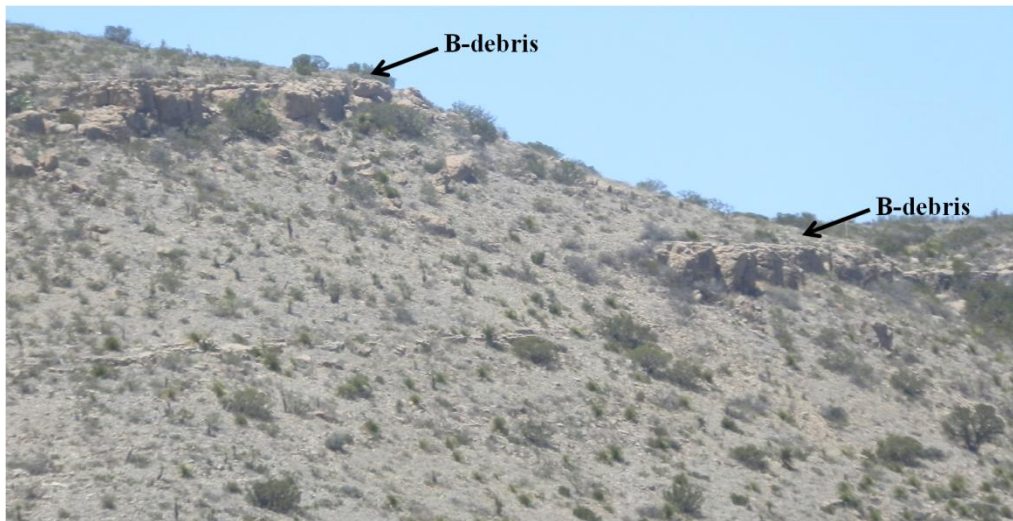


Figure 4.4: Photograph of part of the eastern ridge of Scott Canyon showing a down faulted section.

the process of extension that produced the normal faults that sheared and provided stress on the rock, visible in figure 4.5 (B) as parallel and perpendicular fractures to that of the axis of the canyon. A clear example of closely spaced sets of normal faults that tier and collapse parts of the footwall downward into the graben can be seen on the western flank of Ed Ray Canyon in its northern part (figure 4.6 (A)), where the three parts of B-debris can be seen as normal faulted downed tiered sections that have sunk towards the canyon in three stages. The western flank of Ed Ray Canyon also has multiple examples of normal faults associated with the graben-boundary fault in a variety of tiers at varying elevations as seen in figure

4.6 (B) showing multiple large sections of displacement of the debris along the flank of the canyon.

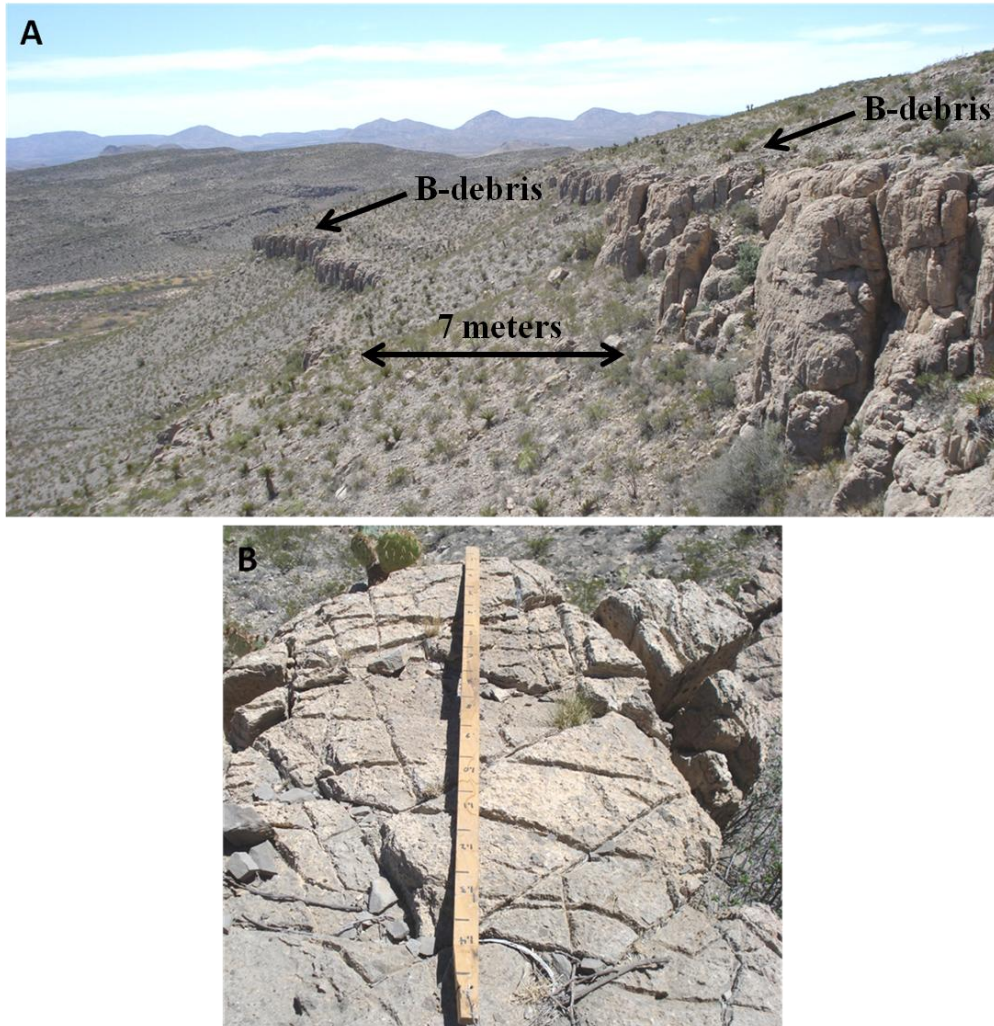


Figure 4.5: Photographs (A), (B) of the western flank of Ed Ray Canyon north of J-Capp road. (A) Shows a down faulted block of the B-debris with a displacement of 7 meters. (B) Top of the debris showing parallel and perpendicular joint fractures.

The western graben-boundary can be seen in Wildcat Canyon on its western side in the base of the canyon (figure 4.7 (A)). The western graben-

boundary fault can also be traced north from this locality (figure 4.7 (A)), where it can also be seen (figure 4.7 (B)) as a down faulted section with another

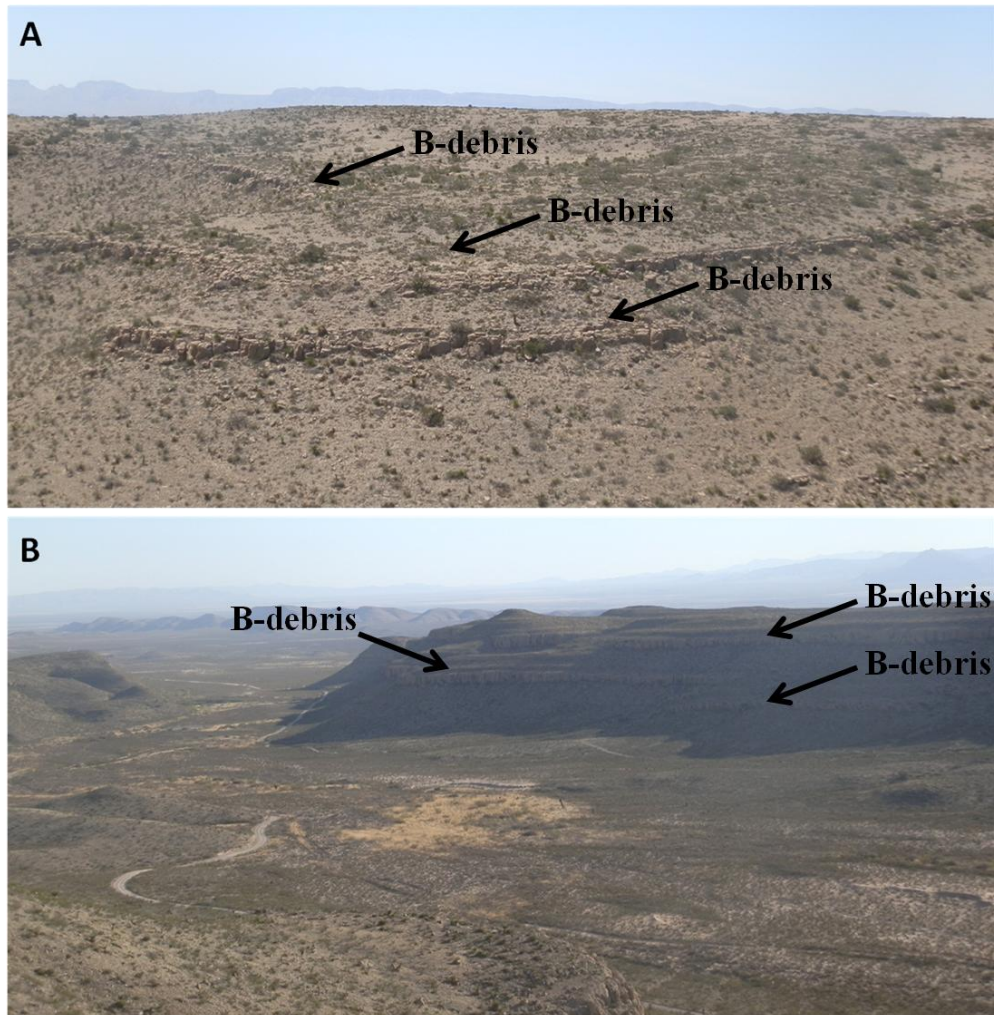


Figure 4.6: Photograph (A) of the B-debris on the western flank of Ed Ray Canyon showing the debris faulted by two close proximity faults that tier the debris into three sections. Photograph (B) showing across Ed Ray Canyon with the southwestern flank of the canyon with several down blocks of the B-debris along the flank.

associated eroding graben block of the B-debris near the base of the canyon. In the northernmost part of Wildcat Canyon, there is a down-dropped graben block

of the B-debris that has not eroded away or been covered (figure 4.8 (A)). A normal faulted three meter displacement can be seen on the right (east) side of the

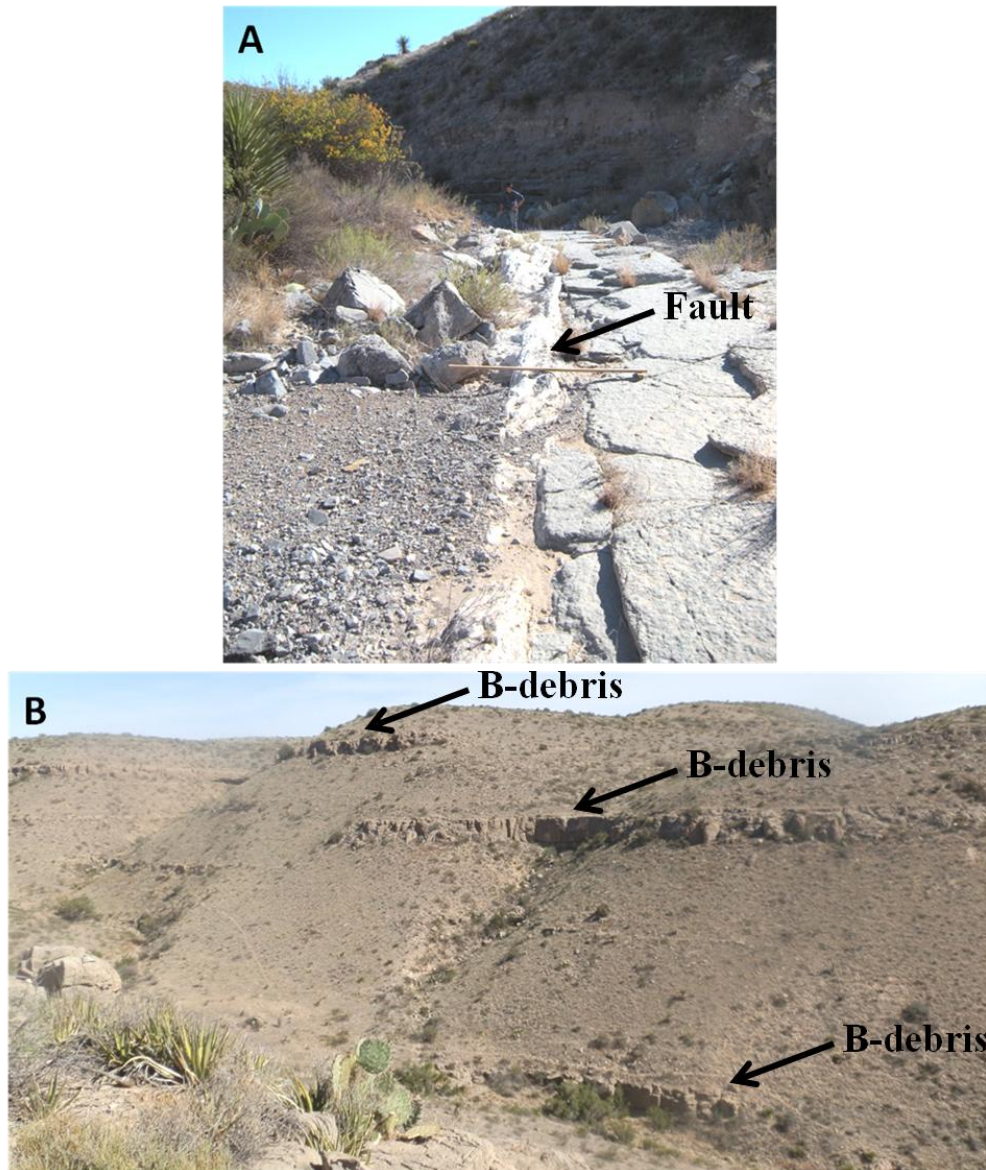


Figure 4.7: Photograph (A) taken facing southward in the base of the Wildcat Canyon, where the western graben-boundary fault is seen. (B) B-debris in the northern part of Wildcat Canyon on the western flank, where two faults have displaced three sections of the debris.

canyon in figure 4.8 (A). Another small close proximity normal fault can be seen slightly to the right of the main fault, but showing less displacement. The main fault can be seen in figure 4.7 (A) and can be seen to down fault other sections on

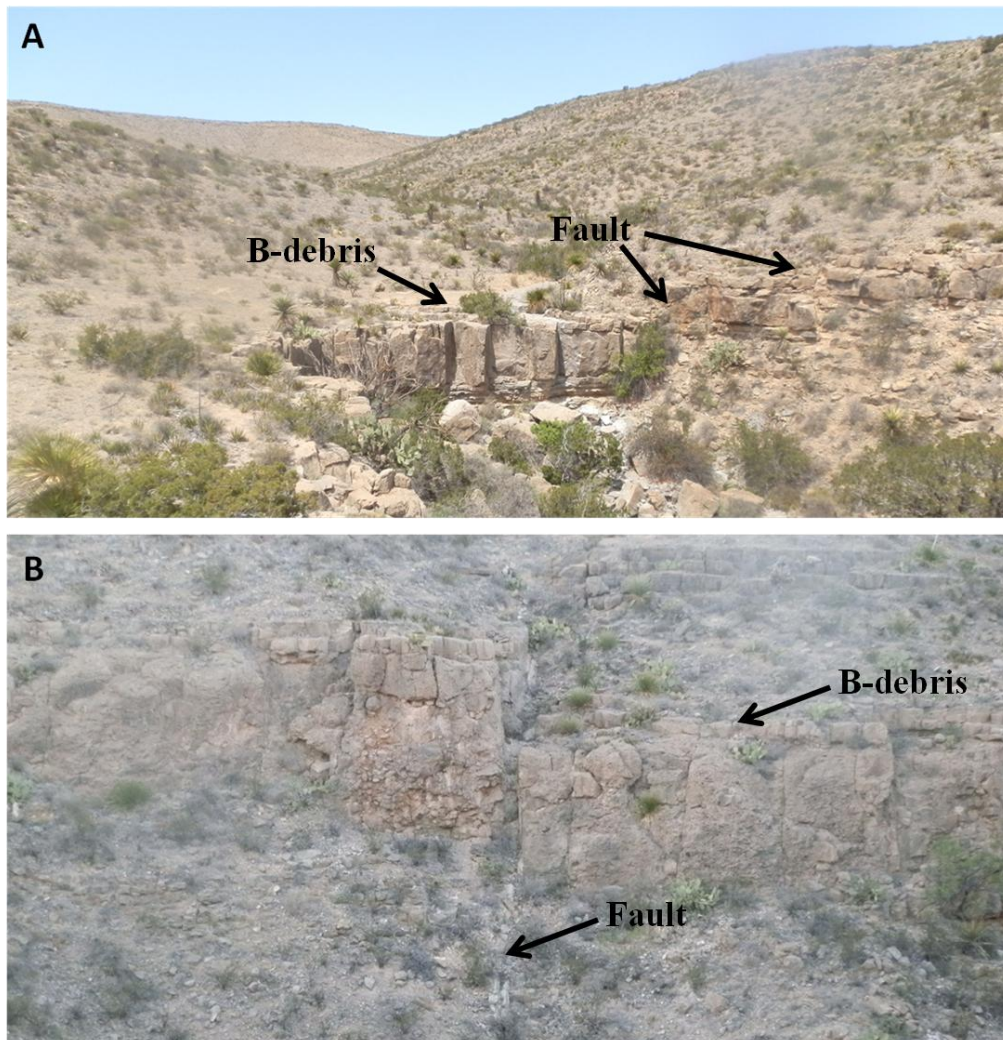


Figure 4.8: Photographs (A) and (B) of the B-debris in Wildcat Canyon, where (A) shows the northernmost part of the canyon with a graben block of the debris is in processes of being eroding into the wash of the canyon. (B) A three meter displacement of the debris from a fault that cuts along the eastern flank of the canyon.

the eastern flank of Wildcat Canyon. A little to the south from where the photograph in figure 4.8 (A) was taken, the same fault can be seen to cut through the B-debris (figure 4.8 (B)), where the down side is towards the canyon. Wildcat Canyon is the only canyon where a graben-boundary fault was directly observed. Overall Wildcat Canyon is an excellent place to observe the graben-boundary fault and associated normal faults that tier and collapse parts of the footwall downward into the graben.

The structural relations of the southern part of the Delaware Mountains cross the study area from west to east can be interpreted by using figure 3.1 and figure 3.2 guides. Starting from the Salt Flats on the western side of Square Mesa is a border fault zone marking the division between the down-dropped Salt Basin to the west and the uplifted strata that makes up the southern part of the Delaware Mountains to the east (King, 1948). Square Mesa is a part of an uplifted horst block bounded on both sides by parallel normal faults (figure 4.2).

Directly east of Square Mesa is an interpreted half-graben (figure 4.2), where it is down on the west side due to the hanging wall slipping, and up on the east side where the WP-section is located. Scott Canyon is a down-dropped graben bounded on both sides by parallel normal faults, also called graben-boundary faults by Smith (1978).

Between Scott and Ed Ray Canyons is an uplifted horst block bounded on both sides by parallel normal faults. Ed Ray Canyon is a down-dropped graben

bounded on both sides by graben-boundary faults. The eastern flank of Ed Ray Canyon has classic examples of normal faults in close proximity that have tiered the strata downward towards the graben. Between Ed Ray Canyon and Wildcat Canyon is another uplifted horst block bounded on both sides by parallel normal faults. Wildcat Canyon is highly faulted, but is considered by the writer to be a small down-dropped graben bounded on both sides by graben-boundary faults as one can be seen in figure 4.7 (A).

Chapter 5

B-DEBRIS

5.1 Introduction

The extensive presence of the B-debris in the southern part of the Delaware Mountains was a decisive factor in selecting an appropriate reference section (the WP-section) to establish its stratigraphic context within the Bell Canyon Formation, and provide a reference section to the study area. The WP-section is capped by the B-debris of Package D (figure 2.1), north-northwest approximately five and half miles from the original locality of its exposure as described by Kennedy (2009) in a road cut along Texas FM road 2185 in the southeast corner of the study area (figure 1.7). Over much of the area of the southern Delaware Mountains the characteristics of the B-debris are very similar to those at the original Kennedy's locality, and as previously described above in this work from the WP-section (Package D unit 8) where it is mostly a megabreccia composed of a conglomerate of allochthonous clasts of various sizes. The source of these clasts is considered to be a nearby shelf edge containing primarily reef and fore reef carbonate facies (Kennedy, 2009), but the actual mechanism of emplacement of the B-debris unit is not known. The B-debris generally consists of three lithofacies zones where the lower part is a carbonate megabreccia, the middle part is a carbonate breccia, and the upper part is a wackestone to a carbonate mudstone. A variety of constituents are present

including small foraminifers, fusulinids (*Polydiexodina*, *Leëlla*, and *Codonofusiella*), brachiopods, ammonoids, mollusks, *Tubiphytes*, bryozoans, sponge spicules, ostracodes, echinoid spines, crinoids, pellets, medium to boulder sized lithoclasts, and very fine- to coarse-grained quartz grains.

5.2 Rheology

The exposures of the B-debris at the reference WP-section and Kennedy's (2009) original locality are significant reference points in the study area. The exposures of the B-debris vary in thickness in the study area from over twenty meters on the top of Square Mesa in the western part of the study area to as thin as a few meters in the northeastern part of the area just to the east of Casa de Piedras road and north of Wildcat Canyon (figure 1.7 and 3.1). Kennedy (2009) described the composite rheology of the B-debris as non-Newtonian Bingham Plastic and Newtonian fluids contributing to a plastic debris flow-like and turbidity current. He further described how the three zones (lower, middle, and upper) of the B-debris were classified from his rheological interpretations of the outcrops at the original locality along a road cut of Texas FM road 2185. Such a debris flow has also been defined by Gani (2004) as a densite, coined for deposition of multiple processes or as a hybrid with several stages of deposition. Kennedy (2009) ultimately determined the B-debris to be a densite from his zoning descriptions.

The first zone (lower part) is identified as a carbonate megabreccia composed of very large clasts over a meter across resting on smaller clasts less than a meter across (figure 5.1 (A)) with about 5% clay content in the matrix

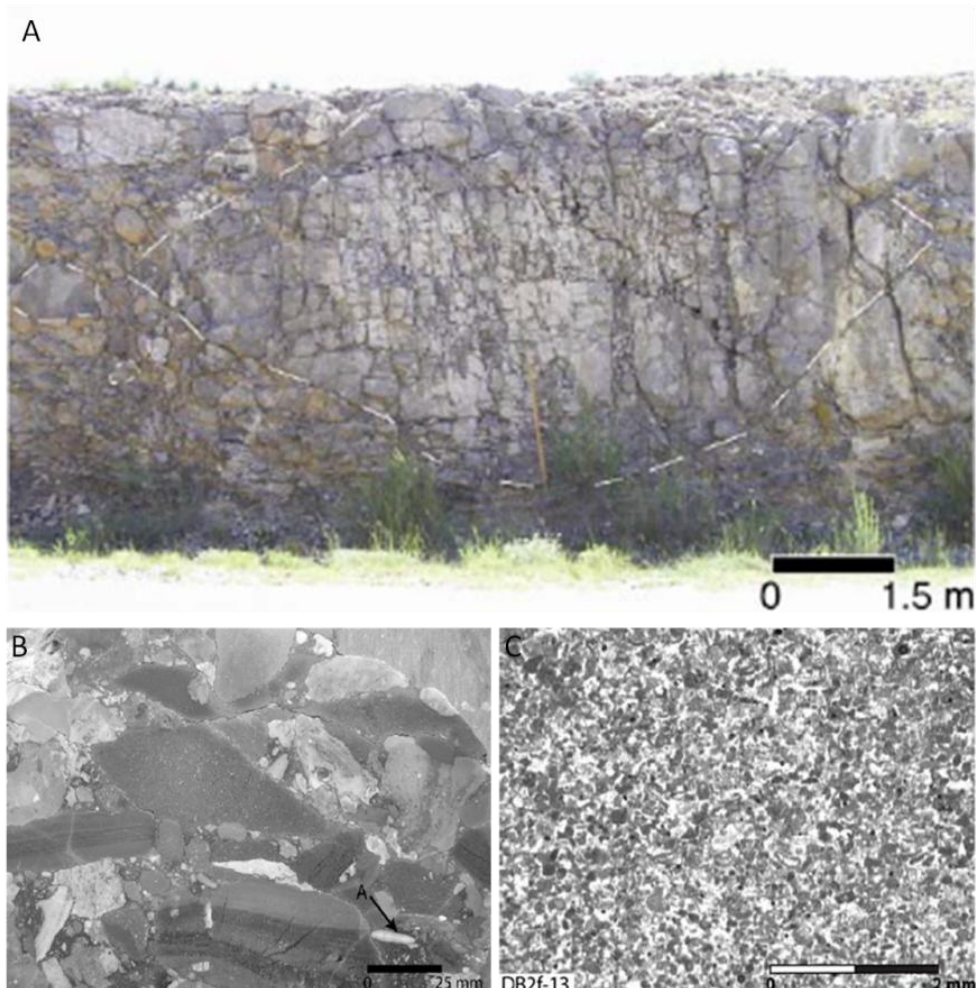


Figure 5.1: Photograph (A) shows the lower zone of the B-debris along Texas FM road 2185 on the south wall side, where a large clast is outlined in white. (B) Shows a thin section of the middle zone of the debris with partial aligned clasts and the arrow points to a *Polydiexodina*. (C) Shows a thin section from the upper zone near the top where it is composed of a fine-grained biomicrite (from Kennedy, 2009).

(Kennedy, 2009). The laminar and debris flow-like non-Newtonian Bingham characteristics provides yield strength and cohesiveness to the B-debris, where the poorly sorted interlocking clasts is the yield strength and the poor clay content provides cohesiveness being the dominant support mechanism. The second zone (middle part) is identified as a carbonate breccia composed dominantly of smaller clasts less than a quarter of a meter across, partially aligned, and with a higher percentage of clay content in the matrix (figure 5.1 (B)) with some outsized floating clasts. This description indicates the environment of deposition was decreasing in energy as compared to the first zone, and whereas the clasts in the middle zone provide yield strength, and the clay content is the dominant sediment support mechanism (Kennedy, 2009). The third and last zone (upper part) is a fine-grained wackestone that grades into a carbonate mudstone (figure 5.1 (C)). The fine-grained composition of the third zone illustrates the dominate support mechanism to be of fluid turbulence lacking in yield strength characteristic of Newtonian fluids contributing to a turbidity current (Hampton, 1975; Kennedy, 2009). Kennedy's (2009) zonal structure and his descriptions of the B-debris will be used to discuss the interpretations of the rheology as seen along the ridges, flanks, and canyon floors within the southern part of the Delaware Mountains.

The top of Square Mesa is capped by the B-debris (figure 3.1) where it is over 20 meters at its thickest on the eastern flank (figure 5.2 (A)). The lower and

middle zones of the B-debris contain very large boulders, some larger than the boulder outlined in

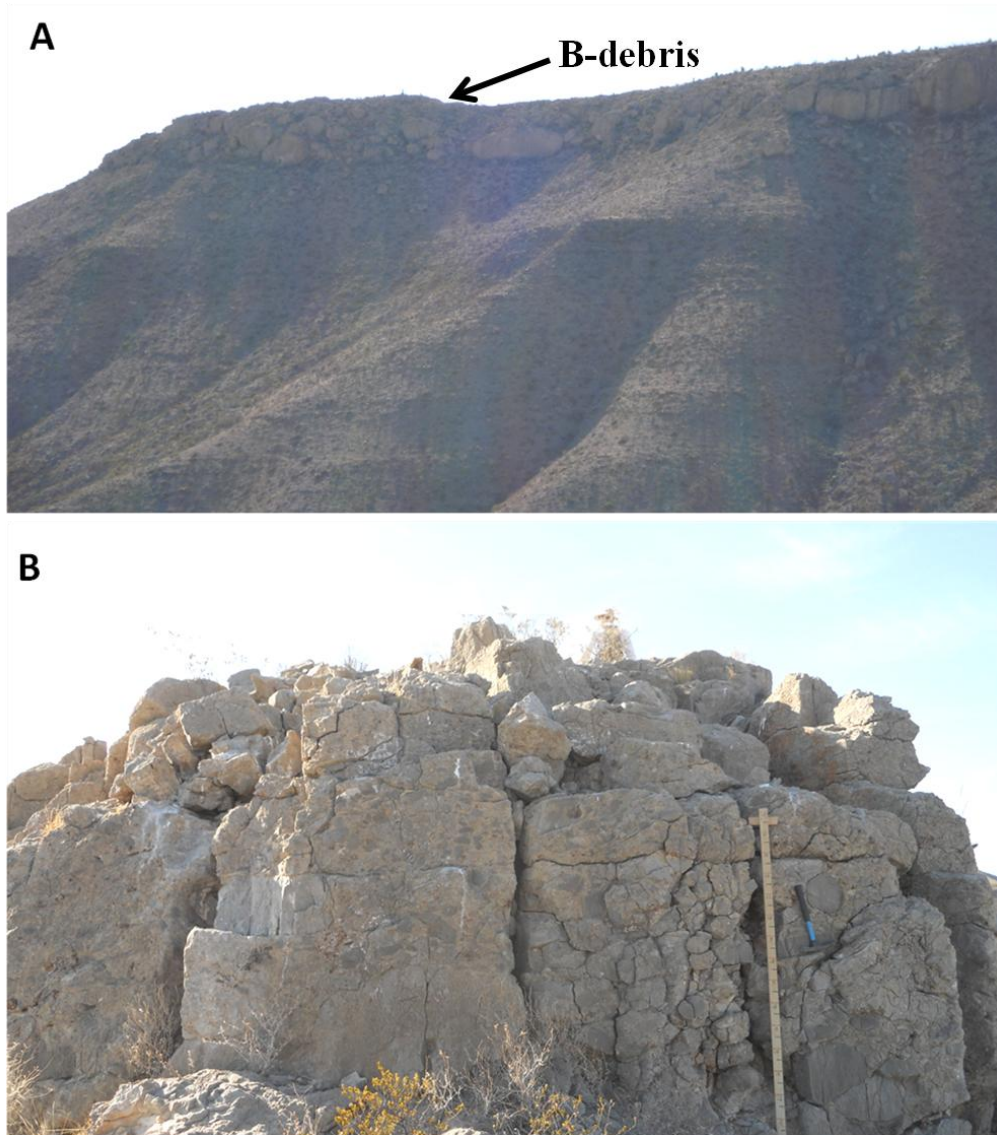


Figure 5.2: Photograph (A) of the eastern flank of Square Mesa capped by the B-debris with very large boulders seen from the exposure. (B) Photograph of the southern side of the WP-section showing part of the lower and middle zones of the B-debris.

white in figure 5.1 (A). Characteristics of the debris are very similar to those previously described from the road cut exposure along Texas FM road 2185; only the lower and middle zones are of a much larger magnitude in both the size of the blocks and in thickness. Unlike in the section on top of Square Mesa, the B-debris is slightly less than four meters thick at the top of the WP-section (figure 1.7) located one and half miles to the southeast and along the southwestern flank of Scott Canyon (figure 2.1). On the south side of the B-debris in the WP-section, the base is partially covered, and the top has been mostly eroded (figure 5.2 (B)). In figure 5.2 (B), the upper part of the lower zone and the middle zone of the B-debris are exposed with subrounded to angular clasts that are less than a meter across in the exposure. This portion of the B-debris is five and half miles north-northwest from the original locality from Kennedy (2009), but the characteristics of the poorly sorted interlocking larger clasts can be seen to be overlain by smaller clasts that appear to be partially aligned with an increased amount of mud matrix (figure 5.2 (B)). Slightly over a mile to the north of the WP-section in the northernmost exposure of the B-debris (figure 3.1), it is about two to three meters thick, but the base is covered. In this northernmost exposure a fractured section of the B-debris in figure 5.3 (A) has part of the middle and upper zones showing clasts that appear to be partially aligned in a more dominating mud matrix, and then fining upwards into the upper zone where it is a wackestone. The topping mudstone appears to have been eroded from the unit in this northern area.

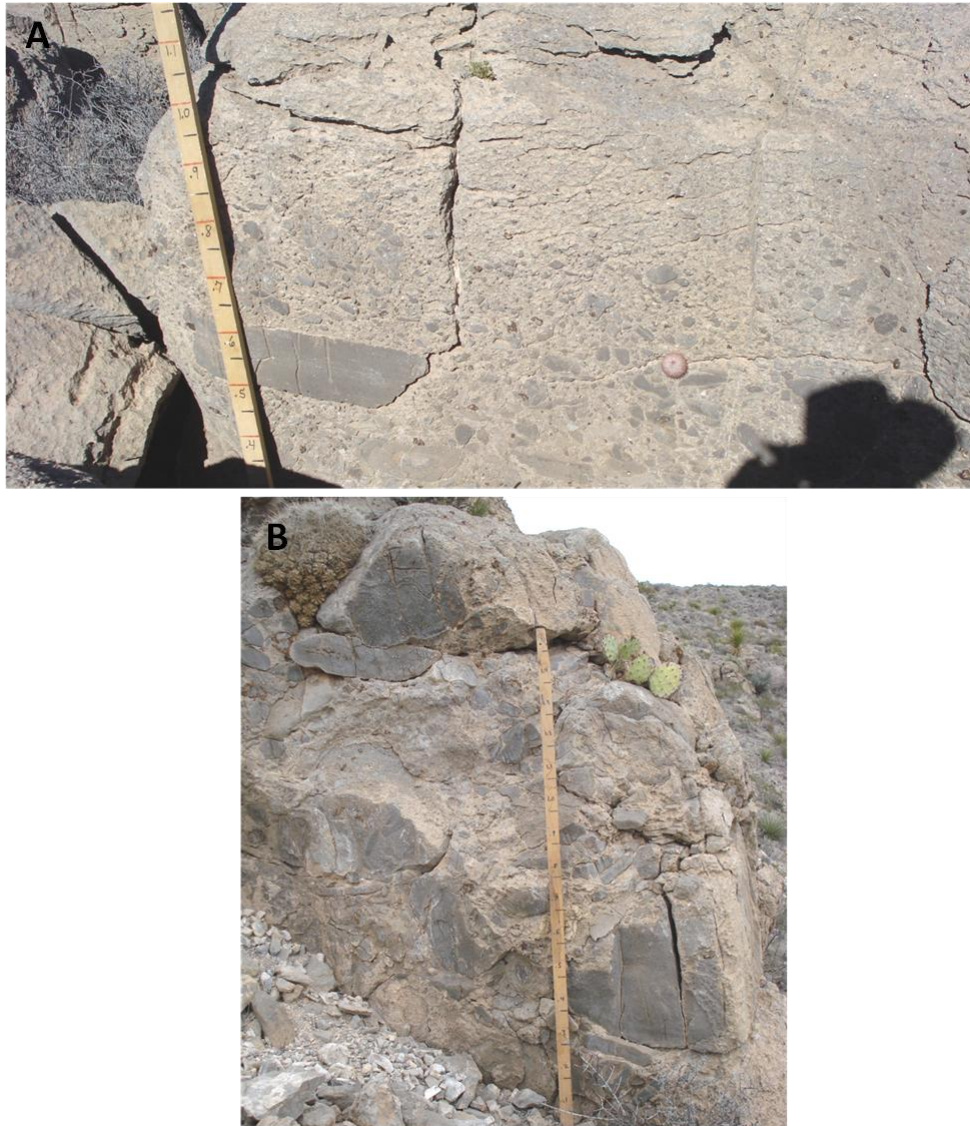


Figure 5.3: Photograph (A) of the northern exposure of the debris north of the WP-section showing the middle zone with partially aligned clasts. (B) Near the northern limit of the B-debris on the ridge between Scott Canyon and Ed Ray Canyon, where the lower zone is exposed with boulders visible.

Approximately two miles southeast from where the photograph of figure 5.3 (A) was taken and on the northernmost exposure of the B-debris between Scott and Ed Ray Canyons (figure 3.1), there are some exposures of the upper part

of the lower zone (figure 5.3 (B)). Measured exposures of the debris in this area range up to five and half meters thick, but the base is partially covered. In figure 5.3 (B) interlocking clasts are less than a meter across, and there appears to be additional mud matrix within the unit between some of the clasts. On top of the ridge directly above where the photograph of figure 5.3 (B) was taken, there has been a lot of erosion with broken up pieces of the middle zone of the B-debris (figure 5.4 (A)). Partially aligned clasts less than a quarter of a meter across can be seen (figure 5.4 (A)) as an indicator of the middle zone. Approximately a mile south-southwest from where the photographs of figure 5.3 (A) and figure 5.4 (A) were taken is an exposure of the B-debris on the western flank of Ed Ray Canyon (figure 5.4 (B)). Part of the lower zone can be seen that quickly transitions into the upper two zones (figure 5.4 (B)). Measured exposures of the B-debris in this area range between up to nine meters thick. There are larger clasts in this section that are over a meter across (figure 5.5 (A)). Continuing south approximately a mile from where the photographs of figure 5.4 (B) and figure 5.5 (A) were taken, there is a massive exposure of the entire B-debris measuring over 12 meters thick (figure 5.5 (B)). Other measured exposures of the debris in this area range between six to sixteen meters thick. In the lowermost part of figure 5.5 (B), there are small clasts and lenses of limestone beds in a laminar-like bed overlain by an interlocking, poorly sorted clast bed that dominates most of the unit (lower zone). Some of the clasts measures over a meter across in this

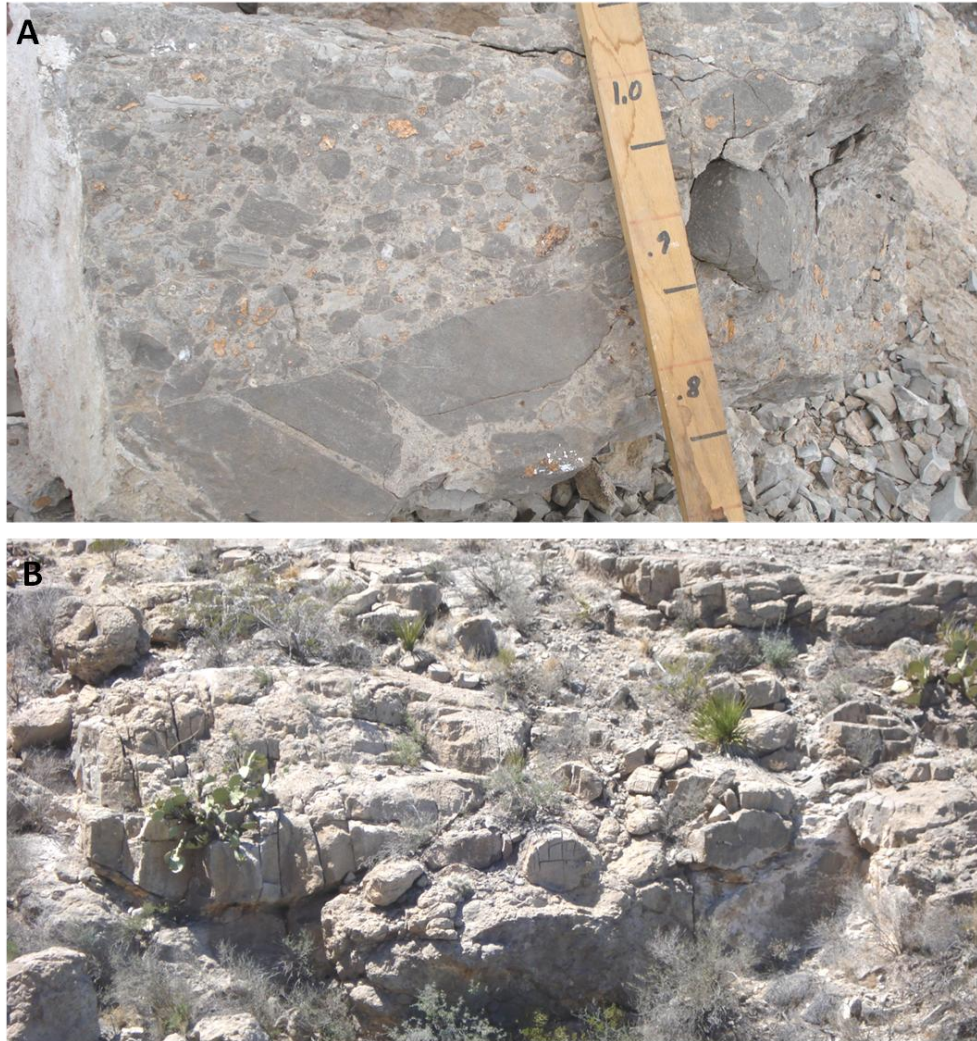


Figure 5.4: Photograph (A) of the ridge between Scott and Ed Ray Canyons, where it shows the middle zone of the B-debris with partially aligned clasts and an outsized clast. (B) Photograph taken on the western flank of Ed Ray Canyon showing mainly the lower zone of the debris as it then quickly fines upwards into the middle and upper zones.

exposure. In figure 5.5 (B) the strata of the lower zone is overlain by strata of the middle zone that has smaller clasts measuring less than a quarter of a meter across with some oversized clasts, and capped by a partially eroded bed of mudstone with no visible clasts or skeletal fragments. Exposures of the B-debris on the



Figure 5.5: Photograph (A) is of a boulder in the lower zone of the debris over a meter and half in length from the western flank of Ed Ray Canyon. (B) Photograph taken near the southern part of the western flank of Ed Ray Canyon, where a complete section of the debris is exposed.

eastern flank of Ed Ray Canyon are similar to those on the western flank, but from the southern part of the canyon to the north it measures in thickness from

eleven meter to three meters, thinning towards the north, as seen in the capping ridges of figure 5.6 (A).

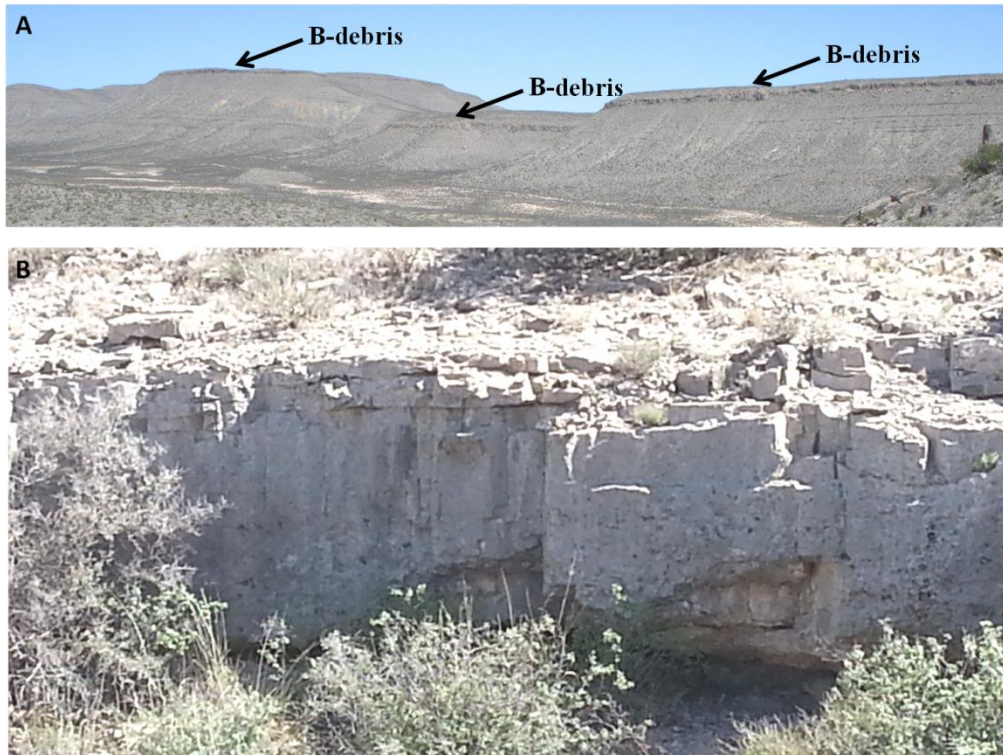


Figure 5.6: Photograph (A) of the eastern flank of Ed Ray Canyon, where the ridges are capped by the B-debris. (B) Photograph of a northeastern exposure of the debris showing the middle and upper zones.

In the northern part of Ed Ray Canyon on the eastern flank, there is continual thinning of the B-debris to the east. Approximately one mile from Ed Ray Canyon on the northeastern edge of the exposure in the north (figure 3.1), were it thins down to an average of about two meters (figure 5.6 (B)). In this area, the lower zone of the B-debris is no longer present (figure 5.6 (B)); the middle zone contains clasts measuring less than a quarter of a meter across, but still

displaying partial alignment, and the upper zone fines upwards from a wackestone into a mudstone.

In Wildcat Canyon, south-southwest of where the photograph in figure 5.6 (B) was taken, the exposures of the B-debris (figure 3.1) vary in measured thickness from three meters to ten meters with no consistent succession, but the lower zone of the unit is present and can be seen in figure 5.7 (A). In the northernmost part of Wildcat Canyon slightly southwest of where the photograph of figure 4.8 (A) was taken on the western flank, there is a massive boulder in figure 5.7 (A) that is longer across than the debris is thick, and the B-debris was measured as four meters thick. The upper part, as seen overlying the boulder in the lower part of figure 5.7 (A), belongs to the middle zone, and the upper zone is eroded back from the edge and covered. In the eastern branch of Wildcat Canyon towards the northern part, the B-debris in figure 5.7 (B) is measured at its thickest to be seven and half meters and contains all three zones. Some boulders seen in figure 5.7 (B) in the lower zone are over a meter across. Another interesting feature of the B-debris about half a mile southwest from where the photograph in figure 5.7 (B) was taken and on the eastern flank of Wildcat Canyon (figure 5.8 (A)). There is a massive boulder of nine meters thick that is higher in height than the surrounding debris thickness. It appears to be subrounded in cross view with only the upper zone resting upon it. There is a complete section of the B-debris

(figure 5.7 (B)) that is four meters thick in the northern part of a southeast branching canyon

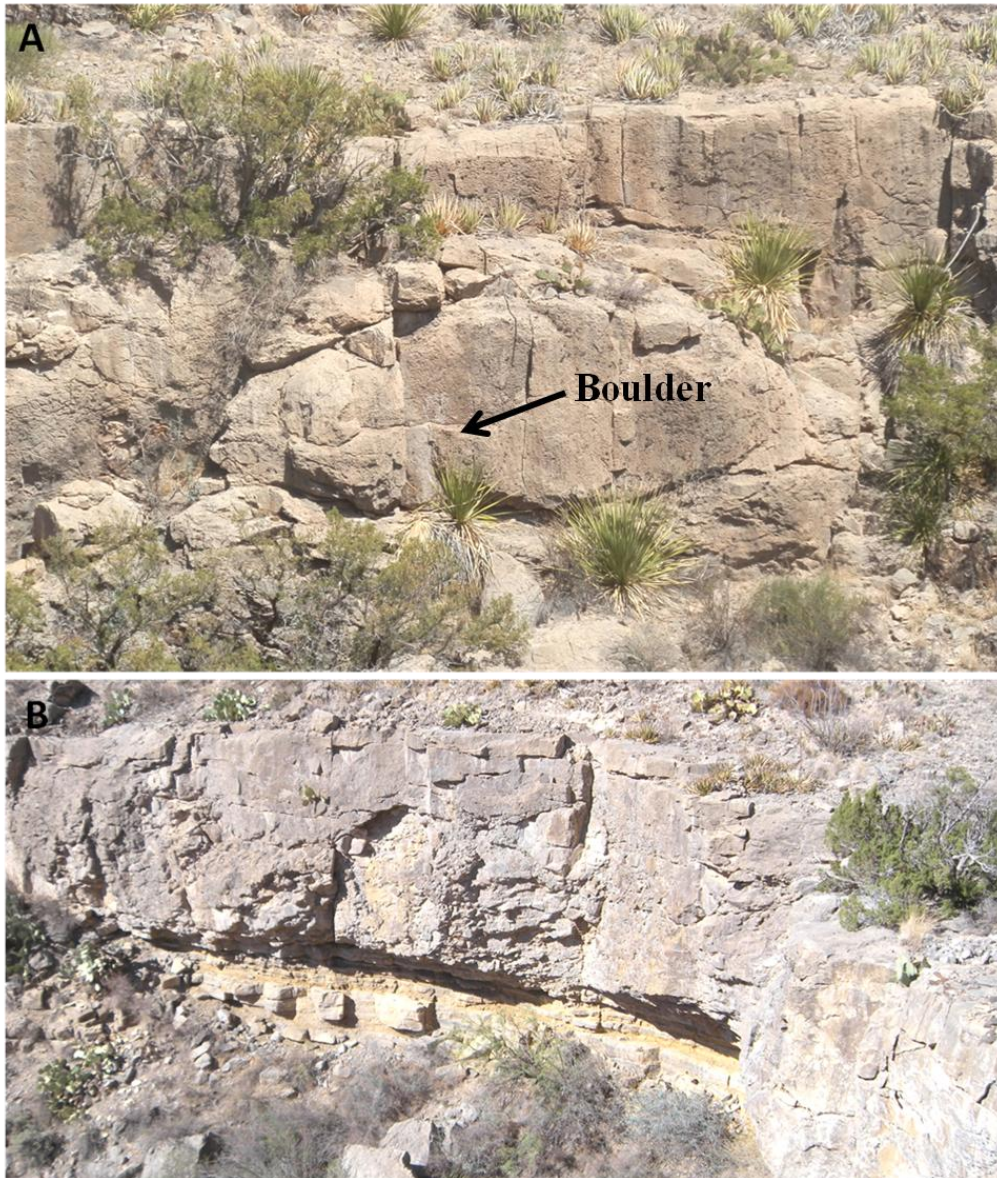


Figure 5.7: Photograph (A) of the debris in the northern part of Wildcat Canyon with a large boulder is exposed in the lower zone with the middle zone draped over the top. (B) The northeastern branch of Wildcat Canyon, where there is a complete section of the B-debris.

in the southern part of Wildcat Canyon. The lower zone is about two meters thick with some large clasts up to three to four meters across. The middle zone is slightly over one meter thick, and the upper zone at the top of the debris is about

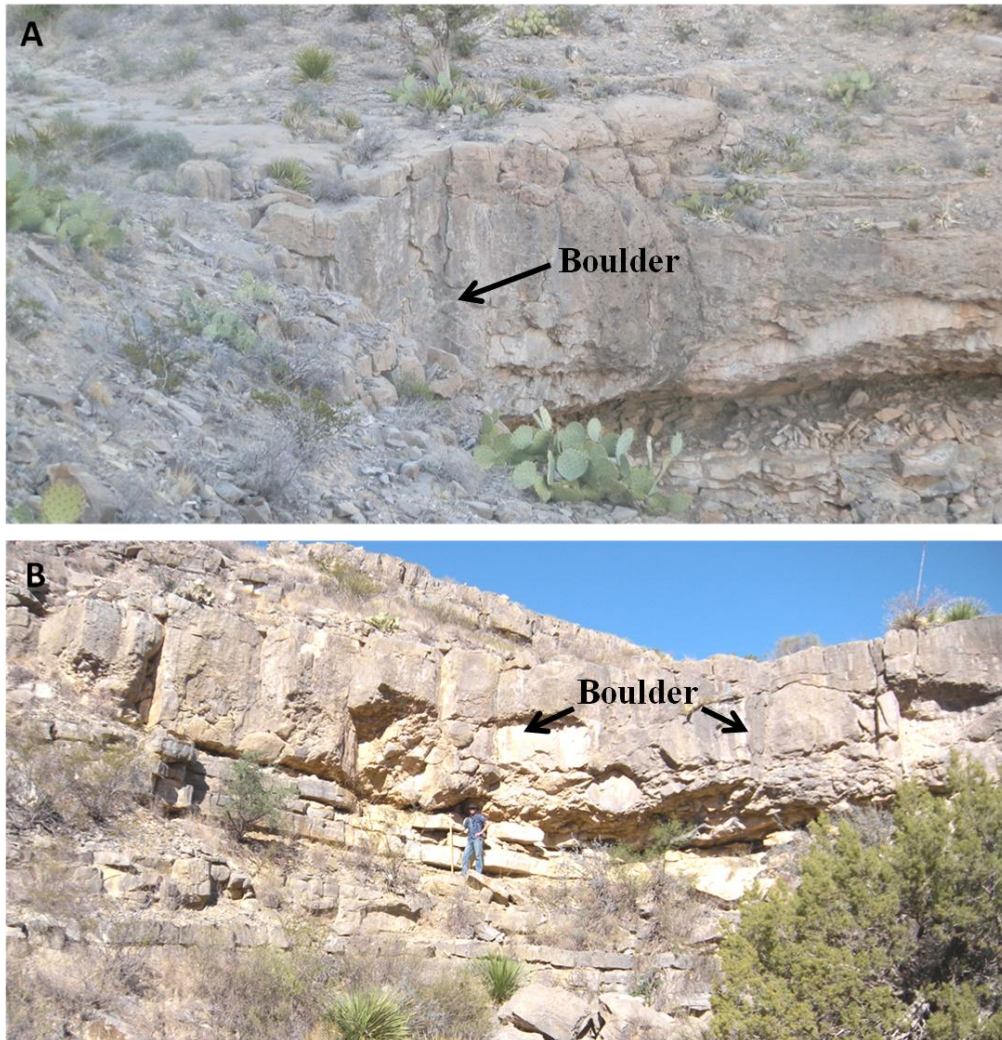


Figure 5.8: Photograph (A) shows a large boulder in the debris higher in height than the lower two zones and draped over by the upper zone of the eastern flank of Wildcat Canyon. (B) Photograph taken in the southeastern branch of Wildcat Canyon, where the lower two zones are exposed and the upper zone is eroded back from the edge.

half a meter thick. The B-debris described in the road cut along Texas FM road 2185 is approximately two and half miles south-southeast from where the photograph in figure 5.8 (A) was taken. The characteristics of the B-debris at the locality shown in figure 5.8 (B) are very similar to those of the road cut section of Kennedy (2009). His zone measurements differ in that the lower and middle zones were each slightly over two meters thick and the upper zone was slightly less than two meters thick. These measurements are in contrast to those of the B-debris shown in figure 5.8 (B), where the lower zone measures two meters thick, middle zone slightly over a meter thick, and the upper zone about half a meter thick.

5.3 Source of the B-debris

The original emplacement mechanism may never be directly known, but Kennedy (2009) did conclude that the B-debris contained clasts characteristic of primarily reef and fore reef facies. Clasts of the B-debris contain faunal elements that have been assigned to the reefal facies of the Capitan Limestone as exposed in the Apache Mountains to the south-southeast of the southern part of the Delaware Mountains (figure 1.2). The source of the B-debris is considered to be the Apache Mountains area, because of the similar faunal elements. The shelfal area of the Apache Mountains during the upper part of the Guadalupian had the Capitan Reef on its shelf edge with a back reef lagoonal area directly behind. It underwent a fault activation phase or a possible seismic event that caused a

massive slide event that slumped downward along the slope and became a debris flow in the basin with enough speed to cause a turbidity current above it (figure 5.9). At its distal ends it thinned to an average of two meters in the exposures of the B-debris seen in the northern part of the study area (figure 3.1).

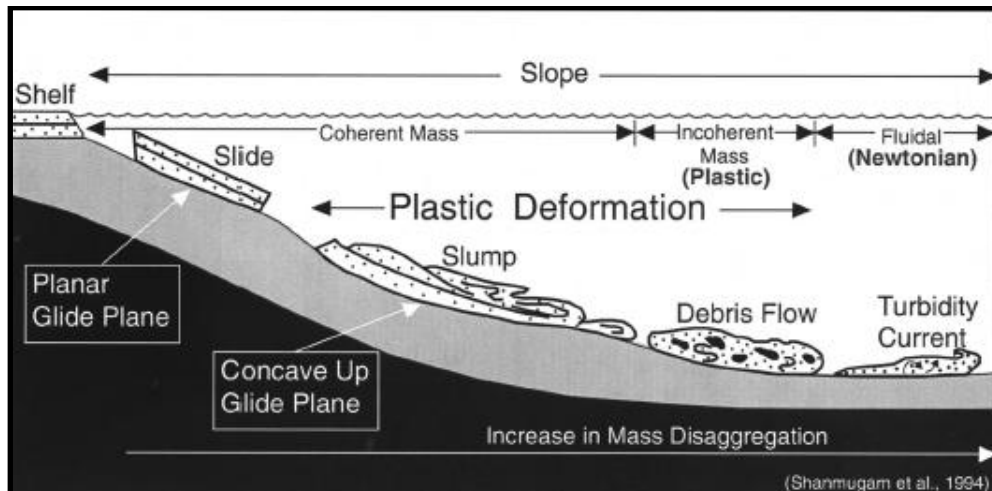


Figure 5.9: Illustration showing the degree of change of gravity-driven bodies as they travel down slope from a shelf representing coherent and incoherent masses (Shanmugam et al., 1994).

Chapter 6

CONCLUSIONS

In the southern part of the Delaware Mountains, the members of the Cherry Canyon and Bell Canyon Formations are not easily recognized lithostratigraphically because these members were originally described in the Guadalupe and the northern part of the Delaware Mountains 35-40 miles to the north. However, biostratigraphic correlations can be made using the microfaunal elements present, especially foraminifers and conodonts. Biostratigraphically, the lower part of the WP-section belongs to the Cherry Canyon Formation because of the presence of several species of the fusulinid genus *Parafusulina* from sample WP-1 up to the last occurrence of the *Parafusulina* in sample WP-60. The first occurrence of the fusulinid species *Leëlla fragilis* is in sample WP-50 suggesting this unit that belongs to the upper part of the Cherry Canyon Formation. Sample WP-60 comes from an interval at the top of the Cherry Canyon Formation that is considered herein to be equivalent in age to the Manzanita Member. The first occurrence of the fusulinid genus *Polydiexodina* in sample WP-63, species *Leëlla bellula* in sample WP-64, and genus *Codonofusiella* in sample WP-65 that marks the lower part of the Bell Canyon Formation that is considered herein to be equivalent in age to the Hegler Member. Lithostratigraphically, a sandstone/siltstone unit is present between the limestone units that are considered to be age equivalent to the Manzanita Member of the Cherry Canyon Formation

and the Hegler Member of the Bell Canyon Formation. As is present in the type area of these two members in the Guadalupe Mountains area, this sandstone/siltstone should be the lowermost part of the Bell Canyon Formation lithologically. It is the opinion of the writer that this transitional basal sandstone/siltstone unit between the stratigraphic equivalents of the Manzanita and Hegler Members makes up much of the covered 8.5 meter section of Package D, unit 1 (figure 2.1).

The minimal extent of the B-debris was mapped by its exposures that encompasses roughly 19 mi² (~30.5 km²) of the southern part of the Delaware Mountains. Other possible thin exposures of the B-debris possibly exist on the Delaware Mountains Ranch to the north of the B-debris map presented herein, but that area was not examined. The B-debris definitely thins significantly and no longer contains the lower zone in the northeastern part of the map area. The edges of the B-debris were mapped in association with older debris beds (the FR unit and the C-debris) along with the identification of some of the major faults in the area. Mapping the faults provided guidance to help determine the multiple repetitions of sections and blocks of the strata, especially of the B-debris, that are down-dropped along the ridges of the canyon flanks in the southern part of the Delaware Mountains. The repetitions of down-dropped strata occurred from uplift and extension of the Delaware Mountains during the Tertiary, causing several horsts and grabens to form, leaving behind the ridges and canyons seen today with

several close proximately faults of down-dropped strata along the ridges.

Mapping the B-debris in the study area provided excellent locations to show the three zones of the flow rheology that make up the B-debris and its limitations of the flow extent observed in the northeastern portion of the study area where the debris no longer contained the megabreccia, lower portion of the debris. All of this study provides a basic guide for future stratigraphic correlations and structural studies in the southern part of the Delaware Mountains.

References

- Beede, J. W., 1924. Report on the Oil and Gas Possibilities of the University Block 46 in Culberson County. *University of Texas Bulletin*, 15(9): 1087-1093.
- Dumble, E. T., 1903. Geology of southwestern Texas. *Transactions of the American Institute of Mining, Metallurgical and Petroleum Engineers*, 33: 913-987.
- Dunbar, C. O., 1944. Geology and paleontology of the Permian area northwest of Las Delicias southwestern Coahuila, Mexico. *Geological Society of America Special Papers*, 52: 35-48.
- Dunbar, C. O. and Skinner, J. W., 1931. New fusulinid genera from the Permian of west Texas. *American Journal of Science*, 5(22): 252-268.
- Dunbar, C. O. and Skinner, J. W., 1937. The Geology of Texas, Vol. 3, Part 2. Permian Fusulinidae of Texas. *University of Texas Bulletin*, 3701: 517-825.
- Dunham, R. J., 1962. Classification of Carbonate Rocks According to Depositional Texture. in Ham, W. E., eds., *Classification of Carbonate Rocks. American Association of Petroleum Geologists Memoir 1*: 108-121.
- Dutton, S. P., Kim, E. M., Broadhead, R. F., Raatz, W. D., Breton, C. L., Ruppel, S. C., and Kerans, C., 2005. Play analysis and leading-edge oil-reservoir development methods in the Permian basin: Increased recovery through advanced technologies. *American Association of Petroleum Geologists Bulletin*, 89(5): 553-576.
- Earth Science Australia website:
<http://earthsci.org/education/teacher/basicgeol/deform/deform.html>
- Gani, M. R., 2004. From Turbid to Lucid: A straightforward approach to sediment gravity flows and their deposits. *The Sedimentary Record*, 2(3): 4-8.
- Garber, R. A., Grover, G. A., and Harris, P. M., 1989. Geology of the Capitan shelf margin subsurface data from the northern Delaware Basin. in Harris, P. M., and Grover, G. A., eds., *Subsurface and Outcrop Examination of the Capitan Shelf Margin, Northern Delaware Basin*. Tulsa, OK, *Society of Economic Paleontologists and Mineralogists*, 13: 3-269.

Girty, G. H., 1908. The Guadalupian Fauna. *United States Geological Survey Professional Paper* 58: 651 p.

Guadalupe Mountains National Park Service website:
<http://www.nps.gov/gumo/naturescience/geologicformations.htm>.

Hayes, P. T., 1964. Geology of the Guadalupe Mountains. *United States Geological Survey Professional Paper* 446: 69 p.

Hill, C. A., 1999. Reevaluation of the Hovey channel in the Delaware Basin, West Texas. *American Association of Petroleum Geologists Bulletin*, 82: 277-294.

Hill, R. T., 1900. Physical geography of the Texas region. *United States Geological Survey Topographical Atlas, Folio* 3: 12 p.

Hills, J. M., 1942. Rhythm of Permian Seas – A Paleogeographic Study. *American Association of Petroleum Geologists Bulletin*, 26(2): 217-255.

Hills, J. M., 1963. Late Paleozoic tectonics and mountain ranges, western Texas to southern Colorado. *American Association of Petroleum Geologists Bulletin*, 47(9): 1709-1725.

Hills, J. M., 1984. The structural evolution of the Permian Basin of West Texas and New Mexico, The geologic evolution of the Permian Basin. *Society of Economic Paleontologists and Mineralogists*, Permian Basin section, Symposium Proceedings, Midland, TX: 8-9.

Horak, R. L., 1985. Trans-Pecos tectonism and its effect on the Permian Basin, Structure and tectonics of Trans-Pecos, Texas. *West Texas Geological Society Field Conference Publication* No. 85-81: 81-87.

Kennedy, W. L., 2009. "Geology of part of the northwestern Apache Mountains, southeast Culberson County, West Texas, USA". Unpublished M. S. Thesis, The University of Texas at Arlington, 84 p.

King, P. B. 1942. Permian of West Texas and southeastern New Mexico. *American Association of Petroleum Geologists Bulletin*, 26(4): 535-763.

King, P. B., 1948. Geology of the Southern Guadalupe Mountains, Texas. *United States Geological Survey Professional Paper* 215: 183 p.

King, P. B., 1949. Regional geologic map of parts of Culberson and Hudspeth Counties, Texas. U.S. Geological Survey, Oil and Gas Investments, Preliminary Map 90, scale 1" = 12,000'.

King, P. B. and King, R. E., 1929. The Pennsylvanian and Permian stratigraphy of the Glass Mountains. *University of Texas Bulletin*, 13(8): 109-145.

King, P. B. and Newell, N. D., 1956. McCombs Limestone Member of Bell Canyon Formation, Guadalupe Mountains, Texas. *American Association of Petroleum Geologists Bulletin*, 40: 386-387.

Lang, W. B., 1937. The Permian Formations of the Pecos Valley of New Mexico and Texas. *American Association of Petroleum Geologists Bulletin*, 21: 1-7.

McNutt, G. R., 1948. "Geology of the southern Delaware Mountains and northwestern Apache Mountains, Texas". Unpublished Ph. D. Dissertation, The University of Oklahoma, 82 p.

Meissner F. F., 1972. Cyclic sedimentation in Middle Permian strata of the Permian basin, West Texas and New Mexico. in Elam, J. C. and Chuber, S., eds. Cyclic sedimentation in the Permian Basin, 2nd edition, *West Texas Geological Society, Publication 72-18*: 203-232.

Nance, H. S., 2014. Middle Permian basinal Siliciclastic Deposition in the Delaware Basin: The Delaware Mountain Group (Guadalupian). Bureau of Economic Geology. The University of Texas at Austin: 80 p. Website: http://www.beg.utexas.edu/resprog/permianbasin/PBGSP_members/writ_synth/delaware%20mountain%20group.pdf.

Nestell, G. P. and Nestell, M. K., 2006, Middle Permian (Late Guadalupian) foraminifers from Dark Canyon, Guadalupe Mountains, New Mexico. *Micropaleontology*, 52: 1-50.

Nestell, M. K., Nestell, G. P., and Bell, G. L. Jr., 2006. Road Log – Day 2. Van Horn to Apache Mountains to southern Delaware Mountains, Texas, Permian (Late Guadalupian-Lopingian). in Hinterlong G., eds., Basinal Facies of the Uppermost Guadalupian: Applicability to Exploration and Development Projects, Field Trip Guidebook Permian Basin Section. *Society of Economic Paleontologists and Mineralogists*, 2006-46: 1-18.

Nestell, M. K. and Wardlaw, R. R., 2010. *Jinogondolella palmata*, a new Gondolellid conodont species from the Bell Canyon Formation, Middle Permian, West Texas. *Micropaleontology*, 56: 185-194.

Newell, N. D., Rigby, J. K., Fischer, A. G., Whiteman, A. J., Hickox, J. E., and Bradley, J. S., 1953. *The Permian Reef Complex of the Guadalupe Mountains region, Texas and New Mexico, a study in Paleoecology*. San Francisco, W.H. Freeman and Company: 1-236.

Richardson, G. B., 1904. Report of a reconnaissance in Trans-Pecos Texas north of the Texas and Pacific Railway. *University of Texas Bulletin*, 23(9): 119.

Silver, B. A. and Todd, R. G., 1969. Permian cyclic strata, northern Midland and Delaware basins, West Texas and southeastern New Mexico. *American Association of Petroleum Geologists Bulletin*, 68: 250-267.

Shanmugam, G., Lehtonen, L. R., Straume, T., Syversten, S. E., Hodgkinson, R., J., and Skibeli, M., 1994. Slump and debris flow dominated upper slope facies in the Cretaceous of the Norwegian and Northern North Seas (61-67N): implications for sand distribution. *American Association of Petroleum Geologists Bulletin*, 78: 910-937.

Shumard, B. F., 1858 (1860). Notice of new fossils from the Permian strata of New Mexico and Texas. *Transactions of the Academy of Science of St. Louis*, 1: 290-297.

Shumard, G. G., 1858 (1860). Observations on the geological formations of the country between the Rio Pecos and the Rio Grande. *Transactions of the Academy of Science of St. Louis*, 1: 273-289.

Smith, A. R., 1978. Sulfur deposits in Ochoan rocks of Southeast New Mexico and West Texas, Geology and mineral deposits of Ochoan rock in Delaware Basin and adjacent areas: *New Mexico Bureau Mines and Mineral Resources, Circular 150*: 71-77.

Sweatt, M. J., 2009. "A Geologic Map and Stratigraphy of upper Guadalupian – lower Ochoan (Permian) Strata along and east of FM 2185 in the northwestern Apache Mountains near Van Horn, West Texas". Unpublished M. S. Thesis, The University of Texas at Arlington, 134 p.

United States Geological Survey Service website:
<http://www.usgs.gov/pubprod/index.html>.

Von Streeruwitz, W. H. R., 1890. Geology of Trans-Pecos Texas, preliminary statement. *Texas Geological Survey*, 1: 217-235.

Von Streeruwitz, W. H. R., 1893. Trans-Pecos Texas. *Texas Geological Survey*, 4(1): 139-175.

Ward, R. F., Kendall, C. G. St. C., and Harris, P. M., 1986. Upper Permian (Guadalupian) Facies and Their Association with Hydrocarbons – Permian Basin, West Texas and New Mexico. *American Association of Petroleum Geologists Bulletin*, 70(3): 239-262.

Wardlaw, B. R., Lambert, L. L., and Nestell, M. K., 2001. Latest Guadalupian-Earliest Lopingian Conodont Faunas from West Texas. *Permophiles*, 39: 31.

Wardlaw, B. R. and Nestell, M. K., 2010. Three *Jinogondolella* apparatuses from a single bed of the Bell Canyon Formation in the Apache Mountains, West Texas. *Micropaleontology*, 56: 195-212.

Wilde, G. L. and Todd, R. G., 1968. Guadalupian biostratigraphic relationships and Sedimentation in the Apache Mountain region, West Texas. in Silver, B.A., eds., Guadalupian facies, Apache Mountain area, West Texas. *Society of Economic Paleontologists and Mineralogists Permian Basin Section Publication* 68-11: 10-31.

Wilde, G. L., Rudine, S. F., and Lambert, L. L., 1999. Formal Designation: Reef Trail Member, Bell Canyon Formation, and its significance for recognition of the Guadalupian-Lopingian boundary. in Geologic framework of the Capitan Reef. *Society of Economic Paleontologists and Mineralogists Special Publication* 65: 63-83.

Wood, J. W., 1965. "Geology of Apache Mountains, Trans-Pecos Texas". Unpublished Ph. D. Dissertation, The University of Texas at Austin, 241 p.

Biographical Information

Johnathon Bogacz has been studying at the University of Texas at Arlington and earned his B.S. degree in Geology with a minor in Physics in 2011 and began his Master's degree that same year. He is presently working as a geologist intern at XTO Energy an ExxonMobil Subsidiary. Future endeavors include his continuation of working in the oil and gas industry as a geologist and to continue the legacy of biostratigraphy in the Permian Basin.